THE DETERMINATION OF MERCURY IN SOIL

By

STEFANIE THERESA PAGANO

A DISSERTATION PRESENTED TO THE GRADUATE SCHOOL
OF THE UNIVERSITY OF FLORIDA IN PARTIAL FULFILLMENT
OF THE REQUIREMENTS FOR THE DEGREE OF
DOCTOR OF PHILOSOPHY

UNIVERSITY OF FLORIDA

1994

UNIVERSITY OF FLORIDA LIBRARIES

To my mother, Rose, and my spouse, Ali, for their unending love and support. You have my unconditional love always.

And to the memory of Marysia Witowski for her integrity, courage, and love of chemistry.

ACKNOWLEDGEMENTS

I would like to thank Dr. James D. Winefordner for his professional guidance during my years at the University of Florida, both undergraduate and graduate. His knowledge of chemistry, enthusiasm for research, dedication to his students, and personal integrity made it both a privilege and pleasure to work for him.

I would also like to thank all the past and present members of the group that I have worked with for their help and support. In particular, I want to thank Ben Smith, Giuseppe Petrucci, and Dennis Hueber for their indispensable experimental and technical advice and assistance on various projects with which I was involved. I want to thank Wilfredo Resto for his guidance on the project presented in this dissertation and also for epoxying the excimer laser to death to keep it from leaking. I would like to thank Nancy Mullins, MaryAnn Gunshefski, Denise Imbroisi, Sue Ohorodnik, Monica Escobar, and Andi Pless for their friendship and moral support. I will surely miss our "Friday lunches." And special thanks go to Donna Robie who incited me to alternate between sanity and insanity for four years, but was always there for me to lean on in the rough times, without exception.

On a more personal note, I would like to thank Michele Riley for putting up with my madness during the first two years of graduate school and for listening to me rant about chemistry subjects she cared nothing about ("assuming a circular horse..."). Her

faith in my ability kept my spirits alive during many valleys. And she finally realized that I am the smartest person she knows, even smarter than Thema.

I would like to thank my entire extended family for their support over the many years that I have been in school. Not one ever doubted that I could achieve the goals I reached for, especially my mother. She always expected me to do the best I could - no more, no less. This helped to support, and not pressure, me.

And finally, I would like to thank Algeisa for filling a part of my life as only she could. Her understanding, love, and support over the past three years have been invaluable to me personally and to the completion of my work here. And now that this period has come to a close, a new one shall begin.

TABLE OF CONTENTS

Abstract of Dissertation Presented to the Graduate School
of the University of Florida in Partial Fulfillment of the
Requirements for the Degree of Doctor of Philosophy

THE DETERMINATION OF MERCURY IN SOIL

By

Stefanie Theresa Pagano

April 1994

Chairperson: James D. Winefordner
Major Department: Chemistry

Over the past 20 years, there has been a ten-fold increase in the concentration of mercury in the soil of the Florida Everglades from anthropogenic sources. The Maximum Contaminant Level (MCL) set by the Environmental Protection Agency (EPA) for mercury in soil is currently 200 parts-per-billion (ppb). Methods of sample digestion and detection must constantly be improved to provide the reliable determination of lower concentrations of mercury in the environment. Based on past EPA protocol, with improvements in methodology and instrumentation, the MCL can be reduced.

In this work, a sample digestion procedure was developed which employed microwave heating of the soil in nitric acid in a high-pressure closed vessel. Sufficient leaching of mercury into the sample solution occurred in five minutes at 59 W/vessel without loss of analyte through overpressurization.

Laser-Excited Atomic Fluorescence Spectroscopy with Electrothermal Atomization (LEAFS-ETA) was used as the detection method. The scheme used a two-step excitation, with λ_1 = 253.7 nm and λ_2 = 435.8 nm. Direct fluorescence was measured at 546.2 nm. Atomization occurred in a pyrolytically coated graphite tube with L'Vov platform, and signal collection was by front-surface illumination. The absolute instrumental limit of detection (LOD) was 14 fg, 1.4 parts-per-trillion (pptr) with a 10 μL sample injection.

A comparison of the results obtained from sample digestion by EPA Series Method 245.5 with measurement by Cold Vapor Atomic Absorption Spectrometry (CVAAS), sample digestion by EPA Series Method 245.5 with measurement by LEAFS-ETA, and sample digestion by the microwave procedure with measurement by LEAFS-ETA showed that microwave digestion of the soil samples was faster and more reliable than by the currently used EPA wet oxidation method, and that the LEAFS-ETA method was more sensitive and selective for the determination of mercury than the CVAAS method.

CHAPTER 1
INTRODUCTION

The contamination of the environment by mercury is an important concern of conservationists throughout the world. Over the last few decades, the level of accumulation of this heavy metal has risen dramatically due to anthropogenic sources. The analysis of soil and sediment for mercury is of particular interest because these media are the ultimate sink for pollutants, and levels of mercury measured there may indicate the significance of overall contamination for the system or area in which the sample was taken. The local and global ramifications of pollution have accelerated the progress in the development of analytical methods for the determination of mercury, especially in real samples.

In 1968, Fujita[1] developed a method using colorimetry to determine mercury residue in rice grains that had been treated with a mercury-containing fungicide. The digestion of the grain was carried out in an oxygen-filled stainless steel bomb containing nitric acid, hydroxylamine hydrochloride, and urea. After digestion, a complicated extraction and separation were performed to isolate the mercury. Finally, colorimetry was used to determine the total mercury concentration.

Wilken and Hintelmann used HPLC to determine the methyl mercury concentration in sediments and suspended particles from one of the most contaminated rivers known, the River Elbe in North Germany.[2] Sediments and suspended particulate

matter (SPM) were first separated from the water phase of the samples by vacuum filtration. The SPM then underwent an HPLC method based on charge neutralization chromatography in which 2-mercaptoethanol is added *in situ* to the eluent to complex the organomercurials on the column during elution. The resulting mercaptoethanol-mercury complex is retained on the reverse phase column, separated, and detected by ultra-violet absorption at 230 nm. The relative standard deviation (RSD) was 2.9%, and the detection limit for methyl mercury was 0.5 ng absolute or 5 parts-per-billion (ppb) dry weight. The average methyl mercury concentration in sediments near an industrial chlor-alkali plant was 2.7 parts-per-million (ppm), nearly seven times the natural background level in the area.

Gas chromatography was used by Lee and Iverfeldt to measure the methyl mercury levels in run-off, lake, and rain waters in Sweden.[3] The methyl mercury was preconcentrated from the water onto a sulfhydryl cotton adsorbent (SCF) using a batch-column two-stage technique followed by capillary gas chromatography with an electron-capture device. The methyl mercury concentrations ranged from approximately 0.04 to 0.68 parts-per-trillion (pptr). The total mercury concentration was also determined by these authors. The samples were first oxidized with BrCl and then reduced by $SnCl_2$. The mercury vapor was collected and preconcentrated on a gold trap and analyzed by a double amalgamation helium dc-plasma atomic emission method developed by Iverfeldt and Linquist[4]. The total mercury concentration ranged from 5 to 15 pptr.

Azzaria and Aftabi used stepwise thermal analysis with Cold Vapor Atomic Absorption Spectrometry (CVAAS) to determine mercury in different phases of soil and

sediment.[5] In this analysis, phases of traces of mercury were estimated by heating the sample in a furnace, allowing the vapor to collect on a gold trap, then stepwise heating to remove the mercury off the gold trap and measuring the absorbance of the liberated mercury at 253.7 nm. The premise of the stepwise heating program is that mercury will be released at different temperatures based on the original form of mercury in the sample. For example, sorbed elemental mercury will be vaporized at a lower temperature than that necessary for mercury in its mineralized form in cinnabar ore.

Various other techniques have been used for the determination of mercury in environmental samples including Zeeman Graphite Furnace Atomic Absorption Spectrometry (AAS)[6], X-ray Fluorescence Spectrometry (XRF)[7], and Helium Microwave Induced Plasma (He-MIP) Atomic Emission Spectrometry (AES).[8] Each technique has its own advantages and disadvantages depending on the type of sample and information desired. For the analysis of mercury in soils, the most commonly used technique is CVAAS, with sample digestion by wet oxidation.

The objective of this dissertation is two fold. First, the determination of mercury in soil and sediment by Laser Excited Atomic Fluorescence with Electrothermal Atomization (LEAFS-ETA) is studied and presented. In this method, the digested sample is introduced into a graphite furnace where the mercury can be directly atomized and contained in a small volume during the analysis. The high number density of mercury atoms in the probed vapor volume allows for the use of small sample volumes (approximately 10 to 20 μL), and preconcentration is not needed. The mercury atom undergoes a two-color excitation process, and the subsequent fluorescence is detected.

Absolute detection limits for aqueous mercury solutions have been reported as low as 90 fg.[9] The analysis of soil and sediment samples by this method is presented in this work.

The second facet of this work is the development of a microwave acid digestion method for the solid sample. The current EPA-approved digestion method for mercury in soil and sediment involves a lengthy and complicated wet oxidation of the sample. It also contains many sources of potential error due to possible analyte loss from the sample and contamination to the sample. The proposed microwave acid digestion method in this work employs only one reagent and five minutes of digestion time. This method utilizes the high efficiency of coupling the microwave energy directly to the reagent which causes an increased rate of digestion due to elevated temperatures and pressures which form in the closed digestion vessel. Microwave acid sample digestion combined with LEAFS-ETA analysis is shown to be a rapid, reliable, and sensitive means of analysis for the determination of mercury in soil and sediment.

CHAPTER 2
MERCURY

Uses of Mercury

Historical Uses

Man's use of mercury dates conclusively as far back as the fifteenth or sixteenth century B.C.[10] This is evidenced by a specimen of quicksilver found in a ceremonial cup in an Egyptian tomb at Kurna. Even before elemental mercury was refined from its natural source, the mercuric sulfide ore cinnabar, ancient peoples used the ore for a wide variety of purposes.[11] Native American Indians used the red ore as war paint for their faces. Crushed cinnabar was used by ancient Greek doctors as an ointment for eyes, burns, and pustules. Mayans used the ore for decorations and pottery from 500 B.C. onwards. Romans used cinnabar to produce the pigment vermillion, which is still regarded as a high-grade paint pigment in the twentieth century.

By the third century B.C., the Greeks knew how to recover mercury from cinnabar ore, and since that time, the applications for the element have been virtually endless. When Isaac Newton turned to alchemy in 1690, he documented his experiences with mercury transformations in his laboratory notebook.[12] Over the years, the chronic effects of mercury intoxication became apparent in his behavior. Fortunately, no

permanent damage occurred, and after his research interests shifted, he appeared back in London in 1696 as a leading scientist.

Other professionals and craftsmen exposed to mercury were not as fortunate. One of the better known mercury poisoning incidents occurred in the hat industry.[10] In order to clean and soften fur used to make felt for hats, the fur was dipped in a solution of mercuric nitrate. During processing, the workers readily absorbed mercury through their skin and inhaled mercury vapor. A common effect of the poisoning was shaking and slurred speech. This phenomenon became known as "hatter's disease." In the United States, it was more commonly called the "Danbury Shakes" because Danbury, Connecticut, was the center for the hat industry. Today, an alternate process is used to treat fur.

In the first half of the twentieth century, one part metallic mercury was added to two parts chalk to produce a finely divided powder, aptly named "grey powder", that was used by the police to lift sweat-formed fingerprints from crime scenes. Over three or four decades, officers who consistently worked with grey powder complained about becoming increasingly irritable, easily embarrassed, shaky, and intolerable of being watched. It was determined that they suffered from various degrees of mercury poisoning, and a suitable compound to replace grey powder was developed.

Mercury and its compounds have also historically been used in medical applications.[10] Until the discovery of penicillin, mercury was used in several forms to treat syphilis. The therapy ranged from applying an ointment to infected skin, to ingesting a "syphilitic cocktail" of mercuric iodide, potassium iodide, and syrup of

sarsaparilla, to actually sitting in a closed chamber containing cinnabar that was subsequently heated to liberate vapors.

In the 1930s and 1940s, mercurial compounds were used in spermicides. These spermicides were often included in contraceptive tablets, jellies, and vaginal douches. Also, ingestion of mercuric chloride was sometimes used by women to induce abortion.

Modern Uses

Although some early processes have been discontinued due to rampant poisonings, the unique properties of mercury still make it valuable in over 3,000 applications in modern industrial and agricultural technology.[13] Because it is a liquid with high thermal conductivity, mercury is very useful as a heat-transfer agent. It is also a successful catalyst in several industrial processes, particularly those involving acetylene.

In the chloralkali industry, metallic mercury is used as a flowing cathode in the electrolysis of brine.[14] Sodium metal is produced at the cathode where it amalgamates with the mercury and flows out of the cell. During this process, chlorine is also produced. The amalgamated metal is later converted to caustic soda (lye or sodium hydroxide). Because chlorine and caustic soda are basic chemical intermediates for products such as bleach, disinfectants, grease-removers, soap, rayon, paper, medicines, textiles, and many more, their production is extremely sizable.

The high toxicity of most mercury compounds makes them very effective bactericides and fungicides.[13] Mercury is employed as a fungicide in the pulp and paper industry, both in the processing and storing of pulp. It is also utilized to control bacteria

in the tanning process of leather and to give fungal resistance to many plastics. In addition, commercial laundries oftentimes use mercury-containing compounds in their laundering chemicals to act as a disinfectant.

In agriculture, a variety of organic and inorganic mercury compounds have been used to treat seed potatoes, flower bulbs, and grain seed to protect them against fungal attack. However, the consequence of dusting food products with mercury results in intoxication and possible death.[15] Therefore, the use of mercury compounds in agriculture has been declining.

Skin antiseptics, such as Mercurochrome® and Methiolate®, are nonprescription mercurials that are used to treat small cuts and bruises and disinfect the skin. Despite the known effects of topically applying mercury ointments to the skin, these products continue to be sold today.[16]

A continued application of mercury that is often overlooked as dangerous is the use of mercury amalgam fillings in the dentistry industry. The typical proportions by weight for a mercury amalgam filling are five parts metal alloy to eight parts mercury.[10] The metal alloy may contain tin, copper, silver, and sometimes zinc. The added mercury allows the amalgam to be pliable while being shaped in the tooth cavity. Then it hardens into a strong, abrasion-resistant material. Although the danger of mercury exposure to the patient is usually minimal depending on the number of fillings the patient has, over time the dentists and their assistants can absorb high amounts of mercury through their hands and inhale vapors emitted as fresh amalgams are inserted into, or the old ones are drilled out of, the patient. Other risks of exposure can occur while the professional is

preparing the amalgam, if a spill occurs and is not cleaned up properly, and if there is poor ventilation in the work place. Many studies have shown that dentists and dental personnel have two to three times the mercury level than control groups tested, and they often suffer from mild, chronic symptoms of mercury poisoning.[17,18,19,20]

These are only a few examples of modern industries that still use mercury, and their applications. These industries can produce a direct contamination of the environment by the use and disposal of mercury products, by-products, and wastes.

Interaction with Soil

Sources of Contamination

Soil is a component of the biosphere that serves a very specific and necessary purpose. It produces the sustenance which is basic for human survival. In addition, it acts as a natural buffer controlling the transport of elements and compounds between the atmosphere, hydrosphere, and the biota therein. Another role of soil is that it acts as a sink for contaminants. Contamination of soil is very persistent, especially by heavy metals; the complete removal of mercury contaminants from soil is nearly impossible. For example, the first half-life of mercury in lysimetric conditions in soil is between 500 and 1000 years.[21]

When investigating sources for soil contamination, the original rocks and minerals that are indigenous to the soil must be considered first.[22] Igneous rocks are categorized into granite and basalt. Of the two types, mercury is more concentrated in granite. Of the types of mineral deposits formed, mercury has a propensity for the chalcophiles,

which are sulfide minerals. Sedimentary rocks consist of shales, sandstones, and limestones. The mercury content in these rocks varies and depends somewhat on the weathering processes present.

Overall, the contribution of mercury to soil from igneous rocks, sulfide minerals, and sedimentary rocks is minimal, on the order of low parts-per-billion (ppb) range. The exception to this trend is when the soil lies on top of an irregular belt of rich mercury-containing ore deposits that encircles the earth. In the western hemisphere, this belt lies along the East Pacific Rise, from northern Alaska to the southern tip of Chile. The primary mercury mining operations in the United States are located in California, Oregon, and Washington.[10] Topsoil in this region has higher concentrations of mercury than average soil in the rest of the country. However, it has not been established whether the higher content is due to natural weathering processes or from redeposition of mercury-containing dust and vapor released by the mining operation.

In any industrialized region, the major source of mercury contamination arises from industrial processes rather than natural sources. The contaminant can reach the soil by following one or more of three general pathways. These pathways are by travelling through the air, the drainage system, or by direct mechanical effects. Atmospheric transport of pollutants is accomplished by the wind. Factors such as wind speed and direction, turbulence, particle size, temperature, and ability of the contaminant to adsorb to particulates influence the extent of the transport. Consideration must also be given to the source of pollution, whether it is from a point source such as a refinery stack, a line source such as a heavily travelled road, or an area source such as the difference between

urban and rural zones. In all cases, the airborne contaminant eventually enters the water or soil fractions of the biosphere. Fluvial transport occurs mainly through drainage systems around the industrial sites. Contaminated water drainage from waste products produced by factories or works can either wash directly onto the soil or seep into local streams and rivers where it is further transported. The resulting contamination may be local or widespread. Gravitational and mechanical transport involve the downslope movement of pollutants from mine or other waste that is located on a hillside, the loss of solid materials from trains or other transportation vehicles, and the direct application of contaminated fertilizers to fields. The use of sewer sludge to produce fertilizers and manures, which are then used in fields, provides the highest form of mercury gravitational contamination.

The two principal industrial sources of mercury pollution are combustion of coal in power plants and emissions from chloralkali plants. In 1989, Meij[23] conducted research in the Netherlands on the fate of mercury in coal-fired plants. As the coal is burned, the native mercury present in the coal will either be concentrated in the coal ash left after combustion, or it will be volatilized and emitted from the air stack. It appears that the amount of mercury vapor vented is inversely proportional to the concentration of HCl present, due to the formation of $HgCl_2$. In his investigation, Meij found that an average of 42% of the mercury is released as vapor from the stack. If a wet flue-gas desulfurization (FGD) scrubber is on the stack, 52% of the emitted mercury is retained. The annual mercury emission by a 600 MW power plant was found to be 25 kg.

Mukherjee[24] reported that in 1987 fuel combustion nationwide released 0.94 tons of mercury to Finnish air and 0.17 tons to Finnish land. He observed that in a coal-fired plant, 7% of the mercury is in particulate form, 92% in vapor form and the rest, 1%, is retained in the process ash.

Pacyna and Münch[25] also found similar results for the emission of mercury vapor from the combustion of coal in Europe. They concluded that between 90 and 99% of mercury in coal is released to the atmosphere in a gas phase, and that the average mercury concentration in bituminous coal from different countries ranges between 0.1 and 1 g/ton.

Maserti and Ferrara[26] measured the concentration of mercury in the air, water, and soil surrounding a chloralkali complex in Pisa, Italy. The complex has been in operation since 1940, but waste treatment facilities to contain mercury contamination were not installed until late 1975. The discharge of mercury from the factory occurs mainly through an effluent channel that leads to the nearby coastal waterway. In the waste water, 90% of the mercury is in particulate form while 10% is dissolved. Between 1984 and 1986, the concentration of mercury in the waste water was 1-3 ppb, and the total mercury discharged into the coastal seawater was 80-160 kg/yr. Although the concentration of mercury in the water is within regulations, the amount discharged in weight per year is still significant, and these values are two orders of magnitude lower than the amount of mercury released before the installation of treatment facilities in 1975. The major increase in mercury levels was confined to a four to five kilometer radius around the plant.

Gonzalez[27] studied the mercury output of a chloralkali plant in central Cuba from 1985 to 1988. This plant has been in operation since the mid 1970s and is equipped with a treatment system for trapping mercury in the waste water. His analysis showed that atmospheric pollution by mercury was restricted to the factory and its surroundings, and that liquid wastes discharged to the Sagua la Grande River caused slightly elevated mercury levels up to the estuarine zone of the river mouth about five kilometers away, but overall contamination was minimal.

In the United States, a growing concern over industrial mercury pollution from wastewater treatment facilities is developing. In 1990, Glass[28] investigated two Great Lake estuaries for new sources of mercury contamination. The study showed that, for the St. Louis River estuary, the highest concentration of mercury in the sediment occurred near the regional Western Lake Superior Sanitation District wastewater treatment facility. By analyzing different waste streams, they concluded that the highest levels were associated with the incineration process in which sewer sludge is burned by using refuse-derived fuel from municipal garbage, and from municipal wastewater inputs. The concentration of mercury in the sediment ranged from 5 ppb to 5 ppm. Most of the samples tested were well above the EPA guidelines for allowable levels of mercury in sediment.

Speciation, Mobility, and Chemical Transformations

By whatever transportation pathway taken, once the mercury reaches the soil, it can undergo a variety of chemical transformations (Figure 2-1).[22] These transformations

Figure 2-1: Chemical transformations of mercury in the environment.

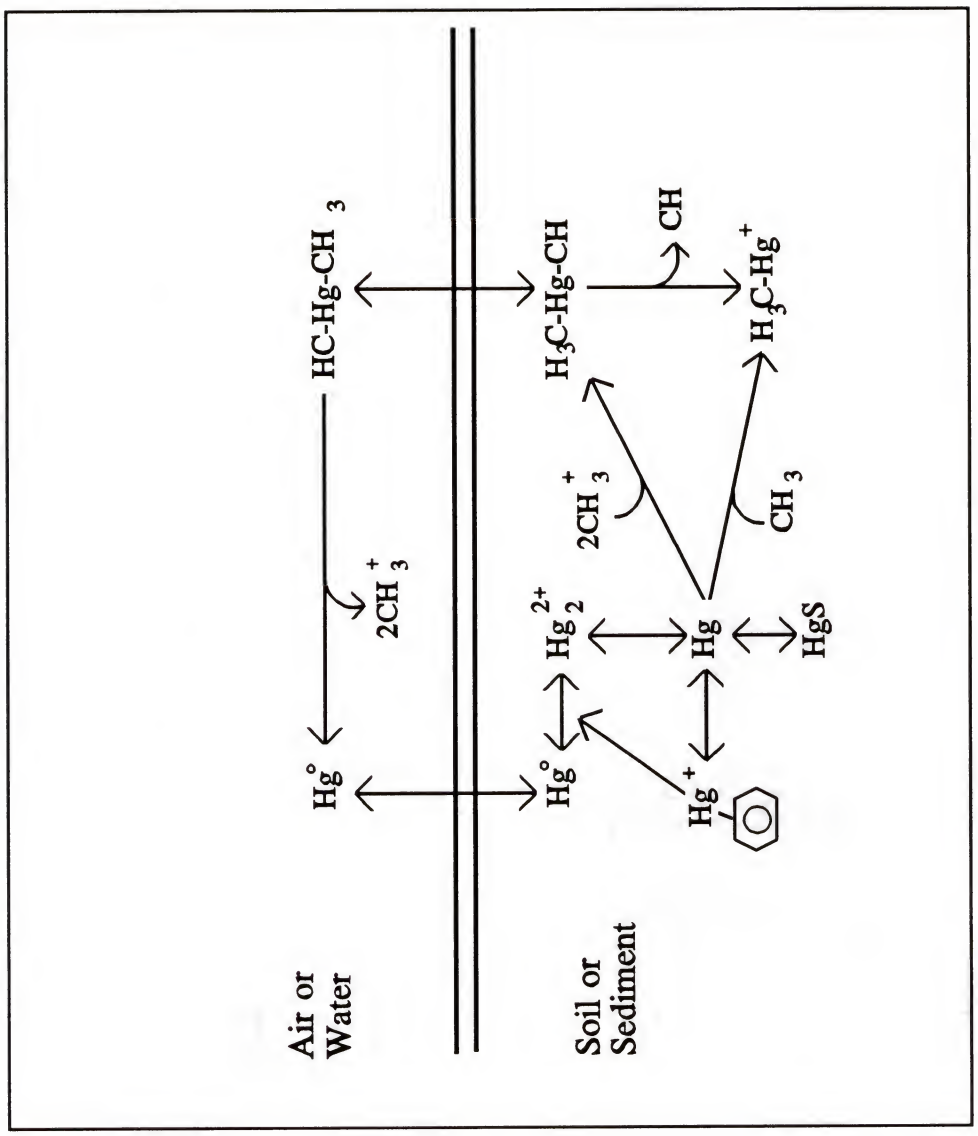
Air or Water
Soil or Sediment
HC-Hg-CH 3
2CH 3 +
Hg°
Hg°
H3C-Hg-CH
CH
H3C-Hg+
2CH 3 +
CH 3
Hg2 2+
Hg
HgS
Hg+

depend upon many different soil processes, such as:[21]

1. Dissolution
2. Sorption
3. Complexation
4. Migration
5. Precipitation
6. Occlusion
7. Diffusion into minerals
8. Binding by organic substances
9. Absorption and sorption by microbiota
10. Volatilization
11. Reduction/Oxidation

The relative importance of each of these processes is controlled by the particular soil properties prevalent at a given location. Soil pH and redox potential appear to exert the greatest influence on which process is dominant.

Schuster[29] found that the physical partitioning of soil organic matter between the dissolved and adsorbed fractions determines the behavior and distribution of mercury in soils with regard to complexation and adsorption processes. The most important ligands in solution are OH^-, Cl^-, and organic anions. The complexation of mercury into $HgCl_2$ or $Hg(OH)_2$ will increase its mobility due to the high solubility of these compounds. Also, the high affinity of mercury for sulfur allows the metal to readily bind to the S-containing functional groups of organic ligands.

In the same vein, Dryssen and Wedborg[30] concluded from their studies that under acidic conditions methyl mercury chloride and methyl mercury will be the dominant species present, whereas in the presence of high sulfide concentrations or neutral to alkaline conditions, the methyl mercury sulfide and hydroxide compounds will be most prevalent.

Wang[31] also found that as the concentration of chloride ions increased, so did the rate of elemental mercury desorption from freshwater sediments. This is an important process in the cycling process of mercury in the environment.

Although the study of adsorption of mercury to humic substances is usually undertaken to demonstrate the subsequent increase in mercury mobility,[32,33] Allard and Arsenie[34] have recently shown that natural organic matter such as humic substances can also reduce Hg(II) to Hg(0) in soils and sediments under anaerobic conditions with low pH and absence of chloride. Previously, it was believed that this reduction occurred only through microbial action.

It is clear that mercury exists in soil and its surrounding water systems in many different forms and undergoes various transformations based on conditions and other species present. Of all these transformations, the most significant is the natural methylation of mercury by microbial processes because of the high toxicity of organo-mercury compounds and the ease with which they are bioaccumulated in plant and animal species.

Bacteria and fungi are known agents of natural mercury methylation.[10] Microbes in the soil remove inorganic mercury that has adhered to food particles or dissolved

organic matter by methylating and discharging it into the surrounding environment. This is accomplished through several mechanisms. Some bacteria and fungi adsorb the mercury on the outside of their cell walls where it is directly reduced to the vapor form. Others absorb the mercury into their systems where it can combine with the cytoplasm and be converted into a different compound. Kerry[35] found that the methylation of mercury in the sediment of a freshwater lake in Ontario was due to sulfate-reducing bacteria. The process of methylation is dependent not only on the concentration of bacteria and inorganic mercury present, but also on pH, redox potential, organic substrate, and temperature.[36] Other organisms present in the soil or sediment can also methylate inorganic mercury biologically, perhaps with enzymes located in the liver.

In addition, Matilainen[37] found that the highest rates of methylation occurred in anaerobic conditions, but that the process of aerobic methylation became increasingly important with increasing concentrations of iron and manganese in the sediment. This supports the theory that methylation is highly dependent on specific environmental conditions present.

Bioavailability, Uptake, and Distribution

In order for a metal to exert toxic effects on an organism, it must first be incorporated inside of it. The degree of bioavailabilty of a metal will be determined by the particular type of organism and the form of the element (free, complexed, lipid-soluble, etc.). There are three generally accepted mechanisms of transport for ionic and molecular species across biological membranes.[38] The first route of transport is by diffusion. It entails a passive transport through pores in the cell membrane. The passage

of free metal ion may be mediated by membrane-bound proteins. For lipid-soluble species such as methyl mercury, passive diffusion provides an extremely rapid course across the cell membrane which may account for the high toxicity of these compounds. The second mode of passage is through facilitated transport. In this mechanism, metals are weakly bound to a receptor ionophore on one side of the membrane, and the complex will then diffuse to the other side where the metal can be released into the cytosol. The third mechanism is by active transport. There can exist a transmembrane proton electrochemical gradient which allows ion channels to form across the membrane. The metal may then enter the organism through the ion channel.

Once inside of the organism, metals have a propensity to bioconcentrate. Lipophilic species, such as methyl mercury, bioconcentrate to a factor of 10^6 to 10^8. This is a function of the rapid diffusion of lipid-soluble compounds across the biomembrane, and for a particular species, it also is a function of the surface area to body weight ratio. For this reason, it is not surprising to conclude that bacteria and algae have the highest organo-mercury concentrations in the food chain because they have the greatest surface area to body weight ratio. This is ecologically important because bacteria and algae retain organic metal species in the food web and can thus cause bioaccumulation in higher order species that feed off them. This is one process by which methyl mercury is bioaccumulated in fish, which in turn can lead to bioaccumulation in other fish, birds, animals, and humans.

For plants, it might be believed that heavily polluted soil and sediment is incapable of supporting much life. However, this is not correct.[22] In actuality, plant

species are very adaptable to their environments. In the case of bioaccumulation of non-essential toxic elements such as mercury, the problem then becomes to what extent the plant can absorb the metal and still flourish, and to what extent this polluted plant will affect the rest of the food chain. In fact, the mercury content in plants and fish is oftentimes used as an indicator of mercury pollution for the environment in which the species lives.[39] By analyzing the mercury concentration in species sampled from a variety of locations, general trends and hot spots of pollution can be established for a particular area or industrial site.

The actual uptake of metals into plants is controlled by soil conditions, in particular the pH and synergistic and antagonistic interactions with other nutrients present. Uptake also varies considerably from species to species and between different varieties within a species. Also, there is a varying spatial distribution of the metal observed among different parts of the plant.

Customarily, mercury may be incorporated into plants by root uptake and foliar uptake.[21] The absorption of metals by roots may be both passive and active, and it is positively correlated with the available pool of mercury species at the root surface. In passive absorption, the metal complex diffuses from the external pool to the root endodermis. Active absorption utilizes metabolic energy and occurs against a chemical gradient. Foliar uptake also ensues by two processes. The first is by the passive penetration of the metal through the cuticula, which is generally considered the major route of entry, especially for a volatile element like mercury. The second mode is by metabolic mechanisms which transport ions across the concentration gradient of the

plasma membrane into the cell protoplast. In 1978, Browne and Fang[40] studied the mechanisms of foliar uptake using labelled Hg vapor. They found that, in wheat, the foliar uptake was controlled by the stomata and confined solely to the leaves. Depending on the element, plant variety, and seasonal conditions, however, the distribution of metal within the plant components can vary. The transport of metals within plant tissues is regulated by movement in the xylem and movement in the phloem; the transport depends on the storage, accumulation, and immobilization processes of the particular plant species.

Biological Consequences of Mercury Exposure

The toxicological and deleterious effects of mercury are highly dependent on the form and dose ingested.[14] The various forms of mercury are generally categorized as inorganic, organic, and elemental vapor. The extent of biological effect and distribution throughout the body are primarily a result of the element's reaction with thiol compounds to form mercury mercaptides. The natural distribution of thiols in the tissues, therefore, determines the degree of reaction and accumulation. This supports mercury's partiality for blood plasma, which contains numerous thiol groupings. Because organo-mercury compounds are highly lipid-soluble and can diffuse easily through cell membranes, they are fairly uniformly distributed throughout the body. On the other hand, inorganic mercury compounds mainly form groupings on proteins. This means that most of the mercury binds to relatively few molecules, and therefore, the distribution of these compounds throughout the body is not uniform.

Table 2-1 shows the common symptoms for various types of mercury poisoning and the representative lethal concentrations of mercury in several target organs.[41]

Inorganic Mercury

Of the three general categories of mercury compounds, the inorganic form is the least toxic. After exposure, approximately 50% of the mercury is transported to the blood plasma and is quickly excreted in urine. In the body, inorganic mercury has a half-life of 40 days, with nearly all of it being eliminated in the first five days after exposure. Acute exposure is rare, and the symptoms include acute gastroenteritis and severe kidney injury.

Mercury Vapor

Inhalation of mercury as a vapor produces initial symptoms of pulmonary irritation and disorders of the central nervous system. About 74% of the vapor is absorbed by the lungs, but it is quickly oxidized to the mercuric ion and passes through the elimination system. The lethal effect of mercury vapor inhalation, therefore, is manifested in renal failure by accumulation of mercuric ions in the kidney.

Methyl Mercury

Methyl mercury poisoning occurs mainly through ingestion, where there is over 95% absorption of the compound by the gastrointestinal tract, and about 50% of the mercury localizes in the liver immediately. Methyl mercury has a half-life in the body

Table 2-1

Mercury Toxicity in Humans

Form of Hg	Symptoms	Concentration in Fatal Poisonings (ppm)			
		Whole Blood	Brain	Liver	Kidney
Organic (Methyl)	Numbness and tingling Loss of vision, hearing, coordination Intellectual deterioration Congenital neurological disorders	2.6	27.0	30.0	22.0
Vapor	Pulmonary irritation CNS disorders Renal failure	2.2	1.3	3.9	30.0
Inorganic	Acute gastroenteritis Severe kidney injury Renal failure	22.0	3.0	56.0	136.0

of 70 days, but unlike inorganic mercury, only 3% is eliminated in the first five days.Symptoms of methyl mercury intoxication include numbness and tingling, incoordination, loss of vision and hearing, and mental deterioration. Congenital disorders can also develop because of transfer across the placental barrier in pregnant women. This form of mercury is particularly toxic relative to the other forms because it is capable of passing through the blood-brain barrier.

Disasters

The epidemic in Minamata, Japan during the 1950s and 1960s sparked man's first widespread interest in the consequence of mercury poisoning.[10] Until that time, growing environmental contamination by mercury was largely ignored. For almost a decade, the people who lived near Minamata Bay, Japan, ate fish and shellfish that contained very high concentrations of methyl mercury. The local waters from which the fish came were polluted by a slaughterhouse located in nearby Tsukinoura, ammunition disposed of at the end of World War II, agricultural chemicals, and the Shin Nihon Chisso Company which was a large chemical-fertilizer factory. By the time the disease was recognized and diagnosed as the result of mercury poisoning, twenty-six people had died and hundreds more suffered from chronic effects.

Only ten years after the Minamata disaster, the largest outbreak of methyl mercury poisoning ever recorded occurred in Iraq.[42] The incident ensued as a result of consumption of homemade bread prepared from seed wheat treated with a methyl mercury fungicide. The repercussions of this catastrophe were over 6,000 Iraqi people

admitted to hospitals throughout the country, with 500 cases ending in death. It is in fact believed that more people were poisoned and died, but did not contact the hospitals.

EPA Regulations

In 1970, President Nixon issued an executive order titled Reorganization Order No. 3 which created the Environmental Protection Agency (EPA).[43] The EPA is an independently run agency that implements and supervises environmental laws and regulations and sponsors environmentally oriented research. There are seven regulatory acts that fall under the supervision of the EPA. They are the Clean Water Act (CWA), Safe Drinking Water Act (SWDA), Clean Air Act (CAA), Toxic Substances Control Act (TSCA), Federal Insecticide Fungicide and Rodenticide Act (FIFRA), Resources Conservation and Recovery Act (RCRA), and the Comprehensive Environmental Response, Compensation, and Liability Act (CERCLA or "Superfund").

Of these seven acts, CERCLA and RCRA deal specifically with solid and hazardous wastes, and they govern the guidelines set for the determination of mercury in soil. CERCLA was enacted in 1980 with the purpose of cleaning up old, improperly constructed, and hazardous-waste disposal sites. RCRA, on the other hand, governs the current and future generation, transport, and disposal of hazardous waste. According to CERCLA restrictions, the contract-required detection limit (CRDL) that must be demonstrated on a laboratory instrument before it can be used to determine mercury in contract laboratory procedure (CLP) samples is 0.2 ppb in solid waste.[44] The maximum contaminant limit (MCL) for mercury in solids is 200 ppb. At this level of mercury contamination, RCRA considers the sample to be hazardous material.

CHAPTER 3
SOIL SAMPLING

One of the most critical factors of metal analysis in soil and sediment is the physical sampling. This is especially true for the analysis of volatile compounds such as mercury. In the ideal case, an individual sample accurately represents all the intrinsic properties from the entire system in which it is taken.[22] Unfortunately, this is seldom the case, and a multitude of samples must be obtained and analyzed in order to accurately portray the total population. Improper sampling can lead to false data or erroneous conclusions drawn from the data. With proper objective sampling, a reduction of costs, an enhancement in the speed at which data are obtained, and an improvement in precision, accuracy, and scientific value of the data can be achieved.

Sampling Plans and Methods

All soils are naturally variable, both horizontally across the surface and vertically down the soil profile. Environmental disturbances introduce an additional variation to these natural variations. All diverse areas must be adequately sampled if conclusions are to be drawn about a population area. The soil sampling strategy can be either judgmental or random.[45] The judgmental plan involves sampling typical or visual differences in the area, and it should be avoided because the results obtained rely heavily on the personal decisions of the surveyor. Random sampling, on the other hand, is probability sampling

and its results rely on probability theory. Several random sampling plans exist, and the particular one to follow depends on the sampling site and type of information desired.

Simple random sampling of an area allows every possible combination of sample units to be selected. The combinations possible are only limited by the sample size, and the number of samples is determined by

$$n=\frac{t^2s^2}{D^2} \qquad \text{(Equation 3-1)}$$

where: t = a number chosen from a "t" table for a chosen level of precision; the degrees of freedom are first chosen arbitrarily and then modified by reiteration.

s^2= the variance which is known beforehand from other studies or estimated approximately by $s^2=(R/4)^2$, where R is the estimated range likely to occur in sampling.

D = the variability in mean estimation of analyte that the analyst is willing to accept.

This type of sampling provides information about the mean and confidence limits, but may not reveal patterns of contamination for an area.

Stratified random sampling employs the subdivision of an area into numerous subpopulations or strata. Random sampling is then performed on each stratum. The purpose of stratification is to break the population down into smaller and more homogenous parcels. Factors that contribute to how each stratum is arranged include topography, type of vegetation cover, type of soil, and estimated exposure to

contamination. This sampling plan allows for the statistical analysis of variability within and between the strata.

For an intended complete coverage of a soil population, systematic or grid sampling is used. In this plan, the samples are taken at regular, fixed distances along a "grid" imposed on the population. The only criterion for the technique is that the location of the first unit selected be randomly chosen. Because of its spatially even coverage, systematic sampling is often used for mapping a location.

Composite sampling is used when only the mean value of an analyte is needed. A number of samples are taken from the population and thoroughly mixed to form a composite. This composite is then subsampled and analyzed. Only the mean value can be measured, and there can be no calculation of the variance of the mean or precision with which it can be measured. The number of samples necessary for the analysis depends on the variability of the analyte and the desired level of confidence.

When sampling vertically down the soil profile, the recommended depth depends on the purpose of evaluation and history of the soil area. The active root zone, from 0 to 30 cm, contains variability due to soil type, climate, vegetation, and historical contamination. The subsoil region, from 30 to 100 cm, is affected by water storage, salt movement, and compactness. The parent material then lies below the subsoil.

Random depth sampling is used when there are no known trends in contamination and the variability of the entire soil mass is desired. Prior to physical sampling, the chosen depth for a sample is determined by the formulation equation

$$\text{Depth} = (\text{Total soil depth analyzed}) \times RN \qquad \text{(Equation 3-2)}$$

where RN = a random number between 0 and 1.

Stratified random depth sampling is used when vertical strata are defined. Samples can be acquired by random methods within each stratum. The depth of a sample taken is determined by using Equation 3-2 after substituting "stratum depth" for "total soil depth."

Discrete depth sampling is often used when sampling for volatile organics. In this method, the sampling depths are predetermined and are usually evenly distributed along the vertical profile, unless more samples from one particular level are desired for a specific reason.

Composite depth sampling homogenizes the whole soil core, and subsamples are drawn and analyzed for the compound of interest. This is an inexpensive method to obtain total information about the specific site of the core; however, all information about variability of analyte with depth is lost.

Apparatus

The type of apparatus used to physically collect the sample will depend on the location of the site, type of soil or sediment, and the amount of interstitial water present in the soil.[38] The crudest device used to collect surface or horizon samples is called the grab sampler. It collects large volumes of samples, but in the process disturbs the sampling area. It also tends to lose a significant amount of fine particles. For large, undisturbed samples, a box corer is preferred.

When depth profiling is required, cylindrical sediment corers are used. They are produced in assorted heights and diameters. Often, they are constructed of metal with an interior plastic liner to prevent contamination. If the sample is not too compact,

corers made entirely of polycarbonate can be used. The leading ends of the corers are bevelled for easier penetration of the solid medium. Once the corer has been imbued with sample, polyethylene end caps are used to seal it. If samples of less than 5 cm depth are needed, individual corers made of polyvinyl chloride (PVC) can be used.

QA/QC and Statistical Analysis of Samples

Quality assurance (QA) and quality control (QC) protocols are used to appraise and minimize errors that occur during all facets of sample collection and analysis.[44] Errors can result randomly or can occur through bias. Bias is delineated as systematic error that can be attributed to sampling, handling, transport, preparation, subsampling, and laboratory analysis variabilities. The EPA has mandated the use of duplicate, split, spiked, evaluation, and calibration samples to minimize the error due to these biases. The random errors due to variability in the population itself, on the other hand, can be evaluated using classical statistical concepts, the most common of which will be defined here.[46]

The most frequently used statistic in soil analysis is the mean value of the samples, $\bar{x}$. It is designated as the arithmetic average of the variable being measured among a collection of samples. The variance, s^2, is defined as the measure of dispersion of individual samples around the mean. The square root of this variance is known as the standard deviation, s. The standard error, s_x, indicates the reliability of the mean, $\bar{x}$, by expressing the precision of the average value, and is defined as the standard deviation divided by the square root of the number of samples, $\frac{s}{\sqrt{n}}$. The standard error is then

used in conjunction with the sample mean to calculate confidence intervals. For example, the values obtained by adding or subtracting two standard errors to the sample mean are said to constitute the 95% confidence limits. Confidence limits for levels higher and lower than 95% can also be calculated from the mean and standard error. Finally, the coefficient of variation (CV) or per cent relative standard deviation (%RSD) is used to express the variability among units on a relative basis. For example, large units such as plant stalk length usually will have a larger variance than smaller units such as pore diameter. The coefficient of variation is calculated as a per cent by dividing the standard deviation by the mean and then multiplying by one hundred, $CV\% = 100\frac{s}{\bar{x}}$.

The evaluation of data error in terms of these and other statistical parameters makes the data results more universally comparable when describing studies by different scientific researchers or methods.

CHAPTER 4
THE FLORIDA EVERGLADES SAMPLING SITE

The Florida Everglades was chosen as an important site to sample soil for two reasons. First, it is already known that the level of mercury contamination in this region has increased significantly over the last two decades, and many plant and animal species depend on the delicate balance of this system.[47] This increase in contamination is presumably due to anthropogenic influences. Second, this area manifests very distinctive geographical conditions in which numerous factors influence the distribution of chemical species throughout its land and waterways. The physical, environmental, and habitatual implications of the sampling site will be discussed briefly in this chapter.

The Everglades are located on the southern tip of the Florida peninsula, bordered on the east by the greater Miami area. It is a complex ecological system that comprises approximately seven million acres of land. Topographically, most of the land is barely above sea level. Because of this, the samples themselves physically range from relatively dry soil to extremely watery sediments.

The combination of geographical location, climate, and water flow has provided the United States with its only true subtropical wilderness. Some of the habitats and some of the animals present here are rare or unseen elsewhere in the United States. The type of water that flows in this area originates from both fresh and sea sources. The

resulting brackish conditions allow for the distinctive transport, accumulation, and partitioning of various chemical species.

The particular environmental conditions of this territory are the life-blood for the specific flora and fauna that thrive here, including many endangered species. The Roseate Spoonbill is a bird that was nearly extinct several years ago. Now, with protected grounds in coastal Texas and Florida Bay in the Everglades, its numbers are increasing steadily. The Brown Pelican is another endangered species found in the Glades. It can be found nesting among the many mangrove keys in Florida Bay and along the Gulf Coast side of the Glades. Our national bird, the Bald Eagle, also dwells in the Everglades. There are only approximately fifty nesting pairs in this region. The largest remaining populations of Bald Eagles are in the Everglades area in Florida and in Alaska. Another species that thrives in this region is the Florida Alligator. The brackish waters of the Everglades provide one of the world's few habitats in which the freshwater alligator and salt water crocodile can be found living together. In addition to these endangered species, the Florida Everglades is home to thousands of other animals and plants. It is also a winter haven for a wide variety of migratory animals.

Because of its unique environment and inhabitants, the Florida Everglades is an important ecological site and its delicate balance must be maintained and kept as pristine as possible. This is why it is vital to monitor, analyze, and control pollutants that contaminate this environment.

CHAPTER 5
SAMPLE PREPARATION TECHNIQUES

Introduction

As was discussed in Chapter 3, serious data errors can result from improper handling, preparation, and storage of samples. This is especially true in the case of mercury. All phases of sample preparation must be fastidiously considered in order to avoid additional contamination to the sample or loss of analyte from the sample. Some of the general procedures for sample preparation in this work are as follows. Acid reagents used in solution preparations were obtained from Fisher Scientific in the grade of Trace Metal Certified. Depending on the specific lot analyses, the average concentration of mercury in the nitric and hydrochloric acids used was approximately 5 parts-per-trillion (pptr). All glassware was thoroughly cleaned in a Liqui-Nox™ soap bath. They were then soaked in a 1:1 concentrated nitric acid to water bath for at least twenty-four hours. Afterwards, they were rinsed twenty times in deionized water and again twenty times in Barnstead water. The glassware was kept in a sealed plastic container separate from all other glassware in the laboratory until needed for use. Standard mercury solutions were prepared in the cleanest hood available in the laboratory to reduce contamination as much as possible. They were prepared from a stock 1000 ppm mercury solution (Mercuric Nitrate in 1.8% HNO_3, Fisher Scientific) that was no older than thirty days relative to the date of first opening the bottle, and from Barnstead

water with a resistivity of no less than 12.0 MΩ·cm. A study of the decrease in mercury signal with respect to length of storage time was conducted with samples stored in Teflon, glass, and polyethylene bottles (Figure 5-1). Teflon bottles were found to hold the concentration of mercury the most constant over time; therefore, all solutions prepared were stored in 30 mL narrow-mouthed Teflon bottles. All samples were analyzed as soon as possible after preparation, usually within one week. After thirty days, all solutions were discarded and fresh ones prepared.

In addition to types of reagents, water, and storage bottles used, the type of pipet tips used in preparing solutions also can contribute to contamination of the sample. For very low determinations of mercury, the pipet tips used in making and transferring solutions can leach mercury out of the plastic tip and into the solution. A study was conducted to determine the amount of mercury leaching occurring by standard pipet tips. The tips used were Fisherbrand Tips suitable for use on Eppendorf pipets. A 20 μL aliquot of water was injected into a graphite furnace for mercury analysis by Laser Excited Atomic Fluorescence Spectrometry (LEAFS). Different grades of water were analyzed in order to overlook contribution of mercury from the water itself. The results showed that a mercury signal was observed from the samples analyzed (Figure 5-2). The pipet tips were then pretreated by soaking in a 1:1 nitric acid to water bath for twenty-four hours and then thoroughly rinsing them. This procedure presumably leaches any mercury out of the tip before it used with the samples. The water samples were analyzed again using the pretreated tips, and the results showed that there was at least a 50%

Figure 5-1: Mercury concentration stability based on type of storage container.

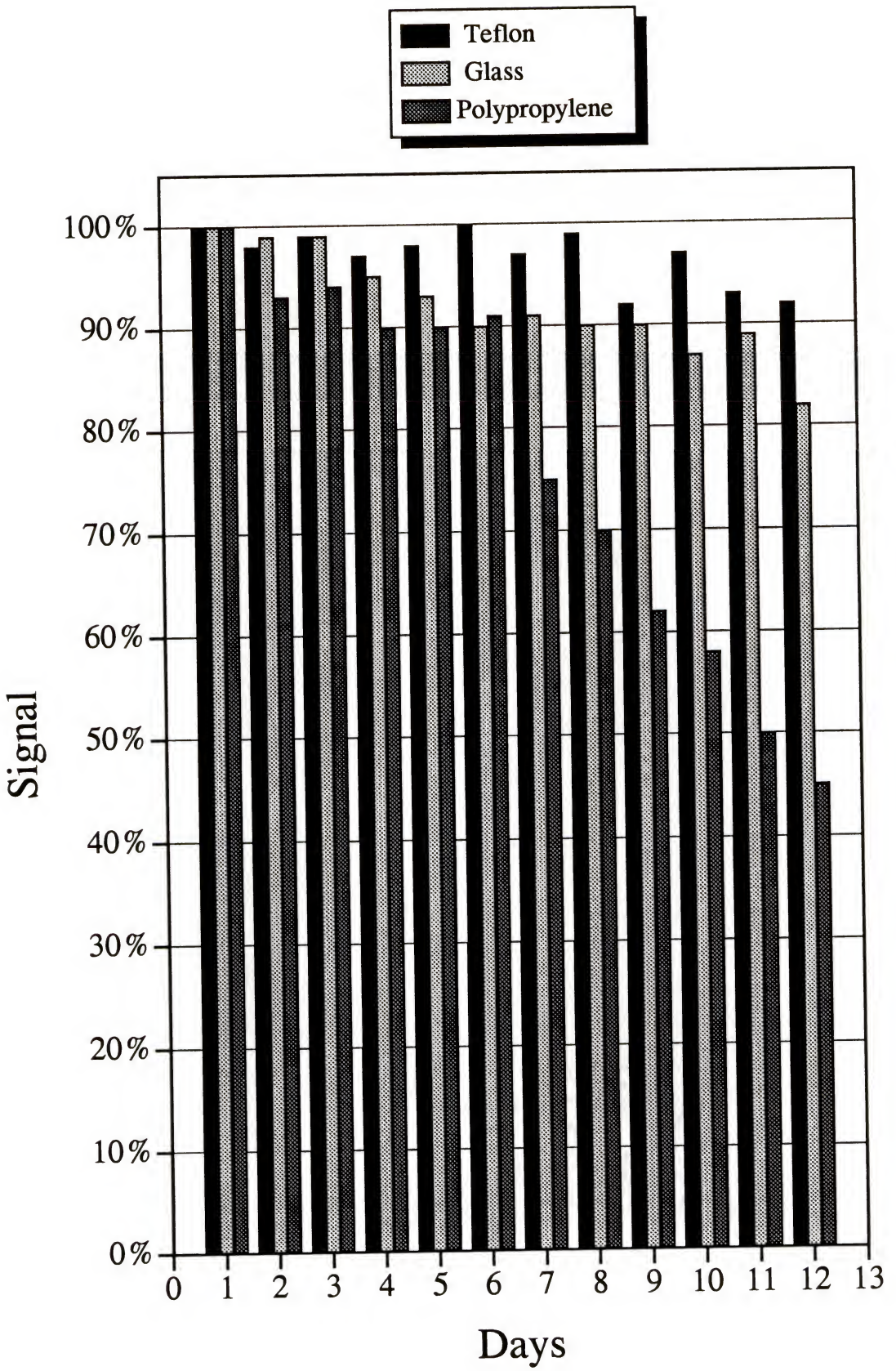
Teflon
Glass
Polypropylene
100%
90%
80%
70%
60%
50%
40%
30%
20%
10%
0%
Signal
0
1
2
3
4
5
6
7
8
9
10
11
12
13
Days

Figure 5-2: Mercury contribution to solutions from untreated pipet tips.

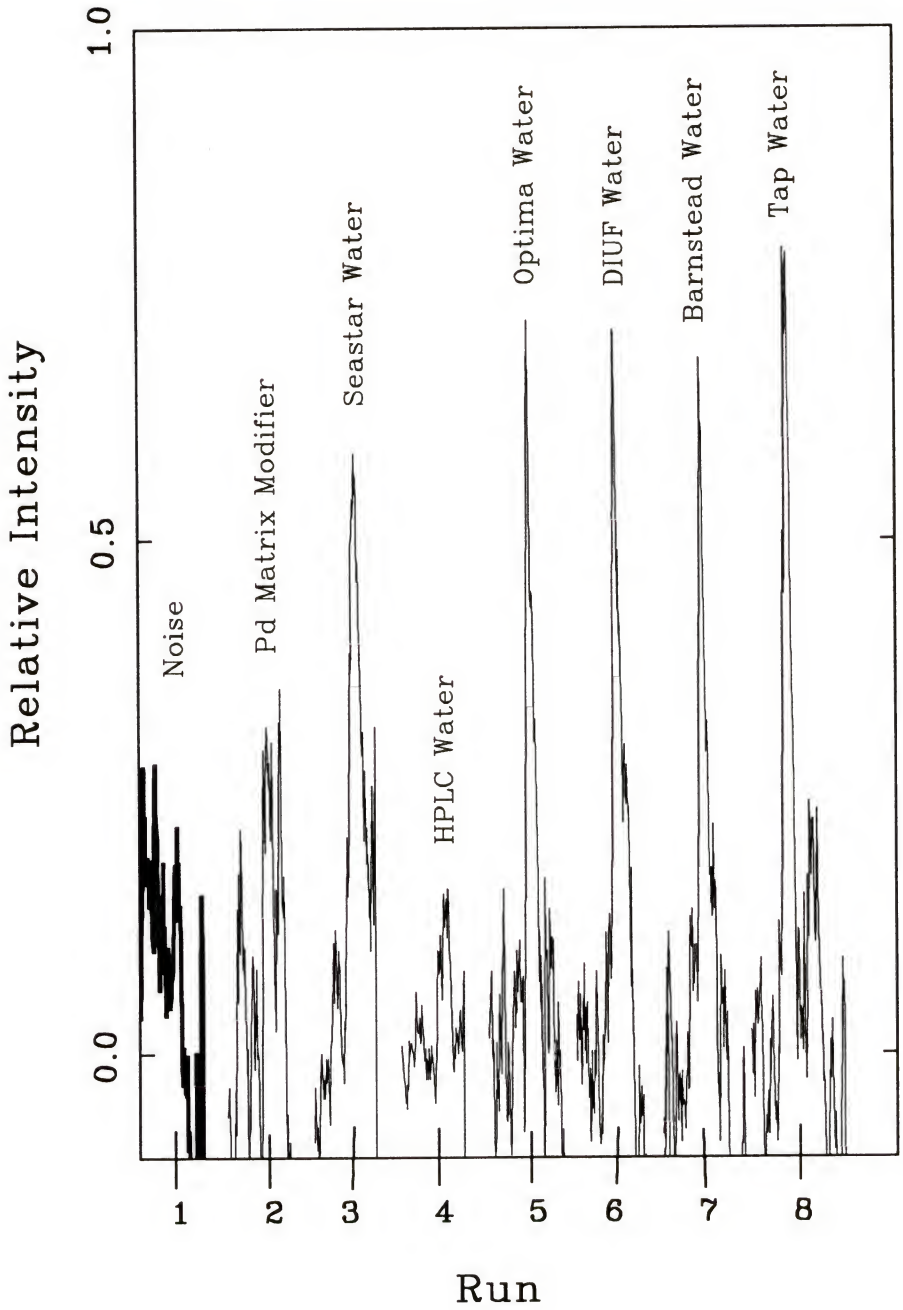
Relative Intensity
0.0
0.5
1.0
Noise
Pd Matrix Modifier
Seastar Water
HPLC Water
Optima Water
DIUF Water
Barnstead Water
Tap Water
1
2
3
4
5
6
7
8
Run

reduction in mercury signal from all samples relative to the previous results, with the Barnstead water showing virtually no mercury at all (Figure 5-3). Because of these studies, it was concluded that standard pipet tips can contribute to mercury contamination of samples. All subsequent preparations and analyses were performed with Fisherbrand Redi-Tips™ Trace Metal Certified Pipet Tips, which have a maximum mercury concentration of only 0.2 ng per tip.

The use of careful preparation techniques can lead to more accurate analyses as well as lower limits of detection. In trace element determinations, the blank sample is oftentimes the highest limiting factor contributing to the total background signal. In previous work, Resto[9] analyzed aqueous mercury standards by LEAFS-ETA and found that the best blank obtainable gave a signal equivalent to 1 ppb mercury. (Figure 5-4). From a calibration plot prepared in that work, the absolute instrumental limit of detection (LOD) was calculated as 9 pptr or 90 fg by extrapolating the linear curve two orders of magnitude past the blank signal value to the laser stray light background noise level. Because the blank value was so high relative to the instrumental background noise, it was difficult to evaluate with certainty how close this instrumental LOD could ever be approached even with improvement of the blank.

In this work, the analysis of aqueous mercury standards was repeated using the same LEAFS-ETA system, but the trace-certified pipet tips were used in the sample preparation. The calibration plot prepared from the results of the analyses showed that the blank value obtained was two orders of magnitude lower than the previous work by Resto (Figure 5-5). This lower blank allowed for the analysis of three more standard

Figure 5-3: Mercury contribution to solutions from pretreated pipet tips.

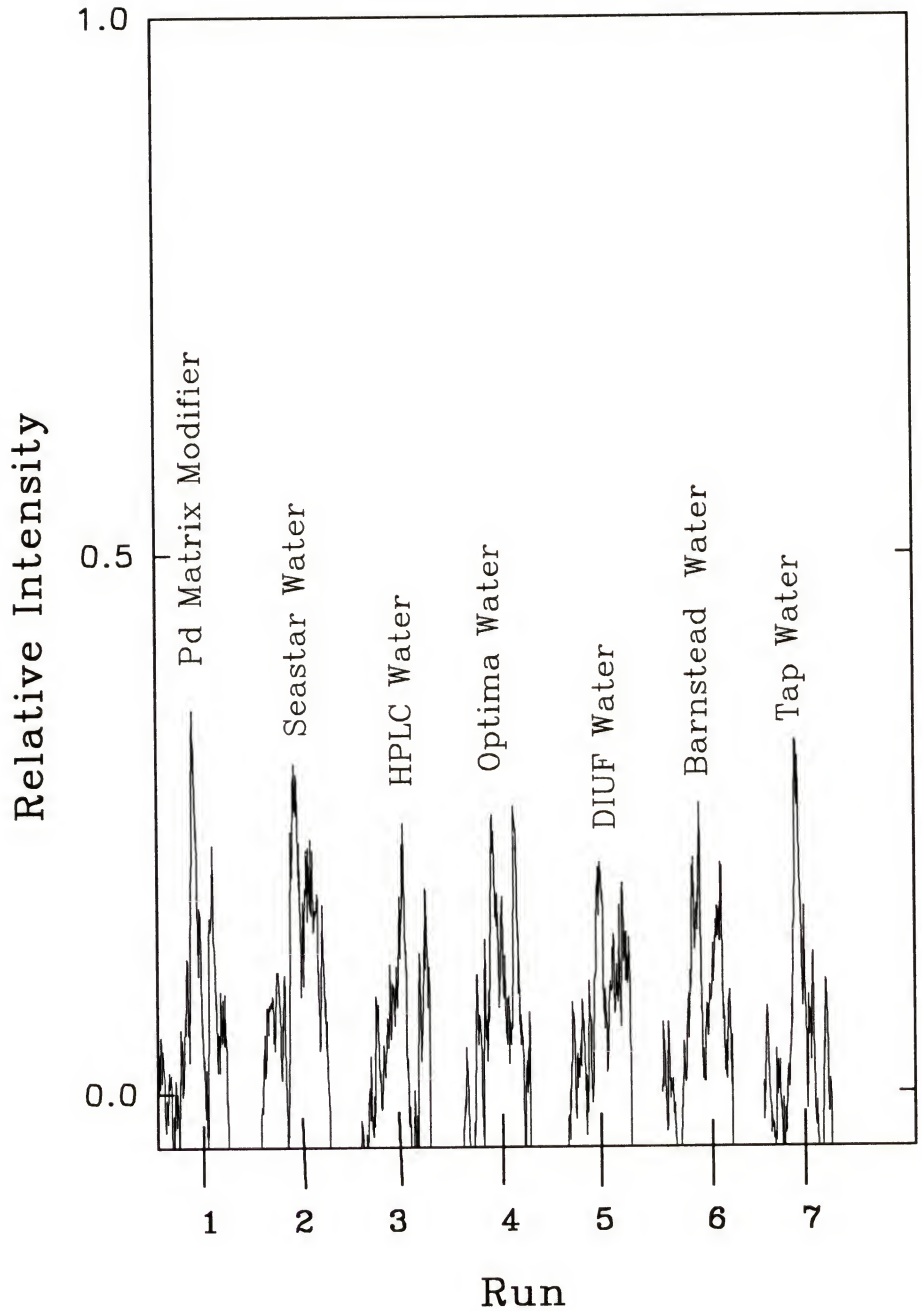
1.0
0.5
0.0
Relative Intensity
Pd Matrix Modifier
Seastar Water
HPLC Water
Optima Water
DIUF Water
Barnstead Water
Tap Water
1
2
3
4
5
6
7
Run

Figure 5-4: Calibration plot of aqueous mercury standards prepared with untreated pipet tips.

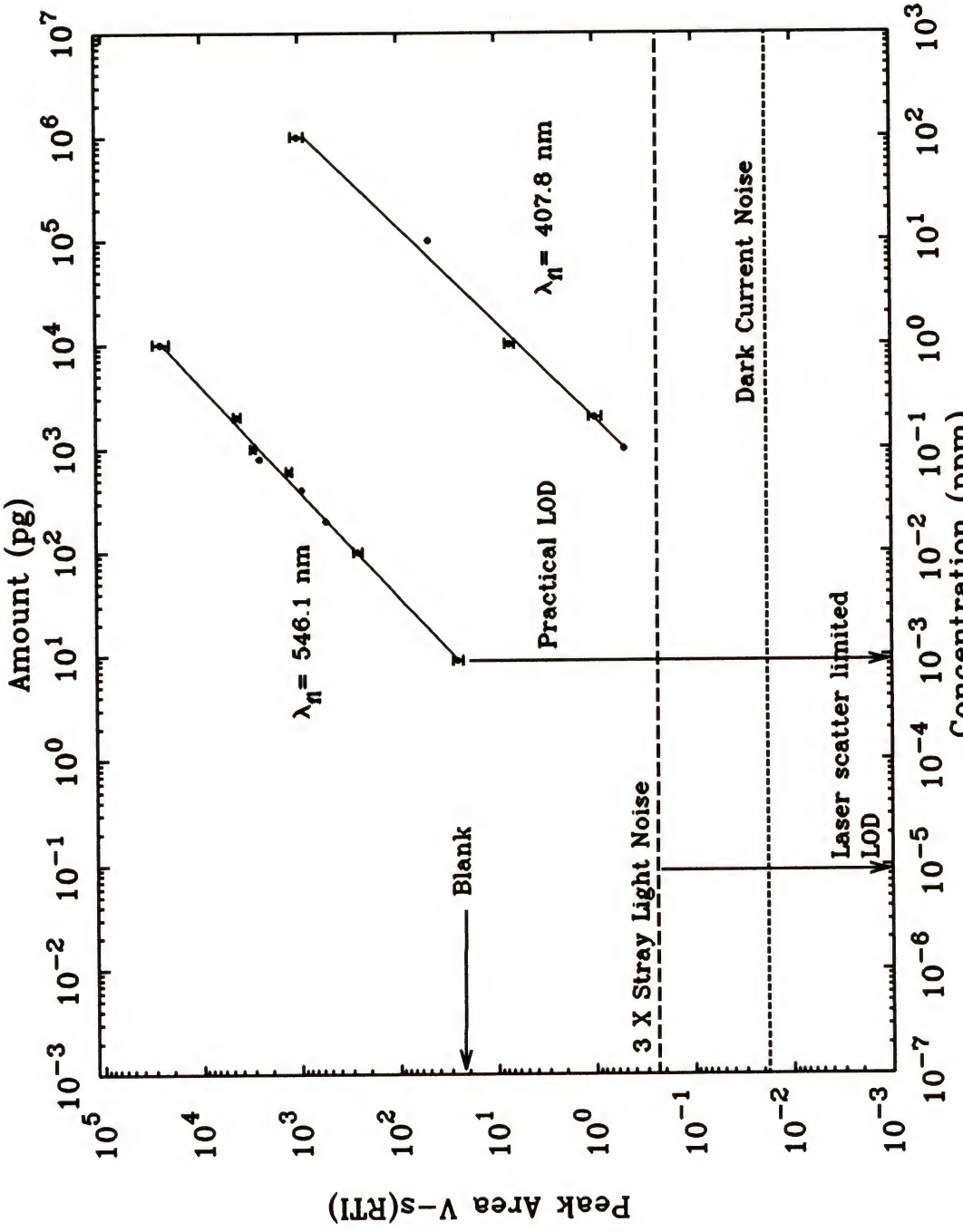
Amount (pg)
Concentration (ppm)
Peak Area V-s(RTI)
λn= 546.1 nm
λn= 407.8 nm
Practical LOD
Blank
3 X Stray Light Noise
Laser scatter limited LOD
Dark Current Noise

Figure 5-5: Calibration plot of aqueous mercury standards prepared with trace-certified pipet tips.

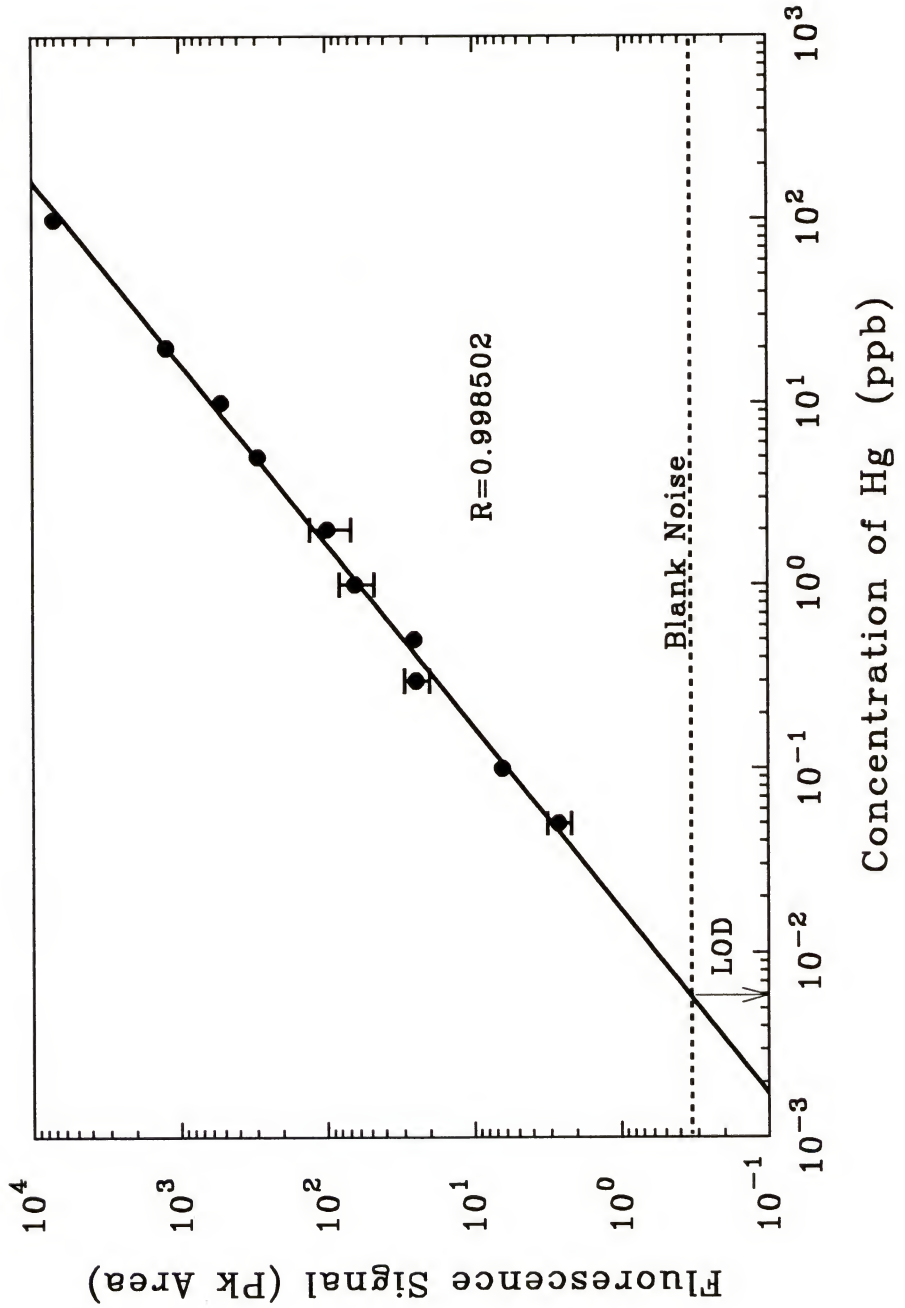
Fluorescence Signal (Pk Area)
Concentration of Hg (ppb)
R=0.998502
Blank Noise
LOD
10^{4}
10^{3}
10^{2}
10^{1}
10^{0}
10^{-1}
10^{-3}
10^{-2}
10^{-1}
10^{0}
10^{1}
10^{2}
10^{3}

solutions between 1 ppb mercury and 50 pptr mercury, and proved the validity of Resto's calculated instrumental detection limit. The instrumental LOD in this work was found to be 6 pptr.

For the determination of mercury in real samples, the solid matrix may either be analyzed directly or it must first be digested and properly prepared. The solid and digestion preparation techniques for soil samples analyzed in this work is discussed in the remainder of this chapter.

Solid Sampling

The sample may be analyzed directly in its solid form if the instrumentation is designed for this capacity. With this type of approach, sample preparation is kept to a minimum in order to reduce possible contamination. Bendicho and de Loos-Vollebregt[48] have thoroughly reviewed solid sampling in electrothermal atomic absorption spectrometry (ET-AAS), and a detailed discussion will not be given here.

Two important parameters in solid sampling is producing a homogenous sample and reducing background matrix effects. Particle size determines homogeneity of the solid sample and has a large influence on the precision and accuracy of the determination; therefore, grinding the sample in a mill may be necessary and is acceptable for soil sample matrices.

Background matrix effects will often interfere with the analysis by producing a large signal that encompasses the analyte signal. Typically, this interference is surmounted by ashing the matrix at a temperature that will burn as much of the

background away as possible without losing any analyte. Ali et al.[49] have shown that direct solid sampling in a tube-cup furnace with AAS has proven to be an accurate, precise, and rapid method of analysis for Pb, Zn, and Mn in standard reference materials (SRMs).

In the case of mercury in soil, however, ashing is a difficult task due to the volatility of the analyte. Figure 5-6 illustrates that the maximum ashing temperature possible for the soil samples without losing a significant amount of mercury is approximately 150 °C. Figure 5-7 depicts the signal obtained from directly analyzing 5 μg of SRM 8406 (60ng/g Hg in River Sediment) in a L'Vov platform graphite furnace using LEAFS and an ashing temperature of 130 °C. Another sample of SRM was then baked at 170 °C for four hours to vaporize the mercury, and then analyzed as described above to observe the portion of the signal due to the background matrix (Figure 5-8). The signals in both cases were virtually the same, indicating that the background matrix was not sufficiently diminished at the maximum ashing temperature to observe the mercury signal, and solid sampling was not a viable preparation technique for the determination of mercury in soil. Therefore, a dissolution method must be employed to digest the sample into a solution suitable for analysis.

EPA Series Method 245.5

As stated in Chapter 1, Cold Vapor Atomic Absorption Spectrometry (CVAAS) is the most commonly used method of mercury analysis in soil. According to the Guide to Environmental Analytical Methods[50], there are three EPA methods available for the

Figure 5-6: Optimization of ashing temperature for SRM 8406.

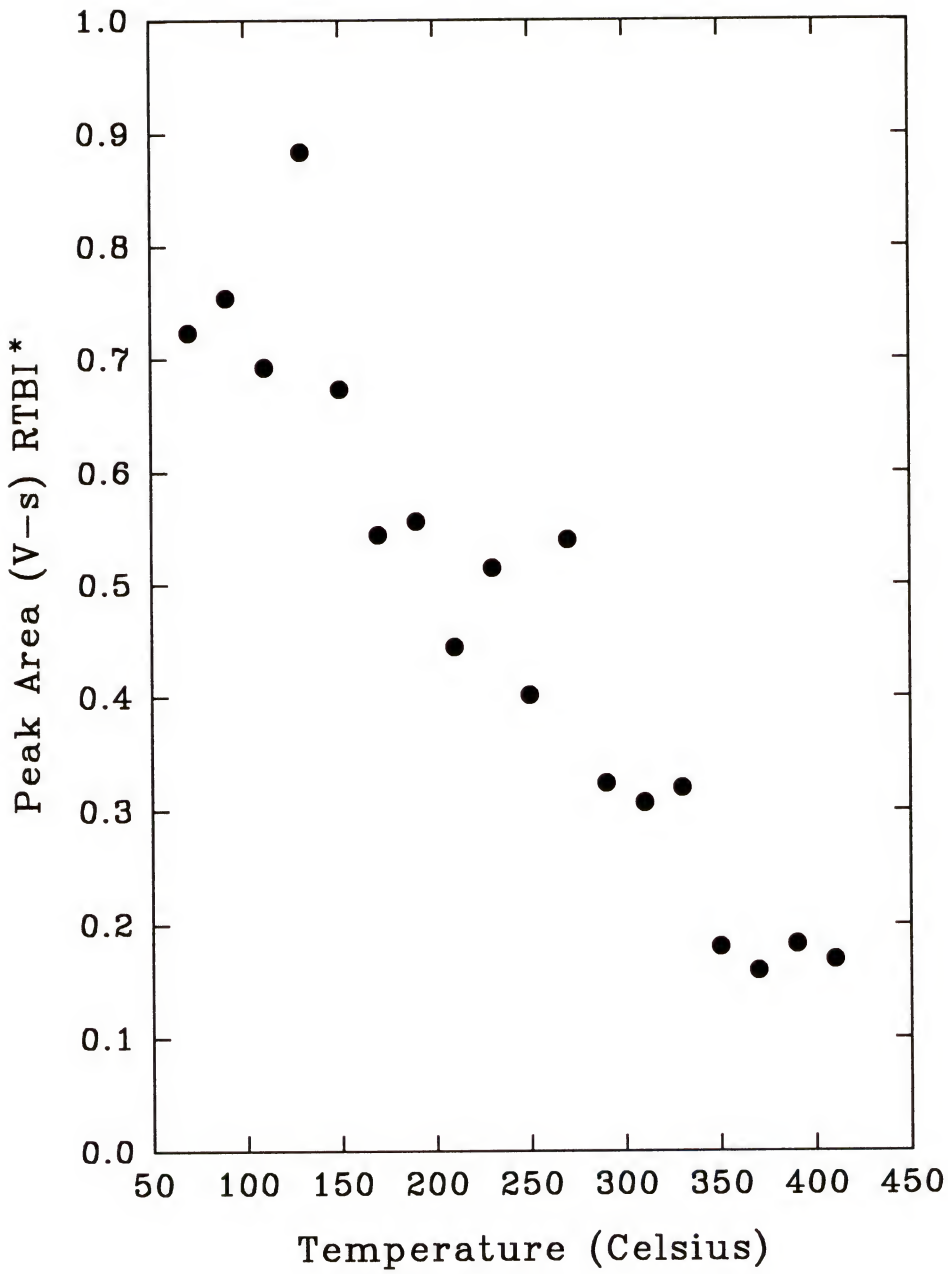

* RTBI = relative to boxcar intensity

Figure 5-7: Signal of SRM 8406 obtained through solid sampling.

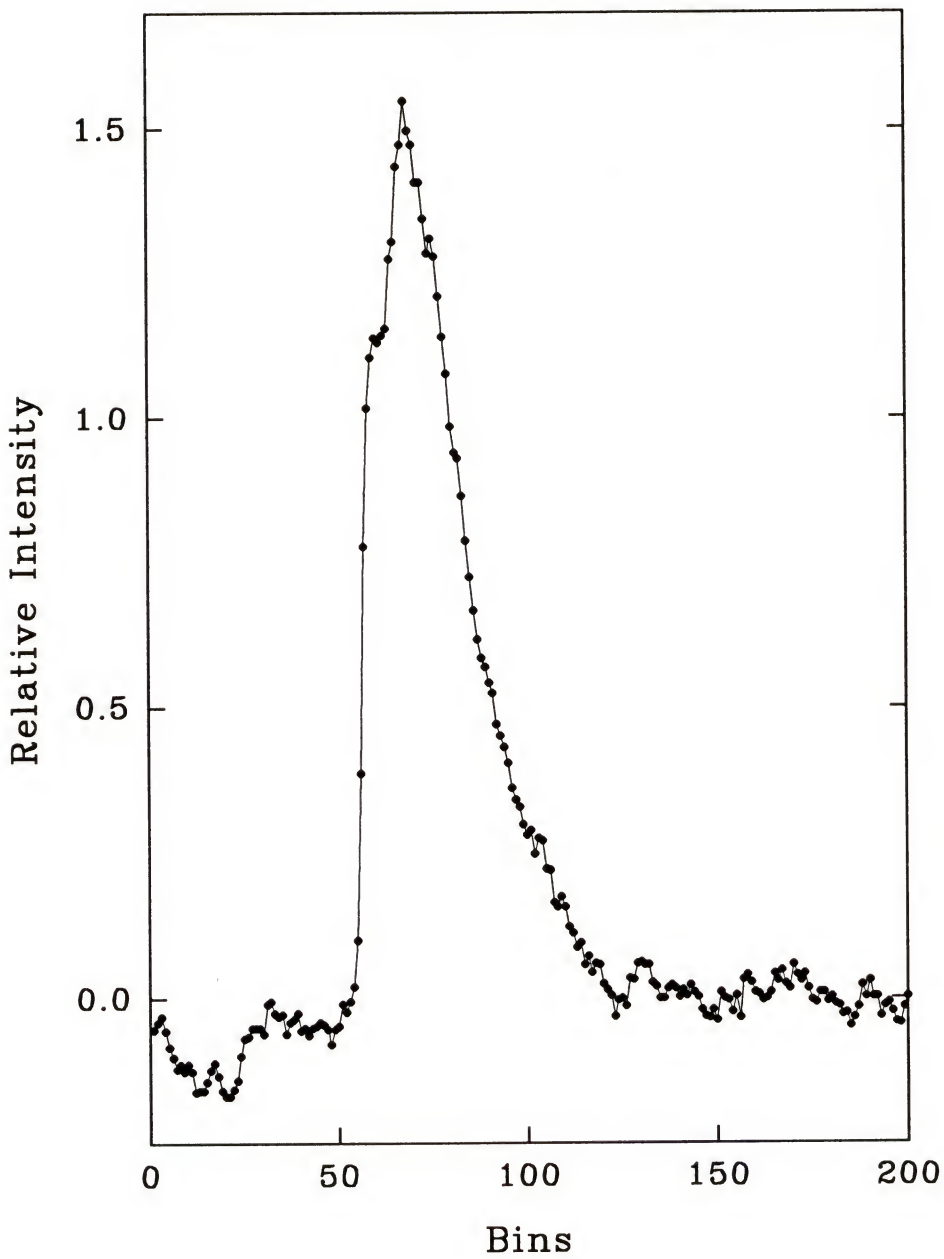
Relative Intensity
1.5
1.0
0.5
0.0
0
50
100
150
200
Bins

Figure 5-8: Signal of SRM 8406, after baking mercury analyte off, obtained through solid sampling.

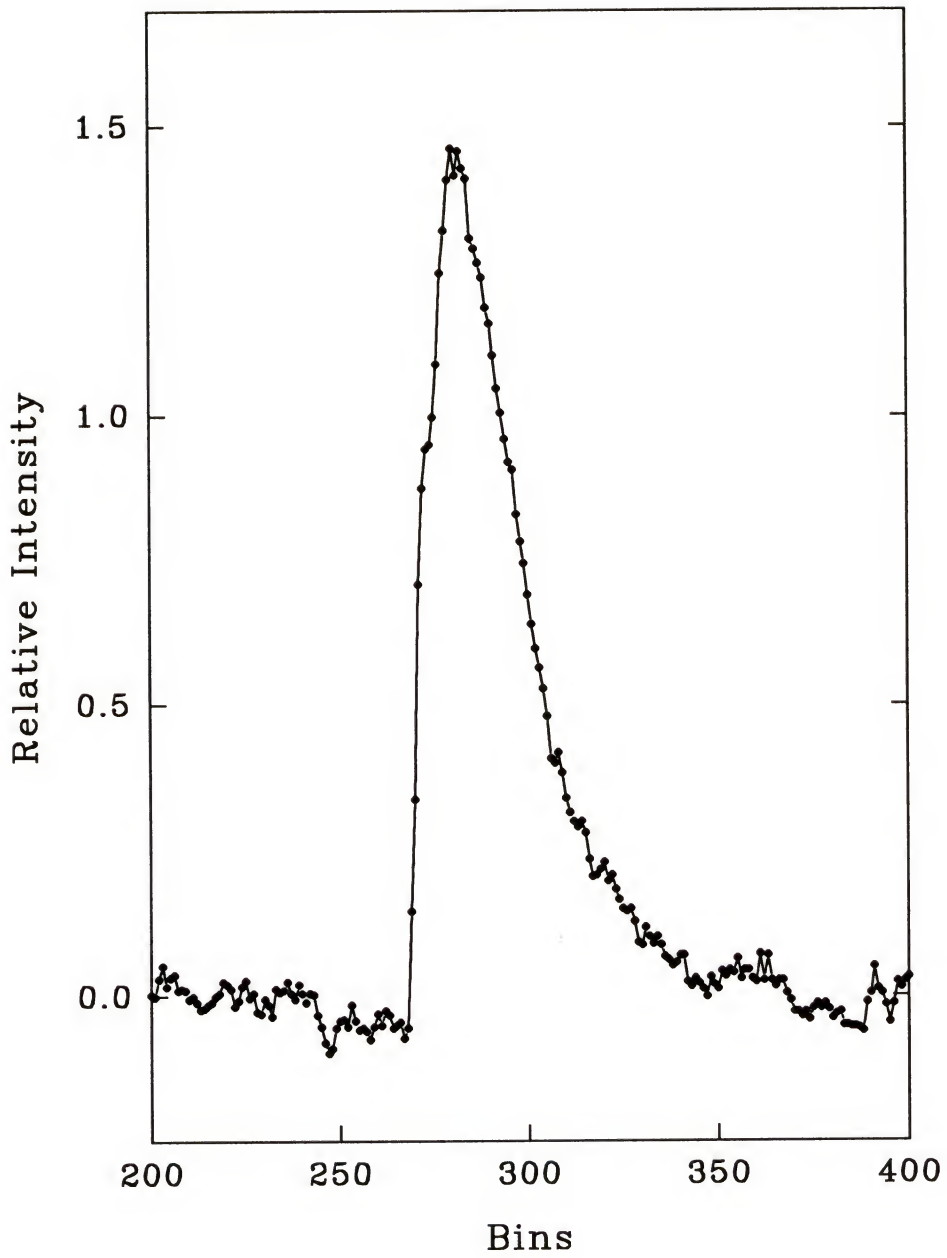
1.5
1.0
0.5
0.0
Relative Intensity
200
250
300
350
400
Bins

preparation of soils and sediments for mercury analysis by CVAAS. They are SW-846 Method 7471, EPA Series Method 245.5, and CLP Inorganic SOW for mercury, and they differ principally in their calibration and QC procedures. In this work, EPA Series Method 245.5 was chosen as the method of soil digestion because the laboratory that was used to perform CVAAS on the soil samples was already set up to utilize that particular method.

The parameters that govern EPA Method 245.5 are as follows. The applicability of the method is for mercury determinations by CVAAS in drinking, surface, and saline waters, domestic and industrial wastes, soils, sediments, and sludges. The quality control standard is a performance sample test in which one blind sample is analyzed per year for mercury, and the results must be within EPA control limits. An optional check is the analysis of a known reference standard once per quarter for mercury. The method detection limit is 0.2 ppb mercury. With a sample volume of approximately 50 mL, this leads to an absolute method detection limit of 10 ng mercury. The expiration of stock standard solutions is not specified; however, the calibration standard solutions must be prepared fresh at the time of the analysis. The initial calibration requires six levels plus a blank. The continuing calibration mandates the analysis of a low-level standard daily or every twenty samples, whichever is more frequent. The %Recovery must be in the range of 90 to 110%. The accuracy and precision parameter requires the analysis of one duplicate sample per every ten samples or per batch of samples if they contain less than ten. Results must again be within EPA control limits. A blank must be used when

preparing a calibration curve, but the method blank is not specified. For the analyses in this work, a blank was analyzed per every ten samples.

For the digestion of the soil samples and SRM 8406 by EPA Method 245.5, seven reagents are added to approximately 0.25 g (dry weight) of sample.[51] Nine milliliters of ASTM Type II water is used to aid in the transfer of solid sample to a BOD digestion bottle. Two milliliters of nitric acid are added to prevent adsorption of sample to the vessel wall. Five milliliters of sulfuric acid and twelve milliliters of potassium permanganate are added to breakdown organics in the sample, including sulfides. Ten milliliters of potassium persulfate are added to assure the oxidation of difficult organic mercurials. After addition of these reagents, the vessel is capped and heated in a hot water bath at 96 °C for one to two hours. During this time as organic material decomposes, vapor builds up in the reaction vessel and is able to escape through a "burping" action. At the end of the required digestion time, the bottle is removed from the water bath and allowed to cool. Twelve milliliters of sodium chloride-hydroxylamine hydrochloride are then added to free any chlorine gas formed as a by-product of the permanganate oxidation step. In the final step, tin chloride is bubbled through the digested sample to reduce the oxidized mercury to elemental mercury for subsequent analysis of the vapor by CVAAS.

This sample preparation method is very time consuming and laborious. In addition, it utilizes many harsh reagents which can increase the likelihood of contamination to the sample and also contamination to the environment after the ensuing disposal.

Microwave Digestion

With the improvement of microwave digestion methods in the past few years, solid sample dissolution has exhibited reduction in systematic errors, reduction in decomposition time, reduction in reagent volume use, and reduction in overall preparation time compared to conventional, hot-plate wet oxidation methods.[52] Systematic errors are minimized because contamination is reduced by using a small volume of highly pure acid for the decomposition process in a closed vessel. The small reagent volume used decreases the amount of decomposition products produced, and the closed system reduces loss of analyte through volatilization and contamination from the atmosphere. Depending on the type of material being decomposed, microwave heating decreases the digestion time by a factor of three to fifteen.

Currently, there is no EPA-approved microwave sample digestion method for mercury in soils and sediments. Several researchers and industrial companies have formulated their own methods, but each is based on the specific properties of the sample analyzed and the instrumentation used. In this work, a prescription-based microwave acid digestion method is formulated for the determination of mercury in soil and sediment samples, and closely follows the quality control and calibration guidelines of established EPA methods.

Theory

A detailed description of the mechanisms by which microwave radiation interacts with solvents and samples is given by Kingston and Jassie.[53] The range of microwave

radiation spans from 300 to 300,000 MHz. In accordance with the International Radio Regulations adopted in Geneva in 1959, the Federal Communications Commission established four microwave frequency bands for industrial, scientific, and medical use. Of these bands, 2450 $\pm$ 13 MHz is the most commonly used frequency and is the frequency of all home microwave units. The heating of a sample by microwave energy is dependent upon the absorptive polarization and ionic conductance of the medium.

Absorptive polarization is due to the molecular dipole rotation and accompanying intermolecular friction that occurs in molecules possessing a significant dipole moment. The principles of the heating that occurs are governed by dielectric loss theory. According to this theory, as microwave energy penetrates a sample, there is loss of energy from the electromagnetic field to the sample at a rate dependent upon the sample's dissipation factor. The dissipation factor is a ratio of the sample's dielectric loss factor to its dielectric constant and is expressed as

$$\tan\delta = \frac{\epsilon''}{\epsilon'} \qquad \text{(Equation 5-1)}$$

where $\tan \delta$ = dissipation factor

ϵ'' = dielectric loss factor

ϵ' = dielectric constant

The dielectric loss factor measures the sample's ability to dissipate microwave energy as heat to the sample, and it depends on frequency and temperature. The dielectric constant, on the other hand, measures the sample's ability to obstruct microwave energy as it tries to penetrate. The larger the dissipation factor is, the greater the sample's

ability to convert electromagnetic energy into heat energy at a given frequency and temperature. Samples that possess a sizeable dipole moment and are free to rotate are likely to have large dissipation factors. This is illustrated by the dissipation factors of water as a liquid and as ice of tan $\delta = 0.1570$ and tan $\delta = 0.0009$, respectively. Teflon PFA has a tan δ of 0.00015, making it virtually transparent to microwave energy, hence its advantage for use as digestion vessel material. Tables of dissipation factors for various substances have been constructed and are readily available for consultation.[54]

Ionic conductance is the second parameter influencing the efficiency of microwave heating. In an applied electromagnetic field, a conductive migration of dissolved ions occurs. This migration produces a current flow that results in IR losses, or heat transfer, due to resistance to the ion flow. The magnitude of current produced by an ion depends on its relative concentration and mobility in the system. Therefore, losses due to this ion migration depend on the size, charge, and conductivity of the ions, as well as their interaction with the solvent molecules. As the ion concentration increases, so does the current, and therefore the heat transfer, because of the greater mobility of the ions.

Temperature is essentially the limiting factor controlling whether absorptive polarization or ionic conductance has the greatest influence on the conversion of microwaves to heat energy. For small molecules, the dielectric loss to a sample from dipole rotation decreases as the sample temperature increases. However, dielectric loss from ionic conductance increases with temperature. Therefore, when heating a microwave-active sample, dipole rotation initially dominates the conversion of microwave radiation to heat, but then ionic conductance dominates at higher temperatures.

Conventional wet oxidation methods of digestion, such as EPA Method 245.5, can take one to two hours or longer to be completed. With microwave heating, digestion can be complete in as little as five minutes. This time difference is due to the relative modes of their sample heating schemes. In conventional methods, the digestion vessel must be conductively heated by a hot plate or hot water bath. After the vessel begins absorbing heat, it must transfer this heat to the sample inside. Convection currents then form in the solution, producing a temperature gradient as vaporization at the liquid surface begins. Therefore, only a small portion of the solution is at equilibrium with the applied heat temperature. These processes increase the time necessary to reach and maintain the boiling point of the acid solvent. In microwave heating, on the other hand, the microwaves travel through the transparent vessel and couple directly to the solvent. This means that, for typical analytical sample sizes, all of the sample and solvent is heated simultaneously. In a closed-vessel system, the boiling point of the acid solvent can be reached in under one minute.

Miller-Ihli[55] superficially compared the method kinetics of a hot-plate digestion to a closed-vessel microwave digestion to illustrate how the higher temperatures obtainable with microwave-assisted digestion increased the reaction rate of the system and decreased digestion time. The Arrhenius empirical relationship given below

$$\frac{\partial \ln k}{\partial T} = \frac{E_a}{RT^2} \qquad \text{(Equation 5-2)}$$

can be written in the integrated form as

$$\frac{k_2}{k_1} = \frac{E_a}{R}\left(\frac{1}{T_1} - \frac{1}{T_2}\right) \qquad \text{(Equation 5-3)}$$

where k = rate constant

T = temperature

E_a = Arrhenius activation energy

R = gas constant

Under most circumstances, the reaction rate increases exponentially with increasing temperature. Microwave digestions are typically carried out at 175 °C; whereas, hot-plate digestions only reach approximately 95 °C. Assuming a nominal activation energy of 80 (kJ/mole), Equation 5-3 yields a rate constant at 175 °C that is 107 times greater than that at 95 °C, and the difference increases with higher activation energies. According to these figures, a digestion that takes five minutes using microwave heating would theoretically take nearly nine hours using a hot plate.

Instrumentation

Microwave oven unit

The key parts of a microwave unit consist of the magnetron, wave guide, mode stirrer, cavity, turntable, and circulator (Figure 5-9).[52] The magnetron produces the microwave energy and is constructed of a cylindrically oriented cathode and anode (Figure 5-10). A magnetic field aligned with the interior cathode is superimposed on the entire diode. The anode contains a ring of mutually coupled resonant cavities. As a

Figure 5-9: Schematic diagram of a microwave instrument unit.

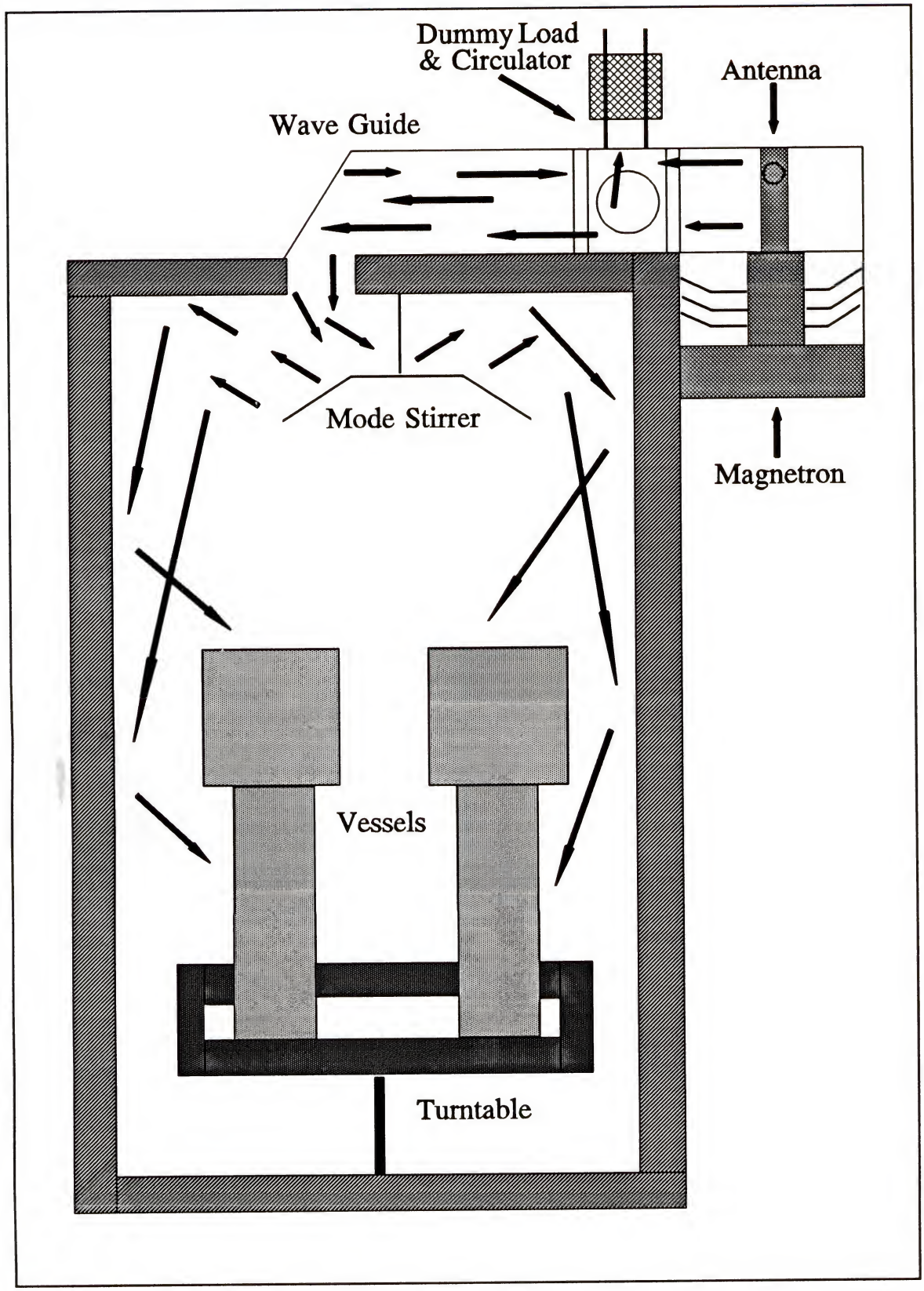
Dummy Load
& Circulator
Antenna
Wave Guide
Mode Stirrer
Magnetron
Vessels
Turntable

Figure 5-10: Magnetron components.

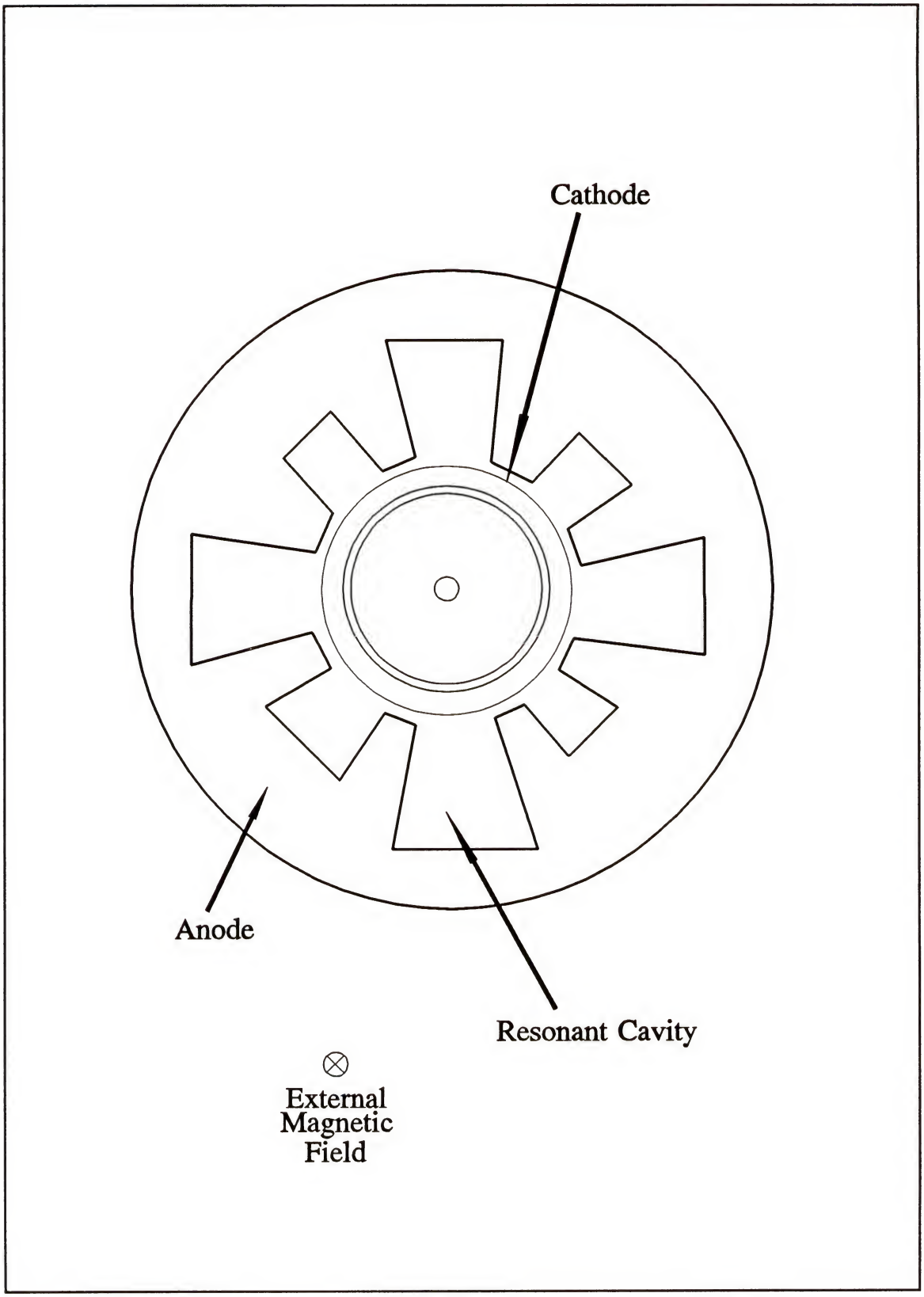
Cathode
Anode
Resonant Cavity
External
Magnetic
Field

potential forms across the diode, electrons are released. The magnetic field induces the electrons to resonate, causing the magnetron to oscillate. An output antenna transmits the energy produced by the oscillating electrons at a fixed frequency to the wave guide cavity. The wave guide is constructed of reflective material and is designed to direct the microwaves to the internal cavity without allowing the wave to be reflected back. At the exit terminal of the wave guide is a fan-shaped blade called the mode stirrer that is used to reflect and mix the energy pattern as it enters the microwave cavity. This allows for a more even distribution of the energy so sample heating approaches independence from positioning. A turntable in the cavity rotating at a minimum of three revolutions per minute is also used to maximize independence of sample positioning. Once the microwaves enter the cavity, they are reflected from wall to wall until all of the energy of the waves has been absorbed by an absorbing material in its path. If the cavity walls are made of metal, they must be protected from corrosion by acid vapors. This is usually accomplished by spraying a Teflon coating on the walls. Sometimes the reflected microwaves may bounce back inside the wave guide and reach the magnetron. The magnetron can be damaged or destroyed by the dissipation of heat from these waves. Therefore, a terminal circulator is usually installed in the wave guide after the output antenna. This component uses ferrites and static magnetic fields to allow microwaves to pass through it in the forward direction but divert reflected reverse microwaves to a dummy load which absorbs the dissipated heat.

The power output of the magnetron is controlled by a process known as cycling. The duty cycle is defined as the time the magnetron is on divided by its time base. The

time base of a modern laboratory microwave oven is 1 s. Most home microwave ovens have a time base of 10 s. This means that for a 50% duty cycle, the laboratory unit would be on for 0.5 s and off for 0.5 s; whereas, the home unit would be on for 5 s and off for 5 s. When heating samples over an extended period of time, a larger time base may cause uneven heating by producing temperature spikes in the sample. Some of the differences between industrial or laboratory microwave ovens and home appliance microwave ovens are compared in Table 5-1.

The power output of the magnetron must be calibrated for each unit in order to be able to transfer digestion methods from one instrument to the next. Equations used for power measurement are derived from elementary heat capacity theory of a given mass at constant pressure.[53] The apparent power output of the magnetron is indirectly determined by measuring the rise in temperature of a quantity of water large enough to absorb all of the energy delivered to the microwave cavity for a given period of time. Usually, one kilogram of water heated at each power level of the unit for two minutes will accomplish this goal. The relationship for evaluating the apparent power is given by

$$P_{absorbed} = \frac{KC_p m \Delta T}{t} \qquad \text{(Equation 5-4)}$$

where P = apparent power absorbed (W)

K = conversion factor for calories per second to watts (4.184 J/cal)

C_p = heat capacity (cal/g · °C)

m = mass of sample (g)

ΔT= final temperature minus initial temperature (°C)

t = time (s)

Deviations from this theoretical equation can occur due to heat loss from the sample vessel to the cavity or, in the case of home microwave ovens unequipped with circulators, from reflected microwaves on the magnetron which can change its output. All ten power levels of the microwave unit used in this work were calibrated using Equation 5-4, and the results are shown graphically in Figure 5-11.

Once the power of the unit has been calibrated, Equation 5-4 can then be used to predict conditions about the digestion. By a simple mathematical transformation of Equation 5-4, the final temperature reached for a sample digested at a certain power for a given time can be calculated using the expression

$$T_f = T_i + \frac{Pt}{KC_p m} \qquad \text{(Equation 5-5)}$$

if the heat capacity of the acid reagent is known. Also, the time of exposure necessary to reach a final temperature can be predicted according to

$$t = \frac{KC_p m \Delta T}{P} \qquad \text{(Equation 5-6)}$$

These thermodynamic relationships hold true for $\Delta T \leq 140$ °C and $t \leq 2$ minutes, after which thermal loss through the vessel wall creates deviations. By using these equations,

Table 5-1

Features of Laboratory vs. Home Microwave Oven Units

Parameter	Industrial Grade	Home Grade
Magnetron time base	1 second	10 seconds
Circulator	Yes	No
Mode stirrer	Yes	Yes
Pressure control	Yes	No
Temperature Control	Yes	No
Isolated electronics	Yes	No
Protected cavity	Yes	No
Safety interlocks	Good	Fair
Safety shield	Yes	No
Cost	$14,000	$100

Figure 5-11: Calibrated power of the microwave oven.

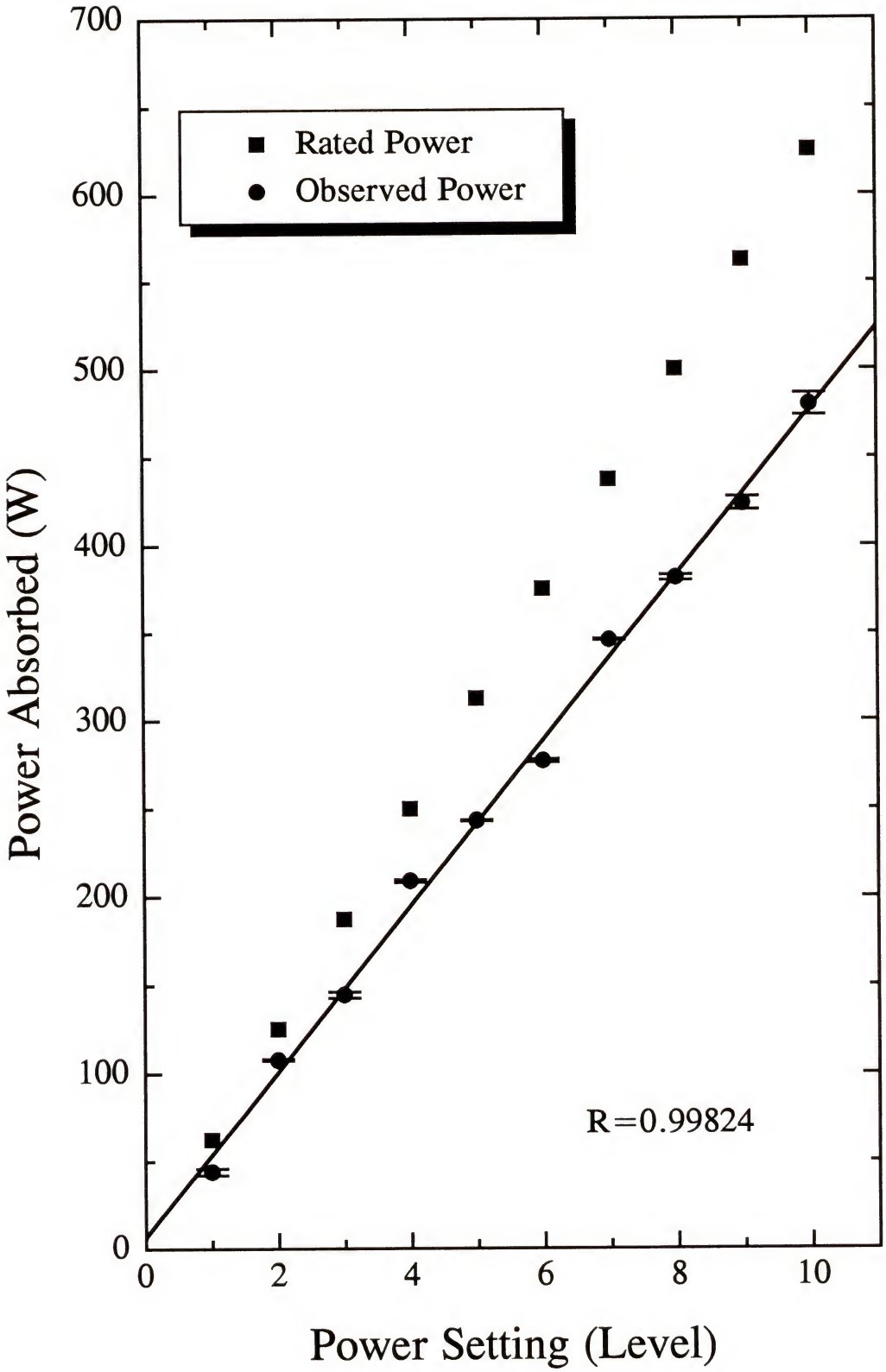
Rated Power
Observed Power
R=0.99824
Power Absorbed (W)
Power Setting (Level)
0
100
200
300
400
500
600
700
0
2
4
6
8
10

the investigator can make educated approximations for initial parameters of power and exposure time necessary for a given digestion. Experimental results will then dictate the final conditions required.

Microwave acid digestion vessel

The high-pressure microwave vessels used in this work were manufactured by Parr Instrument Company.[56] A schematic diagram of the vessel is shown in Figure 5-12. The greatest advantage of using a high pressure closed-vessel system is the rapid decomposition of the sample due to increased oxidation potentials that the acid reagent has when temperatures extend above the normal boiling point of the acid. Also, intermediate reactive products may form at high temperatures, causing some reactions to occur in a high-pressure closed vessel that would not occur under conventional wet oxidation conditions. The complete vessel consists of an inner Teflon sample cup surrounded by a hard polymeric outer casing that is microwave transparent. Teflon is an ideal choice for the sample cup because it is inert to strong acids and high temperatures, as well as transparent to microwaves. It does, however, contain two disadvantages that must be considered when performing the digestions. First, Teflon can creep or flow when subjected to high pressure or load. At temperatures below 150 °C, this difficulty will be negligible, but at higher temperatures this tendency increases and makes it difficult to maintain tight seals. Secondly, Teflon is somewhat porous allowing small neutral molecules to pass through it. Parr has minimized these imperfections by molding their parts from virgin Teflon at optimum pressure. The Parr bombs incorporate replaceable Teflon O-rings that create a tight seal between the inner top rim of the

Figure 5-12: Schematic diagram of a Parr high-pressure acid digestion vessel.

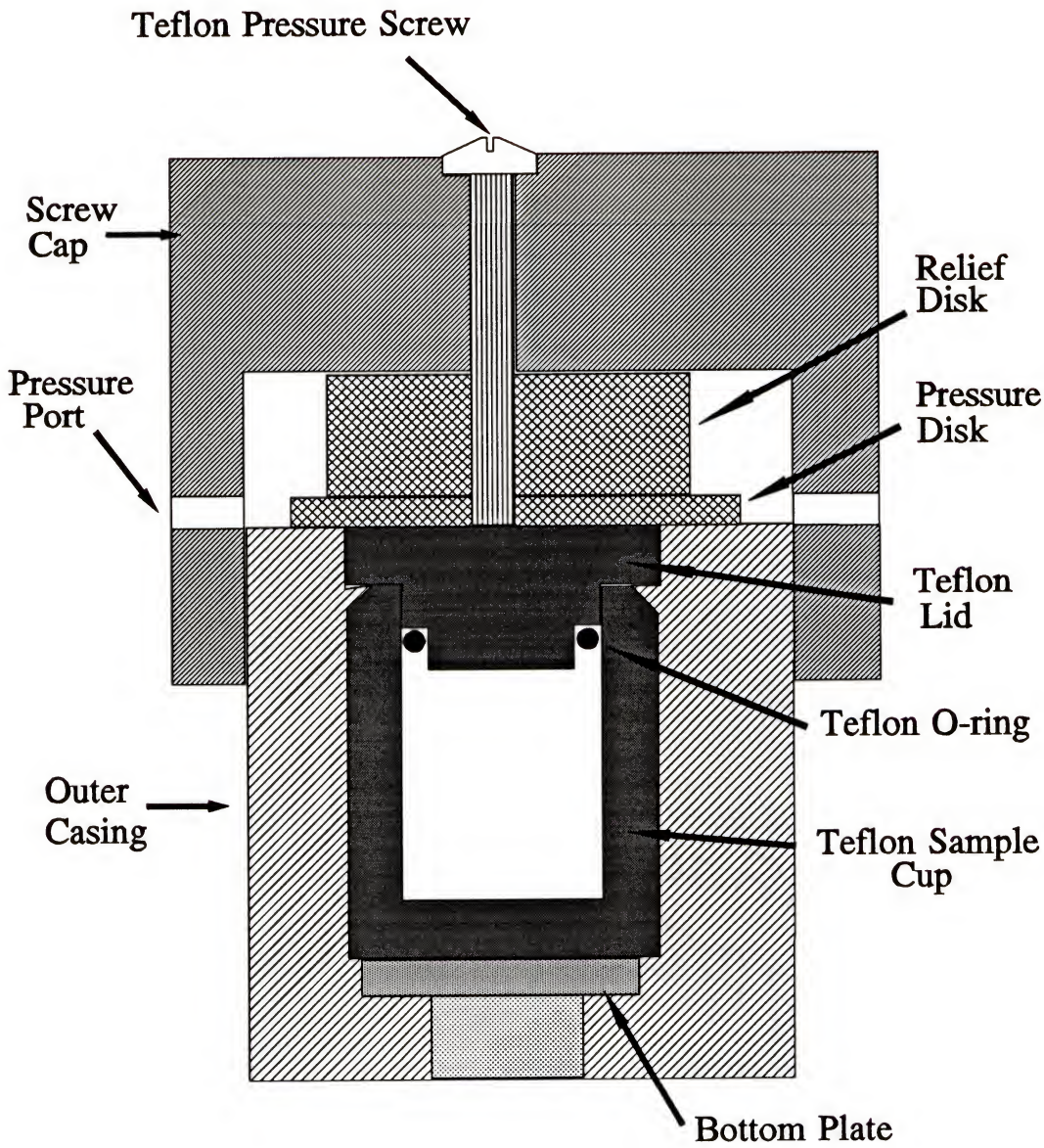
Teflon Pressure Screw
Screw Cap
Relief Disk
Pressure Port
Pressure Disk
Teflon Lid
Teflon O-ring
Outer Casing
Teflon Sample Cup
Bottom Plate

sample cup and its cap when the polymer outer jacket is screwed into place. If the pressure inside the vessel exceeds the maximum allowable value, the O-ring becomes distorted and excess gas pressure can escape from the sample cup by compressing a puck-shaped disk above the sample cup cap and venting through four outlets located at 90° intervals around the top outer jacket's circumference. The retaining screw can serve as a crude pressure indicator by noting the extent of its protrusion from the screw cap. The head of the screw extends approximately 1/32 inch from the flush position for each 500 psi pressure increase within the bomb. After overpressurization occurs, the Teflon O-ring must be replaced. Although the vessel is designed to withstand 80 atm of pressure, potential hazards that could lead to total destruction of the bomb must be addressed. If excessive temperature develops, the vapor pressure of the solvents in the bomb increases, and the integrity of the outer shell decreases as heat is transferred from the inner cup to the outer jacket. Excessive pressure build-up can be caused by this type of overheating, but it may also form from uncontrolled reactions that produce gas themselves. Organic materials liberate a substantial amount of gas and heat upon decomposition, and are more susceptible to causing runaway reactions. Also, if the bomb is physically overloaded, there may be insufficient head space for the expanding vapor, and the resulting pressure build-up may destroy the bomb. This illustrates the importance of strictly adhering to loading limits for organic and inorganic samples in order to safely use the bomb. The loading limits for the 23 mL volume microwave digestion bombs used in this work are 0.1 g of sample and 3 mL of reagent for organics and 1.0 g of sample and 15 mL of reagent for inorganics. Some organic samples, such

as fats, fatty acids, and glycerin, should not be treated with nitric acid in these bombs because explosive nitro compounds may be produced upon digestion. Also, perchloric acid is too unpredictable to be used safely.

History of Microwave Digestion Methods

In the past two decades, many researchers have investigated the use of microwave ovens to assist in sample digestion procedures. In 1975, Abu-Samra and co-workers[57] were the first to report on the use of microwave heating for rapid digestion of biological standard reference materials. Their standards were wet-digested with nitric and perchloric acids in open Erlenmeyer flasks, and the acid fumes were vented to a fume scrubber. Although sample preparation in closed containers has been carried out since the days of Carius in 1860[58], the use of closed-vessel digestion bombs did not enjoy widespread use until the 1980's when improvements in the designs of vessels caused the advantages of closed-vessel digestions to finally outweigh the hazards.[59]

In 1986, Kingston and Jassie[60] reported the digestion of biological and botanical standards in closed Teflon PFA vessels using microwave energy. They also described the modifications of the microwave equipment that allowed for computer-controlled pressure and temperature regulation and feedback. In 1987, Kingston[61] began developing EPA Method 3051, which is a microwave digestion method for Al, As, Ba, Be, Ca, Cd, Co, Cr, Co, Fe, K, Mg, Mn, Mo, Na, Ni, Pb, Se, Tl, V, and Zn in soils, sediments, and sludges. Kingston showed that the proposed method gave faster and more reliable digestions than the parallel hot-plate EPA Method 3050, and in 1991 a collaborative study proved the high degree of precision and accuracy of the method.[62]

The feasibility of home microwave use for digestions was illustrated by Mateo and Sabaté.[63] The modifications made to a home microwave unit used to digest vegetable samples was discussed. Most notably, all interior surfaces of the oven, including electronics and lamps, were protected from possible acid fume leakage by spraying them with a synthetic lubricant containing Teflon particles.

Industrially, the CEM Corporation proposed to the EPA the use of a microwave digestion procedure formulated for thirteen non-volatile elements in domestic and industrial wastewaters.[64] They also have digestion procedures outlined for soils and sediments. Although there still does not exist an EPA-approved microwave digestion method suitable for the determination of mercury in soils and sediments, it is becoming clear by the number of applications that many individual laboratories have their own specific procedures for digestion of various matrices for the analysis of particular elements.

Microwave Digestion Procedure for the Determination of Mercury in Soil

When formulating a new method for microwave-assisted acid digestion of a sample, the general procedure information should include sample type and size, vessel type and size, number of samples simultaneously processed, reagent specifications, preparation of blanks and standards, quality control measures, and microwave power requirements.

Microwave power requirements may be categorized according to whether the method is prescription-based or performance-based.[61] A prescription-based method

establishes compliance by following specific settings, and the analyst must reproduce the settings to achieve similar results. The parameters in this type of method are simply power and time. A sample is heated at a certain power for a given time. The reaction conditions and mechanisms during digestion are not controlled. Because of the different heat loss characteristics of assorted vessels, the prescription settings must be established for each particular vessel type in order to be able to reproduce the temperature profile of a digestion. In contrast, performance-based methods establish compliance by meeting performance criteria whereby actual reaction conditions are reproduced. The reaction mechanisms of the digestion must be controlled, and the parameters in this type of method are temperature, pressure, and time. For example, in this type of method, it would be specified to take the reaction up to 175 °C and maintain that temperature for five minutes. Performance methods are advantageous in that any microwave cavity that meets scientific specifications and can monitor those parameters will be able to reproduce the conditions necessary for digestion in any type of vessel. Pressure and temperature feedback is available in laboratory-grade microwave systems, and computers can be programmed to monitor the pressure and temperature inside the vessel and alter the power output of the magnetron to maintain specified conditions.

In this work, the proposed method of a microwave-assisted acid digestion of soil for the determination of mercury established the following criteria and procedures. The sample set consisted of air-dried soil collected from a marshy region of the Florida Everglades. No more than 0.25 g of sample was digested in one vessel due to the uncertainty of its organic content and possible side reactions possible causing excessive

pressure formation. The digestion vessel used was the 23 mL volume, high-pressure microwave acid digestion bomb manufactured by Parr Instrument Company, Model #4781. This type of vessel has an upper temperature limit of 250 °C, a pressure limit of 1200 psi, and a maximum inorganic loading limit of 1.0 g. Only two samples were analyzed simultaneously due to the small size of the microwave cavity of 0.6 ft^3.

The only digestion reagent necessary for use was Trace-Metal Certified Nitric Acid (15.9 M) purchased through Fisher Scientific. Due to the nature of the soil material, a complete digestion was not essential because the silaceous parent material did not contain a large amount of Hg. Nitric acid was sufficient in leaching the mercury from the sample matrix. Ten milliliters of concentrated nitric acid were added to the sample in the interior Teflon cup. Two types of blanks were prepared for analysis. One consisted of 10 mL of the nitric acid. The other consisted of 10 mL of nitric acid with 0.25 g of a mercury-free soil standard reference material (SRM). The purpose of the two blanks was to determine if the background matrix of the soil would contribute to the blank value. Ten mercury standard solutions in the concentration range of the samples were prepared by spiking the nitric acid reagent with an appropriate amount of aqueous mercury standard stock solution and subjecting these solutions to the same microwave digestion procedure as the soil samples. All digested soil samples, blanks, and standards were diluted to a final volume of 25 mL to decrease the acid content of the solutions to an acceptable level for analysis in a graphite furnace. Dilutions were prepared using Barnstead water with a resistivity of no less than 12 $M\Omega \cdot cm$. Glassware preparation was previously described in this chapter. Storage of all solutions was in Teflon bottles for no longer than thirty days.

Standard quality control protocols were followed for these analyses. The sample set consisted of fourteen unknown soil samples. A batch will be defined here as the number of samples analyzed on a particular day, but containing no more than fourteen samples. A blank was analyzed before and after each batch was run. Each digested sample was analyzed a minimum of three times in order to obtain average values and precision data. One duplicate sample, spiked sample, and SRM sample was analyzed per day. In addition, vapor loss from the digestion bomb was monitored by two methods. First, a small piece of damp pH paper was fastened to the bomb near one of its outlet ports to monitor the liberation of acidic vapors in the event overpressurization occurred. Second, the total mass of the sample cup with lid, sample, and reagent was weighed before and after the digestion to calculate weight loss. According to parameters used in Method 3051[61], weight loss should be no more than ten per cent if the sample is to be considered uncompromised. In the determination of a volatile element such as mercury, the per cent loss should be ≤ 1.

The microwave unit used in this work was a 0.6 ft^3., 600 W microwave oven manufactured by General Electric, Model #JES65T. Because this home-grade microwave oven did not have temperature and pressure feedback control, the method developed was necessarily of the prescription-based type. However, Equation 5-6 was used to predict the exposure time needed to reach a final temperature of 175 °C while operating at power level 2; thereby, the reaction conditions inside the vessel were approximated. This low power level of 107.8 W was chosen because it was not advisable to deliver a large amount of energy too quickly to a sample when there was no feedback control available. For the simultaneous digestion of two samples as previously characterized,

the prescription parameters established were 107.8 W for five minutes, followed by thirty minutes of air cooling. The cooling time could be decreased by running cold water over the bottom of the bomb up to its screw threads. The outer casing should be cool to the touch before opening the bomb.

CHAPTER 6
COLD VAPOR ATOMIC ABSORPTION SPECTROMETRY

History

In 1968, Hatch and Ott introduced the technique that would later be known as Cold Vapor Atomic Absorption Spectrometry (CVAAS).[14] After these researchers digested a rock sample by a wet oxidation method, they added stannous sulfate to the flask, and attached the flask to an aeration apparatus. The liberated mercury vapor passed from the sample solution in a closed system and through the quartz cell of an atomic absorption spectrophotometer where its absorption was measured. The relative detection limit of that early work was 1 ppm Hg.

Since that work was published, there have been hundreds of papers written about the CVAAS determination of mercury. Some of the research has employed standard CVAAS instrumentation with different digestion schemes of the samples. Wet oxidation procedures have been outlined using HNO_3, $HClO_4$, HF, $KMnO_4$, H_2SO_4, $K_2S_2O_8$, $(NH_4)_2S_2O_8$, and $K_2Cr_2O_7$ reagents in numerous combinations and conditions.[65,66,67,68,69,70,71,72,73,74] The use of different reducing reagents, such as $SnCl_2$ and $NaBH_4$, for the liberation of mercury has been investigated.[75,76,77,78] Usually $SnCl_2$ is used in acidic solutions and $NaBH_4$ is used in alkaline solutions. Early studies also included the combustion of samples in an oxygen or ozone atmosphere.[79,80,81]

Other research has focussed on instrumental and sample introduction modifications. Simple modifications include the conversion of a commercial flame atomic absorption spectrophotometer for cold vapor determination[82], improvements in desiccators used to remove water vapor from the absorption cell[83], use of an electrically heated glass tube to replace the desiccators[84], and general modifications from common laboratory materials to improve the sensitivity of the instrument.[85] More elaborate modifications have also been made. Chou and Naleway[86] connected a syringe barrel fitted with a custom designed plunger directly to the absorption cell. This arrangement allowed the transfer of mercury vapor to the cell without dilution effects. The sensitivity of the method was 0.055 ppb or 0.22 ng Hg absolute, and the detection limit was 0.013 ppb or 0.05 ng Hg absolute. De Andrade and co-workers[87] designed a flow cell for the spectrophotometer which used Teflon (PTFE) tape as a membrane phase separator through which elemental mercury could pass but not the carrier solution. The detection limit was 1.4 ppb or 0.66 ng Hg absolute.

The technique of CVAAS has been used for the indirect determination of other ions based on their chemistry with mercury. Chakraborty and Das[88] used CVAAS for the indirect determination of iodide. The method is based on the formation of stable complexes of I^- with Hg(II) and 2,2'-dipyridyl in alkaline solutions, which can then be extracted in EtOAc with an efficiency of greater than 99%. The extracted solution is then analyzed for mercury, from which the I^- concentration can be calculated. The detection limit of this method was 0.68 ppb. Two other research groups developed methods for the indirect determination of iodide based on its interfering effect on the mercury absorption signal.[89,90] In highly acidic solutions, I^- also forms very stable

complexes with Hg(II), which then cause a decrease in absorbance for free Hg proportional to the amount of iodide present. The indirect determination of Sn(II) has been studied by injecting a volume of tin solution into a solution with a high concentration of mercury (1 ppm) in a CVAAS instrument and measuring the amount of mercury vapor liberated.[91] CVAAS has also been used to indirectly determine masses of sulfite ion as low as 30 pg.[92] The technique is based on the reaction of sulfite in solution with Hg(I) to promote its disproportionation to metallic mercury and Hg(II), and the monitoring of vapor released.

Lower limits of detection have been achieved through mercury preconcentration on gold filaments, squares, or foil.[93,94,95] After mercury is released from the sample solution through reduction, the vapor is allowed to amalgamate with the gold apparatus. The amalgamation is then heated to re-release the concentrated mercury which is then analyzed by atomic absorption spectrometry.

CVAAS has been used to determine the mercury concentration in many different types of real samples, including geological materials such as soils, sediments, and ores.[96,97,98,99,100,101,102] Most of the analyses involve a complicated pre-digestion of the sample through wet oxidation, ashing, or combustion techniques. Some analyses also require preconcentration of the mercury with gold gauze or other devices. Currently, detection limits in the pptr range have been reported, although on the absolute level the mass of mercury is still in the ng range.

Theory

Cold Vapor Atomic Absorption Spectrometry (CVAAS) is the technique that is most widely used for the determination of mercury in various types of samples. In this method, the Hg(II) analyte is volatilized not by a flame but through the addition of a reagent such as tin chloride which reduces the mercury ion to its elemental form through the reaction: Sn(II) + Hg(II) → Sn(IV) + Hg(0), hence the name "cold vapor" or "flameless" atomic absorption. After reduction, the intensity of the incident radiation of the source is measured relative to the intensity of the radiation as it passes through the analyte mercury vapor. The theory underlying the detection methodology is based on the absorption law.[103] This law describes the absorption of energy by, and subsequent excitation in, an atom or molecule. In mercury, there is a strong absorption of energy at 253.7 nm promoting electrons from the 6^1S_0 ground state to the $6^3P_1^0$ excited state. The amount of radiation absorbed depends on the thickness of the medium and concentration of absorbing species. Several assumptions must be made in order to derive the absorption law and are listed below.

1. The incident radiation is monochromatic and consists of parallel rays perpendicular to the surface of the absorbing material.
2. The absorbers act independently of each other and are homogeneously distributed and non-scattering.
3. The pathlength crossed is homogeneous over the cross section of the beam.
4. The incident flux is not so intense as to produce optical saturation effects.

The mathematical derivation for absorbance, as given by Ingle and Crouch[103], is as follows. The general expression for the change in radiation flux as it interacts with an absorbing medium is given by

$$d\Phi = -k\Phi db \qquad \text{(Equation 6-1)}$$

where $d\Phi$= change in incident radiant flux

Φ = incident radiant flux on a thin slice of absorbing material

k = proportionality constant called absorption coefficient

db= thickness of the slice

This equation suggests that the change in incident radiant flux as it interacts with the absorbing medium is proportional to the incident radiant flux ($d\Phi \propto \Phi$) and the thickness of the slice ($d\Phi \propto db$). The minus sign indicates attenuation of the beam with increasing thickness.

The absorption in a container of finite thickness, b, can then be obtained by rearranging Equation 6-1 and integrating from zero to thickness to give

$$\int_{\Phi_0}^{\Phi} \frac{d\Phi}{\Phi} = -k\int_0^b db \qquad \text{(Equation 6-2)}$$

which equals

$$\ln\frac{\Phi}{\Phi_0} = -kb \qquad \text{(Equation 6-3)}$$

or

$$\Phi = \Phi_0 e^{-kb} \qquad \text{(Equation 6-4)}$$

where b = finite thickness of pathlength

Φ_0= incident flux

Φ = transmitted flux

Equation 6-4 illustrates that the flux decreases exponentially with increasing distance.

Figure 6-1: Schematic instrumentation for CVAAS.

Although it is clear from this equation that the absorption coefficient, k, is concentration dependent, sometimes it is stated explicitly by defining k as k = k′ c, where k′ is an absorption coefficient independent of concentration. Now Equation 6-4 becomes

$$\Phi = \Phi_0 e^{-k'bc} \qquad \text{(Equation 6-5)}$$

In terms of direct observation during the absorption process, usually the transmittance or absorbance is measured. These terms are defined as

$$T = \frac{\Phi}{\Phi_0} = e^{-kb} = e^{-k'bc} = 10^{-abc} \qquad \text{(Equation 6-6)}$$

and

$$A = -\log T = abc \qquad \text{(Equation 6-7)}$$

where a = absorptivity ($L \cdot g^{-1} \cdot cm^{-1}$)

The absorptivity, a, is a proportionality constant that can be used when b is in units of cm and c is in ($g \cdot L^{-1}$). Equation 6-7 is known as the Beer-Lambert Law.

Instrumentation

The instrumental components of a cold vapor atomic absorption spectrophotometer consist of a source, absorption cell, aeration or sample cell, monochromator, and detector as shown in Figure 6-1. The most commonly used source is a mercury hollow cathode lamp because, when operated properly, hollow cathode lamps can produce atomic line

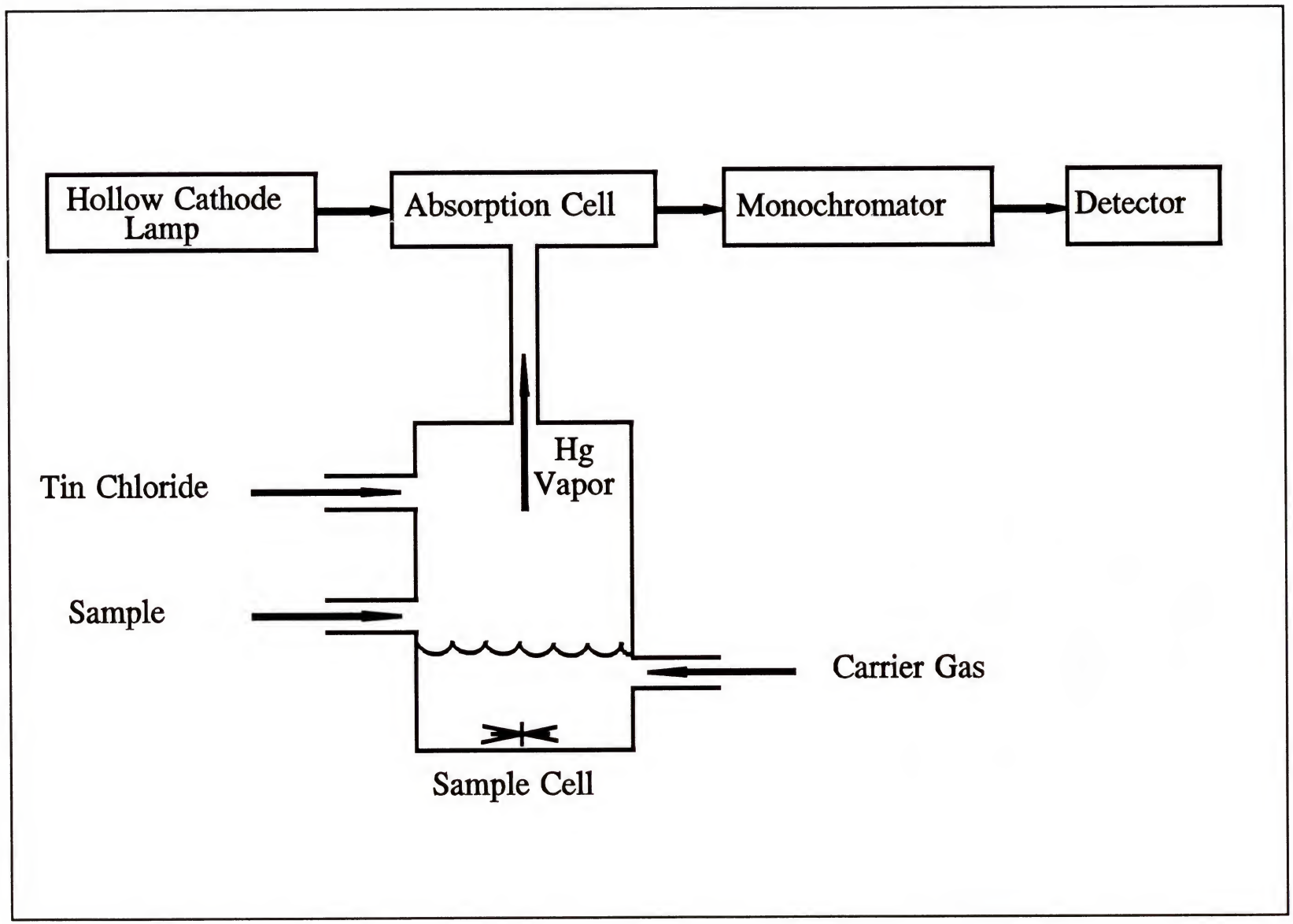
Hollow Cathode Lamp
Absorption Cell
Monochromator
Detector
Hg Vapor
Tin Chloride
Sample
Carrier Gas
Sample Cell

widths of only 0.01 to 0.02 Å. The mercury hollow cathode lamp emits radiation at 253.7 nm which passes through the absorption cell (made of a material transparent to this wavelength, such as quartz), through the monochromator (which filters out background and stray light not of the 253.7 nm wavelength), and its intensity is measured by the detector (usually a photomultiplier tube). Mercury ions in the sample solution are reduced to elemental mercury by the addition of tin chloride, and the mercury vapor is swept into the absorption cell with the aid of a carrier gas, such as nitrogen. In this work, a Perkin Elmer 5000 Atomic Absorption Spectrophotometer was used. Its parameter settings were: monochromator setting = 253.6 nm, lamp current = 0.6 mA, and slit (H) = 0.7 nm.

CHAPTER 7
LASER-EXCITED ATOMIC FLUORESCENCE SPECTROMETRY WITH ELECTROTHERMAL ATOMIZATION

Laser based spectroscopic techniques have emerged in recent years as effective methods for the detection of trace elements in extremely low concentrations or minuscule absolute amounts. According to Omenetto[104], in some industries where it is necessary to be able to analytically detect species at the parts per trillion level, laser based methods may be the only possible option.

Laser-Excited Atomic Fluorescence Spectrometry with Electrothermal Atomization (LEAFS-ETA) is one such technique that combines the extreme sensitivity and selectivity of LEAFS with the excellent analytical performance of the graphite furnace as the means of atomization.

History

The first publication of experimental work employing LEAFS-ETA was by Neumann and Kriese[105] in 1974. Their investigation used a flashlamp-pumped dye laser system for the analysis of lead. In this study, the graphite furnace was shown to be a superior atomization cell compared to the flame, which was the most commonly used atomizer at that time. The supremacy of the graphite tube cell is due to the extremely high atom density produced in the furnace during atomization, coupled with

low interferences from the inert environment. Since these initial studies two decades ago, a number of elements have been determined by LEAFS-ETA from both standard aqueous and real samples and by using various instrumental configurations.

Some of the research conducted with this technique has focussed on the characterization of the graphite furnace atomization cell. Falk and Tilch[106] used model calculations to estimate the atomization efficiency of electrothermal atomizers with either cup or tube geometries. They found that tube atomization had an efficiency of more than 50%; whereas, cup atomization was typically less than 5%. The values of these estimations were confirmed by atomic absorption measurements.

Wei et al.[107] studied variations in the signal-to-noise (S/N) obtained relative to the type of tube illumination used. Both transverse and front-surface illumination of the furnace were investigated. Their findings showed that the illumination efficiency was better in front-surface than transverse illumination, thereby affording front-surface illumination a greater sensitivity.

Preli and co-workers[108] constructed a short-tube electrothermal atomizer that was 8 mm long for use as the atom cell in the LEAFS-ETA analysis of Ag, Co, Cu, In, Pb, Tl, and Mn standard solutions. An excimer-pumped dye laser was used to excite nonresonance fluorescence in the first six elements and resonance fluorescence in the last one. Detection limits showed that this short tube atomizer gave results comparable to the best reported values for LEAFS in a cup ETA, and calibration curves were linear over 4 to 6 orders of magnitude.

Other research with LEAFS-ETA has centered on the various laser systems used for excitation. In 1989, Vera and co-workers[109] used a Nd:YAG-pumped dual dye laser system to study the double-resonance excitation of In, Ga, and Yb atoms from standard aqueous solutions. Collisional coupling between the highest level populated by the laser excitation and nearby levels produced several fluorescence transitions in the UV region. Fluorescence collection was at 90° into a double monochromator equipped with a solar blind photomultiplier tube (PMT). The absolute detection limits obtained were 2, 1, and 220 fg for In, Ga, and Yb, respectively.

Vera et al.[110] also evaluated three separate laser pumps, namely the nitrogen, copper vapor, and Nd:YAG lasers, to pump a tunable dual dye laser system for the analysis of Pb, Ga, In, Fe, Ir, and Tl atoms from standard aqueous solutions. Their studies produced absolute detection limits in the femtogram and subfemtogram range for all elements. In addition, their work suggested the importance a commercial graphite tube furnace system has in the determination of trace elements by laser based methods, especially if complicated matrices are present.

In addition to the determination of atoms in aqueous solutions, various real samples have been analyzed. In 1986, Bolshov and co-workers[111] used a LEAFS method with the electrothermal atomizer under vacuum conditions to determine the Co concentration in a synthetic tin standard, vegetable samples, and quartz glass. Limits of detection were in the pptr range. This study also showed that vacuum atomization decreases matrix interferences as a result of collisionless expansion of the atomized sample components. In 1988, this same research group compared atomization under

vacuum and argon atmospheric conditions.[112] Although matrix interferences are worse in the argon atmosphere, detection limits are worse under vacuum. They concluded that, with the use of steps to minimize matrix interferences, the argon atmospheric conditions in the furnace were more advantageous than vacuum conditions.

Between 1989 and 1992, Bolshov and co-workers[113,114,115] demonstrated the sensitivity of the LEAFS-ETA method for determining Pb and Cd in ice and snow samples taken from the Antarctic. The concentration limits of detection for these elements were in the pptr range, with absolute values as low as 10 fg. The sample size analyzed was between 20-50 μL, and no preliminary chemical treatment or preconcentration steps were necessary. The results were in excellent agreement with values found by isotope mass spectrometry and atomic absorption spectrometry. However, these latter techniques required time-consuming pretreatment and sample volumes as large as 50-100 mL.

Remy and co-workers[116] analyzed the gold content of river water by single-step excited direct line fluorescence in a commercial graphite tube atomizer. A specially designed dual monochromator setup was used to correct non-specific background fluorescence resulting from a high concentration of molecular NaCl and $MgCl_2$ in the matrix. The gold concentration was found to be 6 pptr, which corresponded to 300 fg in the 50 μL sample volume.

LEAFS-ETA has also shown promise for monitoring the long-term effectiveness of the filtering systems in trace-metal clean rooms. Liang et al.[117] used a vacuum to draw air through a jet and impact it against the inner surface of a graphite furnace.

Atomic absorption spectrometry detected the particles collected at the ng/m^3 level, while LEAFS detected the particles at the pg/m^3 level. Short-term reproducibility was 13-24% depending on the air concentration of the metal, and long-term reproducibility of the two sets analyzed seven months apart was 23%. Because of the low concentrations of metals involved, accuracy tests were not empirically possible. However, the accuracy was expected by these researchers to be within a factor of 2 or 3 of the actual value, based on the theoretical aspects of impaction.

In this work, the analysis of soil samples and a river sediment standard by an excimer-pumped tunable dual dye laser system with electrothermal atomization of the sample and fluorescence collected by front-surface illumination to a double monochromator and detection by a PMT is presented. The solid samples were prepared by a conventional wet oxidation method and a novel microwave acid digestion, as outlined in Chapter 5.

Theory

In Laser-Excited Atomic Fluorescence Spectrometry (LEAFS), resonant laser radiation is absorbed by the atom, causing electrons to be promoted from a lower state to a higher excited state for a given transition. The subsequent relaxation of the electrons produces fluorescence, which is then collected by optical lenses and focussed through a spectrometer and detected. In general terms, the analyte signal, S_A, is proportional to the Einstein coefficient for spontaneous emission, A_{21}, the number density of the excited state, n_{exc}, and the duty cycle of the detector, ϵ, as shown in the expression below.[118]

$$S_A \propto A_{21} n_{exc} \epsilon \qquad \text{(Equation 7-1)}$$

The excited state number density is very large in LEAFS, however, it is only maintained approximately during the laser pulses, which is a few ns per laser firing.

There are many different schemes used in LEAFS analysis. In this work, a two-color excitation scheme was used for mercury which utilized a dual dye laser system pumped by one excimer laser. The first dye laser was used to excite the electrons from the 6^1S_0 ground level of mercury to the $6^3P_1^0$ excited state. Its intensity had to be sufficient to cause optical saturation of the excited level. The second dye laser then promoted the electrons from the $6^3P_1^0$ state to the 7^3S_1 level. Again, optical saturation had to be achieved. Three fluorescence lines emanating from this highest excited level could be monitored, but the fluorescence emanating to the $6^3P_2^0$ level was chosen because of its high spontaneous emission coefficient relative to the other two pathways. Table 7-1 lists some of the fundamental parameters involved in the transitions studied in this work.[119]

General Fluorescence Flux Expressions

For a mathematical treatment of LEAFS theory, some basic fluorescence flux expressions must be defined.[9] The total fluorescence flux, Φ_F, produced in a given volume, V, by an absorption length, l, is given by:

$$\Phi_F = (\Phi_{\lambda m})_0 Y \alpha \qquad \text{(Equation 7-2)}$$

Table 7-1

Fundamental Parameters for Mercury Transitions

Transition Wavelength (nm)	Absorption Oscillator Strength (dimensionless)	Spontaneous Emission Coefficient (s^{-1})
253.7	0.025	1.3×10^7
435.8	0.11	4.0×10^7
546.1	0.15	5.6×10^7

where: $(\Phi_{\lambda m})_0$ = spectral radiant power at the central line (W)

α = the fraction absorbed (dimensionless)

Y = fluorescence power yield (dimensionless)

The fluorescence power yield, Y, is given by:

$$Y=\frac{A_{ji}}{A_{ji}+k_j} \qquad \text{(Equation 7-3)}$$

where: A_{ji} = Einstein coefficient of spontaneous emission (s^{-1})

k_j = collisional de-excitation rate (s^{-1})

Under optically thin conditions, the fraction absorbed, α, is given by:

$$\alpha=8.82\times10^{-13}\lambda_m^2\ n_i\ f_{ij}\ l \qquad \text{(Equation 7-4)}$$

where: λ_m = wavelength of the transition (m)

n_i = number density (m^{-3})

f_{ij} = absorption oscillator strength (dimensionless)

l = absorption pathlength (m)

Substituting the expressions in Equations 7-4 and 7-3 into 7-2, the total fluorescence flux under optically thin conditions is given by:

$$(\Phi_F)_{n_i l\to 0}=8.82\times10^{-13}\lambda_m^2 n_i\ f_{ij}\ l(\Phi_{\lambda m})_0\left(\frac{A_{ji}}{A_{ji}+k_j}\right) \qquad \text{(Equation 7-5)}$$

Fluorescence Flux under Optically Saturated Conditions

In order to obtain the maximum fluorescence signal, saturation conditions in which the rate of excitation is equal to the rate of de-excitation must be achieved. This is easily accomplished with the use of a pulsed dye laser as the source. For a multi-level

system, a population inversion occurs in which the population of the upper level is greater than the population of the lower level. Under saturation conditions, the fluorescence signal becomes independent of the quantum efficiency. The mechanism of level population now becomes dominated by the source induced radiative excitation and de-excitation rate coefficients. However, the non-specific scatter signal remains directly proportional to the source intensity. If nonresonance fluorescence is monitored, the magnitude of the scatter signal can be greatly reduced or eliminated.

Mathematically, under saturated conditions the fluorescence flux is given by:

$$\Phi_F = h\upsilon A_{ji} n_i V^* \qquad \text{(Equation 7-6)}$$

where: h = Planck constant ($J \cdot s$)

υ = frequency (Hz)

A_{ji} = Einstein coefficient of spontaneous emission (s^{-1})

n_j = number density of the excited state (m^{-3})

V^* = volume of collected fluorescence (m^3)

Because the rate of excitation and the rate of de-excitation are equal under these conditions, the following expression is given for the case of a 2-level atom:

$$\left(\frac{B_{ij}(E_\lambda)_i}{c}\right) n_i = \left[k_j + A_{ji} + \frac{B_{ji}(E_\lambda)_i}{c}\right] n_j \qquad \text{(Equation 7-7)}$$

where: B_{ij} = rate of stimulated absorption ($nm \cdot m^3 \cdot s^{-1} \cdot J^{-1}$)

$(E_\lambda)_i$ = spectral irradiance of level i ($W \cdot m^{-2} \cdot nm^{-1}$)

n_i = number density of ground state (m^{-3})

c = speed of light ($m \cdot s^{-1}$)

k_j = collisional deactivation rate (s^{-1})

A_{ji} = Einstein coefficient of spontaneous emission (s^{-1})

B_{ji} = rate of stimulated emission ($nm \cdot m^3 \cdot s^{-1} \cdot J^{-1}$)

n_j = number density of excited state (m^{-3})

The general expression for spectral irradiance, $(E_\lambda)_0$, is defined as:

$$(E_\lambda)_0 = \frac{\partial Q}{\partial t \partial S \partial \lambda} \qquad \text{(Equation 7-8)}$$

where: Q = energy (J)

t = time (s)

S = area (m^2)

λ = wavelength (nm)

The spectral irradiance, $(E_\lambda)_0$, is related to the spectral energy density, $(U_\lambda)_i (J \cdot m^{-3} \cdot nm^{-1})$, by the expression:

$$(U_\lambda)_i = \frac{(E_\lambda)_i}{c} \qquad \text{(Equation 7-9)}$$

Substituting Equation 7-9 into 7-7 simplifies that expression to:

$$B_{ij}(U_\lambda)_i n_i = [k_j + A_{ji} + B_{ji}(U_\lambda)_i] n_j \qquad \text{(Equation 7-10)}$$

The statistical weights of the two levels, g_i and g_j, relate B_{ij} and B_{ji} by:

$$B_{ij} = \frac{g_j}{g_i} B_{ji} \qquad \text{(Equation 7-11)}$$

Now, by substituting Equations 7-3 and 7-11 into 7-10, dividing by $B_{ji}(U_\lambda)_0$, and substituting Equation 7-9 and rearranging, the following expression is obtained:

The spectral irradiance for which the fluorescence signal is 50% of its maximum

$$\frac{g_i n_j}{g_j n_i} = [1 + \frac{A_{ji} c g_i}{Y B_{ij} (E_\lambda)_i g_i}]^{-1} \qquad \text{(Equation 7-12)}$$

value is called the saturation spectral irradiance, $(E_\lambda^s)_0$ ($W \cdot m^{-2} \cdot nm^{-1}$), and is given by:

$$(E_\lambda^s)_i = \frac{A_{ji} c}{Y B_{ij}} \cdot \frac{g_i}{(g_i + g_j)} \qquad \text{(Equation 7-13)}$$

Using the relation:

$$n_j = n_M (1 + \frac{n_0}{n_1}) \qquad \text{(Equation 7-14)}$$

where n_M= maximum number density (m^{-3}), and combining it with Equations 7-6, 7-12, and 7-13, the fluorescence flux expression for a 2-level atom system is given by:

$$\Phi_F = h\upsilon A_{ij} V^* n_M (\frac{g_i}{g_i + g_j})[1 + \frac{(E_\lambda^s)_0}{(E_\lambda)_0}]^{-1} \qquad \text{(Equation 7-15)}$$

When a high intensity source is used, such as a laser, $(E_\lambda)_0 \gg (E_\lambda^s)_0$ and the term $[1 + (E_\lambda^s)_0 / (E_\lambda)_0]^{-1}$ goes to unity. Thus, the total fluorescence flux is now given by:

$$\Phi_F = h\upsilon A_{ij} V^* n_M \frac{g_i}{(g_i + g_j)} \qquad \text{(Equation 7-16)}$$

Efficiency of Detection

In order to estimate the efficiency of detecting atoms with a LEAFS system, several assumptions must be made.[120] First, the residence times of the atoms in the probe volume is much greater than the duration of the laser pulse. Second, only one

photon per atom can be emitted during each laser pulse. Third, the atoms are uniformly distributed in the atom cell. Fourth, the LOD is limited by intrinsic noise sources. Assuming these conditions are valid, the number of atoms detected during a single laser firing, N_d, is given by:

$$N_d=\epsilon_0 N_s \qquad \text{(Equation 7-17)}$$

where: ϵ_0 = overall atomization efficiency

N_s = number of atoms in the cell

The overall atomization efficiency is comprised of three parameters:

$$\epsilon_0=\epsilon_a\epsilon_p\epsilon_d \qquad \text{(Equation 7-18)}$$

where: ϵ_a = fraction of atoms atomized by cell

ϵ_p = fraction of atoms probed by the laser and observed by the detector

ϵ_d = probability that a given free atom in the probe volume emits a photon during the probing time

The atomization efficiency, ϵ_a, is the number of free atoms in the atomizer, N_a, divided by the number of atoms put in the cell, N_s,:

$$\epsilon_a=\frac{N_a}{N_s} \qquad \text{(Equation 7-19)}$$

For furnaces, typical atomization efficiencies range in value from 0.1 to 1.

The spatial probing efficiency is equal to the probe volume, V_p, which is the volume illuminated by the laser and observed by the detector, divided by the total volume occupied by all the free atoms, V_s,:

The term V_s assumes a uniform atom density distribution in the total volume, and its

$$e_{ps}=\frac{V_p}{V_s} \qquad \text{(Equation 7-20a)}$$

value is assumed to be the volume of the furnace tube.

The temporal probing efficiency is given by:

$$\epsilon_{pt}=f\tau_r\leq 1 \qquad \text{(Equation 7-20b)}$$

where f = repetition frequency of the laser (Hz)

τ_r= residence time of atoms in the furnace (s).

The overall probing efficiency, ϵ_p, is given by:

$$\epsilon_p=\epsilon_{ps}\epsilon_{pt} \qquad \text{(Equation 7-20)}$$

The approximate expression for detection efficiency for a 2-level atom with saturation is given by:

$$\epsilon_d=f_c\, f_d\, A_{ji}\eta(\frac{\Omega}{4\pi})T \qquad \text{(Equation 7-21)}$$

where: f_c = fraction of atoms that fluoresce (dimensionless)

f_d = fraction of photons collected over a solid angle (dimensionless)

A_{ji} = Einstein transition coefficient (s^{-1})

η = quantum efficiency of detector (dimensionless)

$(\Omega/4\pi)$ = fractional solid angle over which fluorescence is collected in probe volume (dimensionless)

T = laser pulse duration (s)

Substituting Equations 7-19, 7-20, and 7-21 into Equation 7-17 gives the expanded

general expression for the number of atoms detected during a single laser pulse:

$$N_d = \frac{N_a V_p f_c f_d A_{ji} \eta \Omega T}{N_s V_s 4\pi} \qquad \text{(Equation 7-22)}$$

In LEAFS, the signal to noise ratio is proportional to the square root of the laser's repetition rate, $P^{1/2}$, and the detection limit can be improved by using a high repetition rate laser. Because of this, Equation 7-22 is sometimes modified to include this factor:

$$N_d = \frac{N_a V_p f_c f_d A_{ji} \eta \Omega T P^{1/2}}{N_s V_s 4\pi} \qquad \text{(Equation 7-23)}$$

Instrumentation

The basic instrumentation used in LEAFS consists of an excitation source, atom reservoir, wavelength selector, detector, signal processor, and readout device. Some of the fundamental characteristics of these components will be discussed, as well as the specific instrumentation used in this work. Figure 7-1 depicts a schematic of the instrumental configuration used in this research investigation.

Excitation Source

In LEAFS, a tunable laser system is used as the excitation source. It must be capable of producing many wavelengths to probe atoms with sensitive lines throughout

Figure 7-1: Schematic of instrumental setup for LEAFS-ETA.

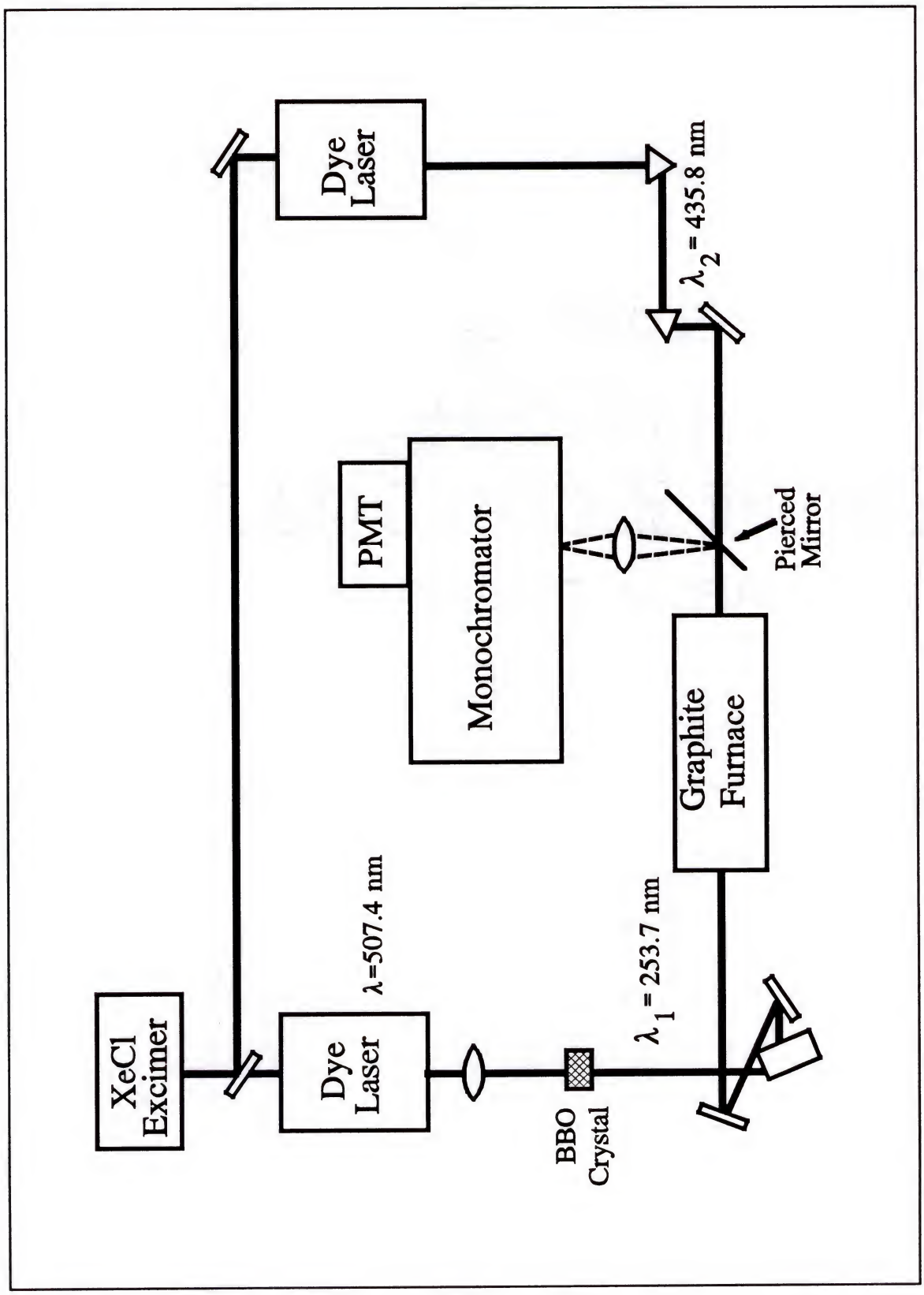
XeCl Excimer
Dye Laser
λ=507.4 nm
BBO Crystal
λ1 = 253.7 nm
Graphite Furnace
Monochromator
PMT
Pierced Mirror
λ2 = 435.8 nm
Dye Laser

the visible and UV regions. The type of system that has this wide range of capabilities employs tunable dye lasers pumped by pulsed nitrogen Nd:YAG, or excimer lasers.[120]

The pump laser emits light of a set frequency and fixed wavelength. This wavelength varies with the particular type of laser. The dye laser that is being pumped will only lase at wavelengths longer than the incident pumped wavelength. Excimer pump lasers are the most efficient for absorption by dyes that lase in the near-UV and visible regions. Xenon chloride excimer lasers, in particular, are the most efficient of the excimer lasers for an extensive range of dyes. Table 7-2 and Table 7-3 show the characteristics of pump lasers and excimer pump lasers, respectively.[103] In this work, a XeCl excimer laser (Lumonics TE-860-4, Lumonics, Ontario, Canada) was used to pump two dye lasers (Molectron DL-14, Laser Photonics, Orlando, FL) at a frequency of 10 Hz. Its output energy was approximately 70 $mJ \cdot pulse^{-1}$.

In a dye laser, the dye absorbs the pump laser radiation and emits fluorescence over a range of wavelengths characteristic of the particular dye used. Optically, the pump beam enters the dye laser cavity where it is divided by two beam splitters and transmitted to the oscillator dye cell and amplifier dye cell. A grating in the laser oscillator cavity is used to select the wavelength produced by changing the angle of the grating. However, the laser is tunable only over a narrow range of approximately 10 nm. The dye lasers used in this work, λ_1 and λ_2, were spatially and temporally aligned and used Coumarin 500 and Coumarin 440 (Exciton 05000 and 04400, Exciton, Dayton, OH) to produce fundamental outputs at 507.4 nm and 435.8 nm, respectively. The dye lasers' energies were measured with a calibrated pyroelectric Joulemeter (Model J3-09C,

Table 7-2

Characteristics of Pump Lasers

Pump Source	Range of Tunability (nm)	Peak Power (kW)	Pulse Duration (ns)	Repetition Rate (Hz)
Flashlamp	220-960	100-500	250-750	1-10
N_2	400-970	1-100	1-8	1-100
Nd:YAG	195-500	100-10000	5-10	1-30
Excimer	217-970	100-1000	10-20	1-500
CW	400-1000	0.1-5	0.015	10^3-10^6

Table 7-3

Characteristics of Excimer Pump Lasers

Laser Medium	Wavelength (nm)	Output Energy per Pulse (J)	Average Output Power (W)
ArF	193	0.2-0.3	10
KrCl	222	0.03	1
KrF	248	0.3-0.4	18
XeCl	308	0.08-0.2	8
XeF	351	0.08-0.15	7

Molectron Detector, Incorporated, Portland, OR). The Joulemeter was calibrated for termination on a 50 Ω resistor, and its output voltage was monitored on an oscilloscope (Hewlett Packard Model 54503A, Hewlett Packard, Colorado Springs, CO), with the peak amplitude of the voltage proportional to the laser pulse energy. The typical output energies of λ_1 and λ_2 were approximately 2.4 and 1.9 $mJ \cdot pulse^{-1}$.

Frequency doubling

The most important UV radiation bands needed for atomic fluorescence are in the 190 to 369 nm range. In practical terms, however, the dyes used for tunable wavelength generation lase at wavelengths longer than 320 nm. Consequently, the shorter wavelengths necessary are obtained by using a frequency conversion technique, such as frequency doubling, sum or difference frequency generation, and Raman shifting. For the first transition in the mercury excitation scheme used in this work, a wavelength of 253.7 nm was produced from the fundamental wavelength of 507.4 nm by the use of frequency doubling.

The fundamental principle underlying frequency doubling is second harmonic generation (SHG) in which the wavelength output of the dye laser is halved using a frequency doubling crystal. Two incident laser photons with a frequency, ν_1, are absorbed by a non-centrosymmetric crystal in its ground state. Upon radiational deactivation back to its ground state, only a single photon of frequency, ν_2, is emitted. The optical efficiency of this process for most commercial crystals is between 10 to 40% depending upon the pump power. The efficiency can be improved by using a lens to focus the dye laser beam into the crystal. However, tight focussing can cause damage

to the crystal material. Therefore, an optimum arrangement must be determined to compromise between high efficiency and crystal life. In this work, a BBO doubling crystal was used to convert the 507.4 nm line of λ_1 to 253.7 nm with an optical efficiency of approximately 11%.

Atom Reservoir

Several types of atom reservoirs or cells have been used in conjunction with LEAFS including flames, plasmas, and glow discharge devices.[120] In this work, an electrothermal atomizer or graphite furnace was used (Perkin-Elmer HGA-400, Perkin-Elmer, Norwalk, CT). Figure 7-2 illustrates the main components of the furnace tube housing, tube, and platform. Electrothermal atomizers are designed in many different forms, such as rods, cups, boats, and tubes. Dittrich and Stärk[121] showed that the tube atomizer had better sensitivity and detection power due to a higher heating rate, a higher atomization efficiency, a longer residence time, and a more homogeneous temperature. Pyrolytically coated graphite tubes containing L'Vov platforms were used as the sample cell in this work. The graphite tube is pyrolytically coated to seal the open pores of the graphite, which reduces the reactivity of the surface. Welz et al.[122] conducted scanning electron microscopy studies of various tube surfaces under different operating conditions. Their work made visible the various processes, transformations, and degradations that occur on the surface of and within the tubes over time. The L'Vov platform is used to allow the sample to atomize at a time when the furnace temperature is theoretically at

Figure 7-2: Components of a graphite tube furnace
A. Cross-section view
B. End-on view.

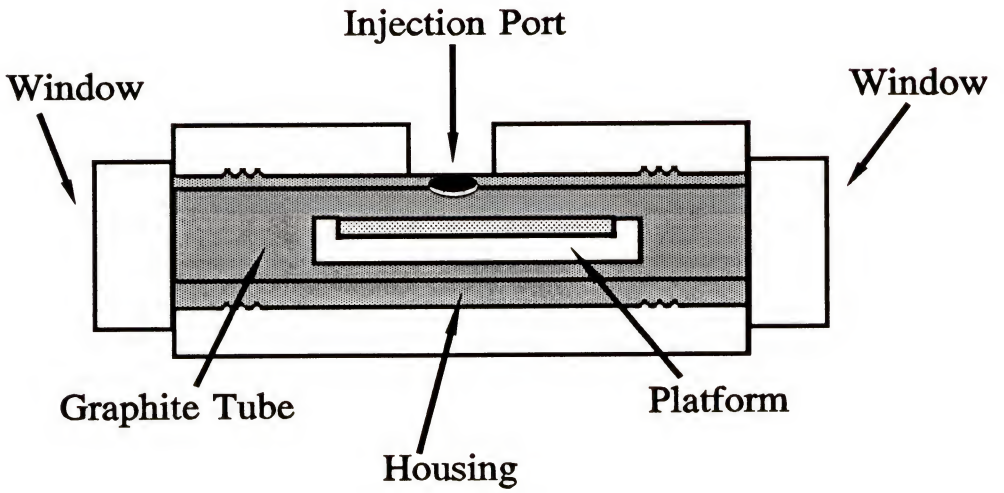
Injection Port
Window
Window
Graphite Tube
Platform
Housing

(A)

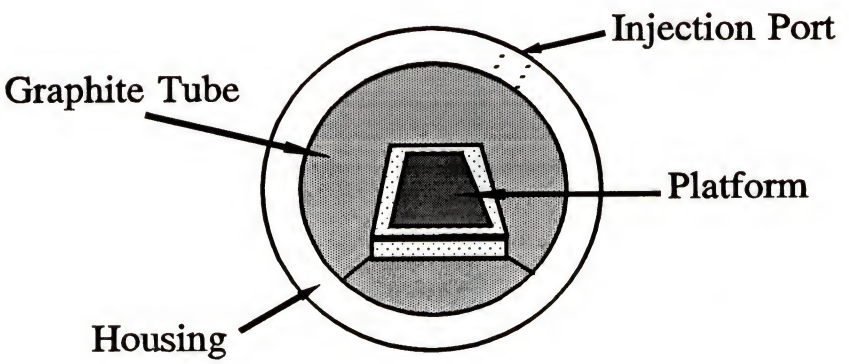
Injection Port
Graphite Tube
Platform
Housing

(B)

equilibrium, as opposed to heating it with a thermal gradient directly off the tube wall. A thorough review of platform furnace theory and processes is given by Wu et al.[123]

Much literature has been generated over the years concerning fundamental processes occurring in the graphite tube such as analyte release mechanisms and transport,[124,125] distribution and reactions within the furnace,[126] effects of matrix modification,[127] and general interferences occurring in graphite furnaces.[128] A detailed description will not be included here.

In this work, the furnace program was optimized to dry the aqueous sample without losing the mercury analyte, and palladium chloride was used as a matrix modifier. The furnace window mounts were slightly tilted so that the window angle was not directly perpendicular to the laser excitation beam, which minimized collection of the reflected laser radiation by the monochromator.

Signal Collection, Detection, and Processing

The fluorescence signal produced after the excitation of the analyte can be collected either by right-angle or front-surface illumination. Wei et al.[107] compared front-surface illumination with right-angle collection and concluded that the front-surface arrangement had better illumination and collection efficiencies (as much as a factor of 10 larger than right-angle collection), thereby producing lower detection limits with this arrangement. Figure 7-4 shows the front-surface collection, as was used in this work. With this arrangement, the fluorescence emanating from the graphite tube atom reservoir is reflected off a pierced mirror and collected with an achromat lens (focal length =

Figure 7-3: Front-surface illumination signal collection arrangement.

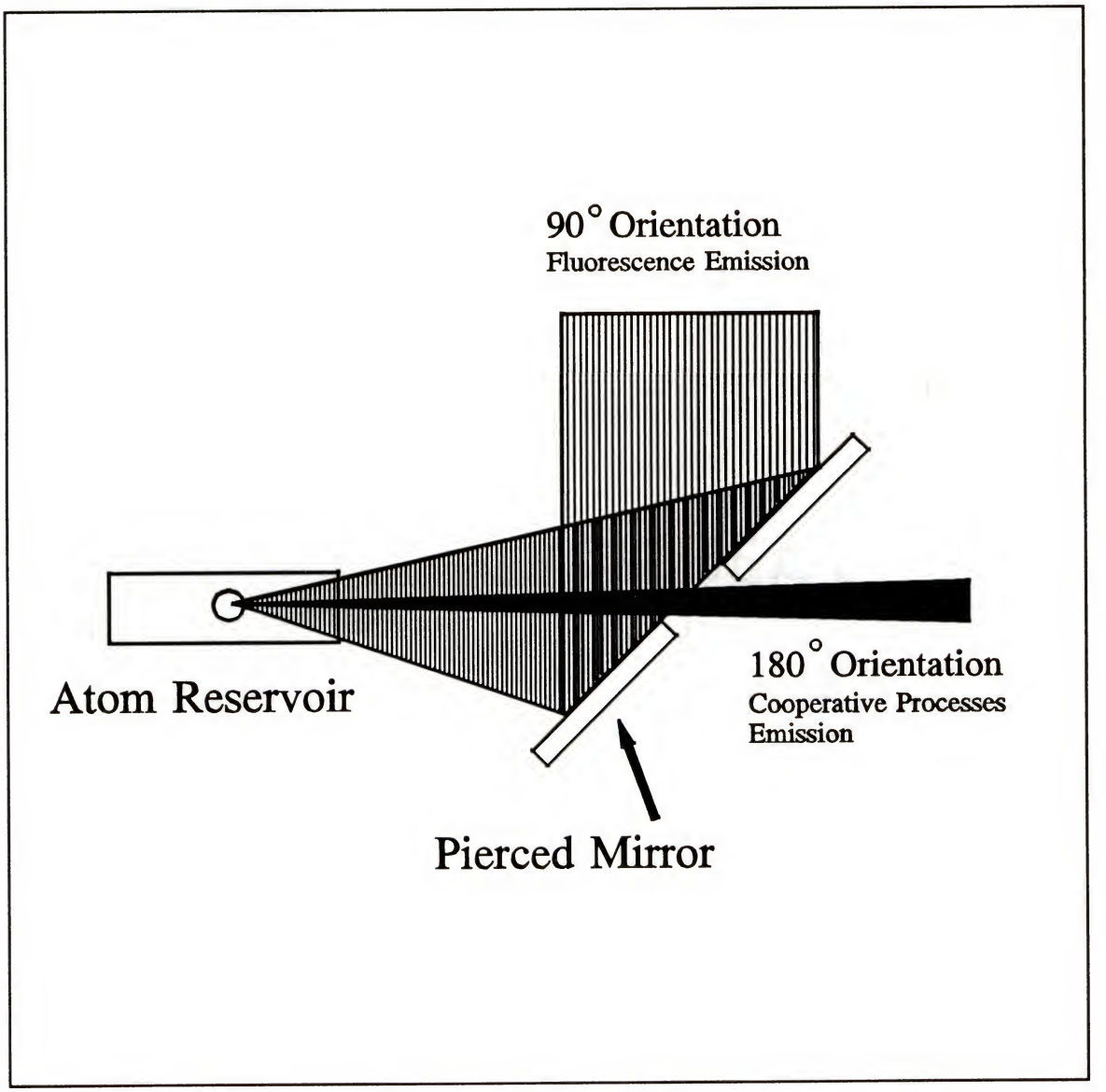
90° Orientation
Fluorescence Emission
Atom Reservoir
180° Orientation
Cooperative Processes
Emission
Pierced Mirror

10 cm, $f/\#2$). An aperture was used in front of the lens in order to match the $f/\#$ of the collection optic with the monochromator $f/\#$, where the lens $f/\#$ = focal length/diameter. The achromat lens imaged the fluorescence on the monochromator entrance slit set at 1 mm, and then passed through the double monochromator (focal length = 22 cm, $f/\#4$; SPEX 1680, 500 nm blazed gratings, SPEX, Edison, NJ), with detection by a PMT (Hamamatsu 1P28, Hamamatsu, Bridgewater, NJ).

If the fluorescence signal was sufficiently intense to saturate the PMT, neutral density filters (ORIEL Corporation, Stratford, CT) were placed in front of the monochromator entrance slit to attenuate the signal. The optical density, D, of a given filter is defined as:

$$D=\log_{10}\frac{I_0}{I_T} \qquad \text{(Equation 7-24)}$$

where: I_0 = incident power (W)

I_T = transmitted power (W)

The transmittance of the filter is calculated by the expression:

$$T=10^{-D} \qquad \text{(Equation 7-25)}$$

Several filters can be stacked together and used collectively to produce greater attenuation of the fluorescence because the optical densities of the filters are additive. The total optical density then becomes:

$$D_{Total}=\sum D_i \qquad \text{(Equation 7-26)}$$

where: D_i = optical density of each individual filter used.

The PMT was terminated in a 1200 Ω load resister. The signal produced was

processed by a boxcar (Stanford SR250, Stanford Research, Palo Alto, CA) with a 1 s time constant and by an analog-to-digital interface (Stanford SR245, Stanford Research, Palo Alto, CA). A computer was used to collect and store all signals. The electronic detection system was externally triggered by a fast photodiode triggered by the XeCl excimer pump laser.

CHAPTER 8
EXPERIMENTAL RESULTS AND DISCUSSION

CVAAS with EPA Method 245.5 Sample Digestion

Experimental Results

Because the most commonly used standard method for analysis of mercury in soil employs digestion of the sample by an appropriate EPA-approved wet oxidation method followed by analysis by CVAAS, the fourteen soil samples under investigation in this work were analyzed according to the aforementioned technique, and the results obtained were used as a reference to the LEAFS-ETA method with microwave digestion.

The standard mercury solutions, soil sample solutions, and standard reference material (SRM) solutions were prepared by EPA Method 245.5 as outlined in Chapter 5. The CVAAS instrumental system used was the Perkin-Elmer 5000 AAS. The parameters on the instrument were optimized by the operating laboratory and pre-set at the following values: time = 0.5 s, energy = 58 μJ, lamp current = 0.6 mA, slit(H) = 0.7 nm, and wavelength = 253.6 nm. All digestions and analyses carried out by this method took place in the Department of Environmental Engineering Sciences at the University of Florida.

In order to determine the mercury concentrations in the soil samples, a calibration curve was prepared through the analysis of mercury standard solutions. A graph of the

absorbance peak height produced versus the mass of mercury present in each solution was plotted (Figure 8-1). The resulting line generated through regression was linear over the mercury range studied, with a coefficient, R, of 0.99843. No data were produced on the precision of each measurement because the entire sample solution was sacrificed in the analysis.

The digested soil samples were then analyzed by CVAAS, and their mercury content was calculated using the equation for the line produced from the calibration curve. Controls used to observe any matrix effects from the soil samples include the analysis of two samples spiked with a known mass of mercury added and analysis of SRM 8406 (River Sediment, 60 ng/g). Table 8-1 summarizes the results obtained from these analyses.

Discussion

The first point to note from the results in Table 8-1 is that the concentration of mercury decreases the further in depth the sample was taken. This trend illustrates the increase in mercury contamination to the soil in recent years. A ^{210}Pb dating of the soil samples was performed[129], and Figure 8-2 shows the marked increase of mercury in soil after the onset of the industrial revolution in the beginning of the 20th century and then another sharp increase after the mid 1970's.

The second issue to note is that the mercury value obtained for SRM 8406 is lower than its certified value of 60 ng Hg per g sample. This suggests that either the digestion was not complete, there was a loss of mercury in the digestion or analysis

Figure 8-1: Calibration curve of mercury standards digested by EPA Method 245.5 and measured by CVAAS.

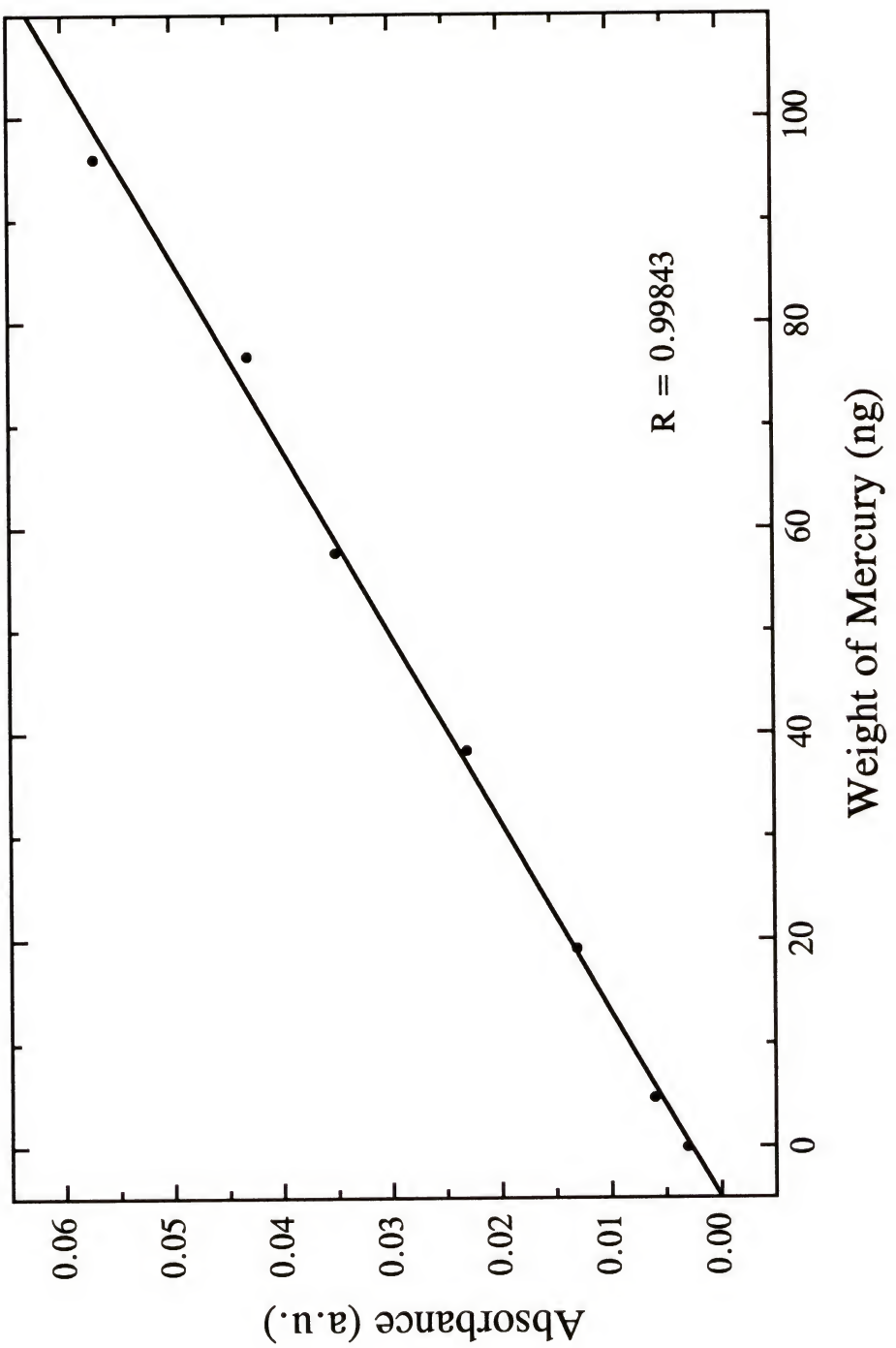
Absorbance (a.u.)
0.00
0.01
0.02
0.03
0.04
0.05
0.06
0
20
40
60
80
100
Weight of Mercury (ng)
R = 0.99843

Table 8-1

Mercury in Soil Samples Digested by EPA Method 245.5 and Analyzed by CVAAS

Core Depth (cm)	Sample Mass (g)	Absorbance (a.u.)	Digested Mass of Hg† (ng)	Conc. of Hg in Sample (ng/g)
0-2	0.2507	0.017	28	104
6-8	0.2515	0.014	23	82
6-8	0.2538	0.018	28	109
8-10	0.2577	0.023	37	143
10-12	0.2503	0.014	21	82
12-14	0.2529	0.012	17	67
14-16	0.2514	0.014	15	60
14-16	0.2495	0.009	11	46
22-24	0.2495	0.008	10	38
24-26	0.2520	0.007	8	31
26-28	0.2483	0.006	6	24
28-30	0.2520	0.006	6	24
30-32	0.2496	0.006	6	24
34-36	0.2500	0.006	6	24
22-24(s)*	0.2520	0.013	19	74
30-32(s)*	0.2566	0.010	13	52
SRM 8406	0.2537	0.009	11	45

* sample spiked with 20 ng mercury

† $Mass\ Hg(ng) = \frac{Absorbance(a.u.) - 2.7351x10^{3}(a.u.)}{5.4937x10^{-4}(\frac{a.u.}{ng})}$

Figure 8-2: Change in mercury concentration in soil over a period of years.

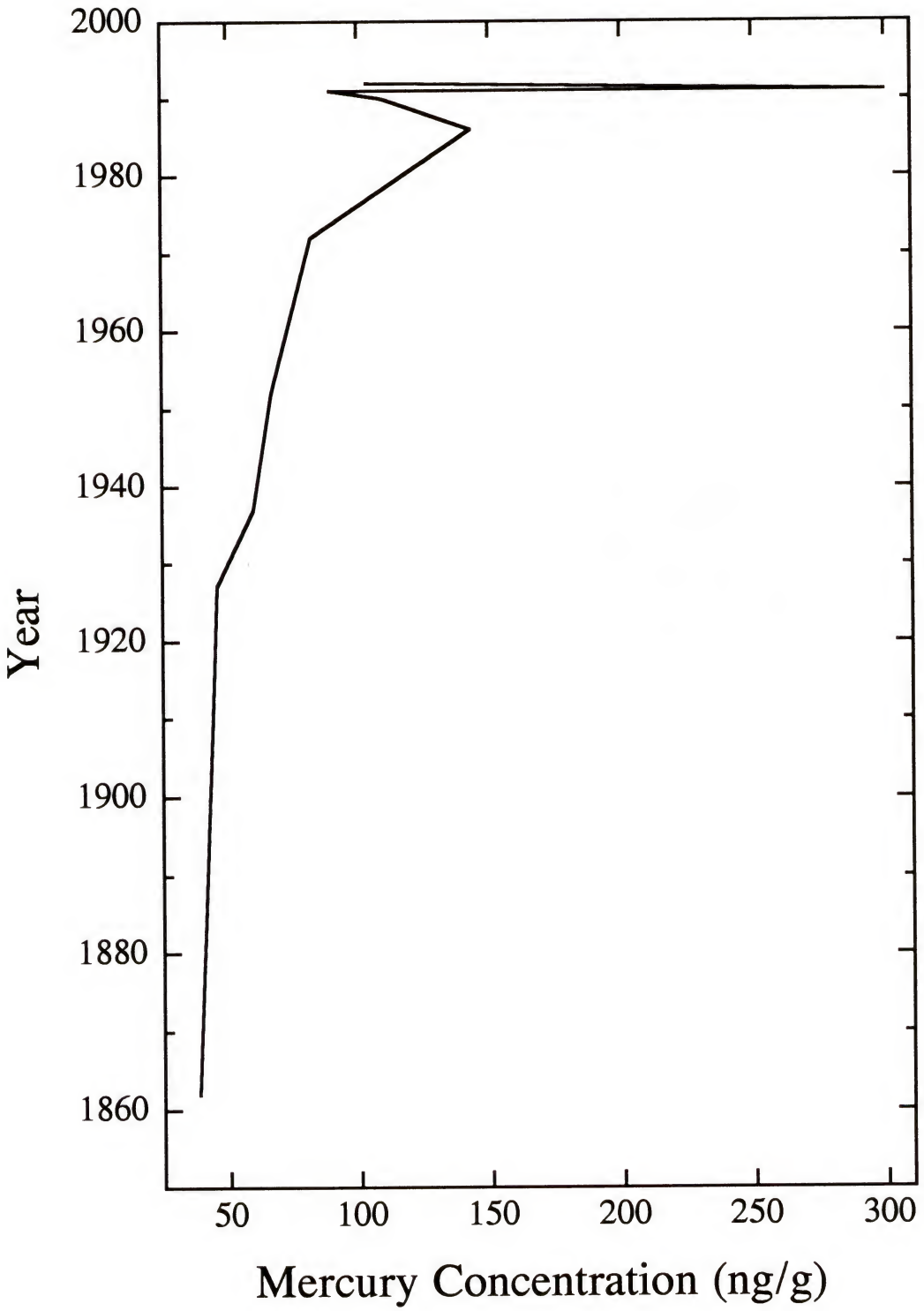

*Based on data from Table 8-1.
Data point at 300 ppb Hg taken from previous study.

processes, there were matrix effects for which the standard solutions do not compensate, or there could be a combination of any or all these factors.

LEAFS-ETA with EPA Method 245.5 Sample Digestion

In order to determine if LEAFS-ETA is a viable method for the detection of mercury in soil, the samples tested were initially digested according to the EPA-approved method to keep as many variables as possible constant when comparing the results from the LEAFS analysis to those from CVAAS. The set of standards and samples measured by the LEAFS-ETA method were actually sub-sampled from the solutions prepared for the CVAAS analysis to minimize variations due to the digestion procedure. This was accomplished by pipetting 2 mL of the digested solutions into 30 mL Teflon bottles. The LEAFS-ETA instrumental operating procedures for the analyses then had to be optimized.

Sample Pretreatment

The digested sample solutions contained very high concentrations of acids. The acid concentration of a solution being injected into a graphite furnace should not be greater than approximately 10%. At concentrations higher than 10%, the acid can interfere with the analyte signal and can also increase the degradation rate of the graphite tube, especially with the presence of H_2SO_4. Two means by which the acid concentration can be reduced are by diluting the sample with water or neutralizing the sample with a base.

Solution dilution was first chosen, but it was eliminated for the following reason. The concentration of the standard solutions subsampled was between 0 and 2 ppb Hg. Because the sample volume injected into the furnace was 10 μL, this translated into the measurement of 0 to 20 pg Hg. The 2 mL solutions would have to be diluted to 20 mL to obtain an acid concentration of approximately 10%; thereby, the resulting mass of mercury analyzed would be between 0 and 2 pg Hg. With these small masses, the measurements at the lower end of the standard solution set would be unreliable and may produce large uncertainties in the results.

Because the samples could not be diluted, neutralization of the solutions was evaluated. Both NaOH and KOH were used to neutralize the acidic sample solutions, and produced similar results. As the number density of the Na or K atoms increased relative to the mercury atoms, the analyte signal decreased (Figure 8-3). One possible explanation for this phenomenon is spectral interference by one or more species in the neutralizing solutions. This argument was dispelled after absorbance studies showed that the neutralizing solutions exerted no effect on either excitation wavelength of 253.7 nm or 435.8 nm, and neither solution appeared to affect the fluorescence wavelength of 546.1 nm.

Stern-Volmer Interference Analysis

Another possibility was physical interferences due to the interaction between the analyte and metal atom species. When two dissimilar atoms collide, there can be an exchange of electronic excitation energy according to the general equation:

Figure 8-3: Decrease in mercury signal as a function of metal atom number density.

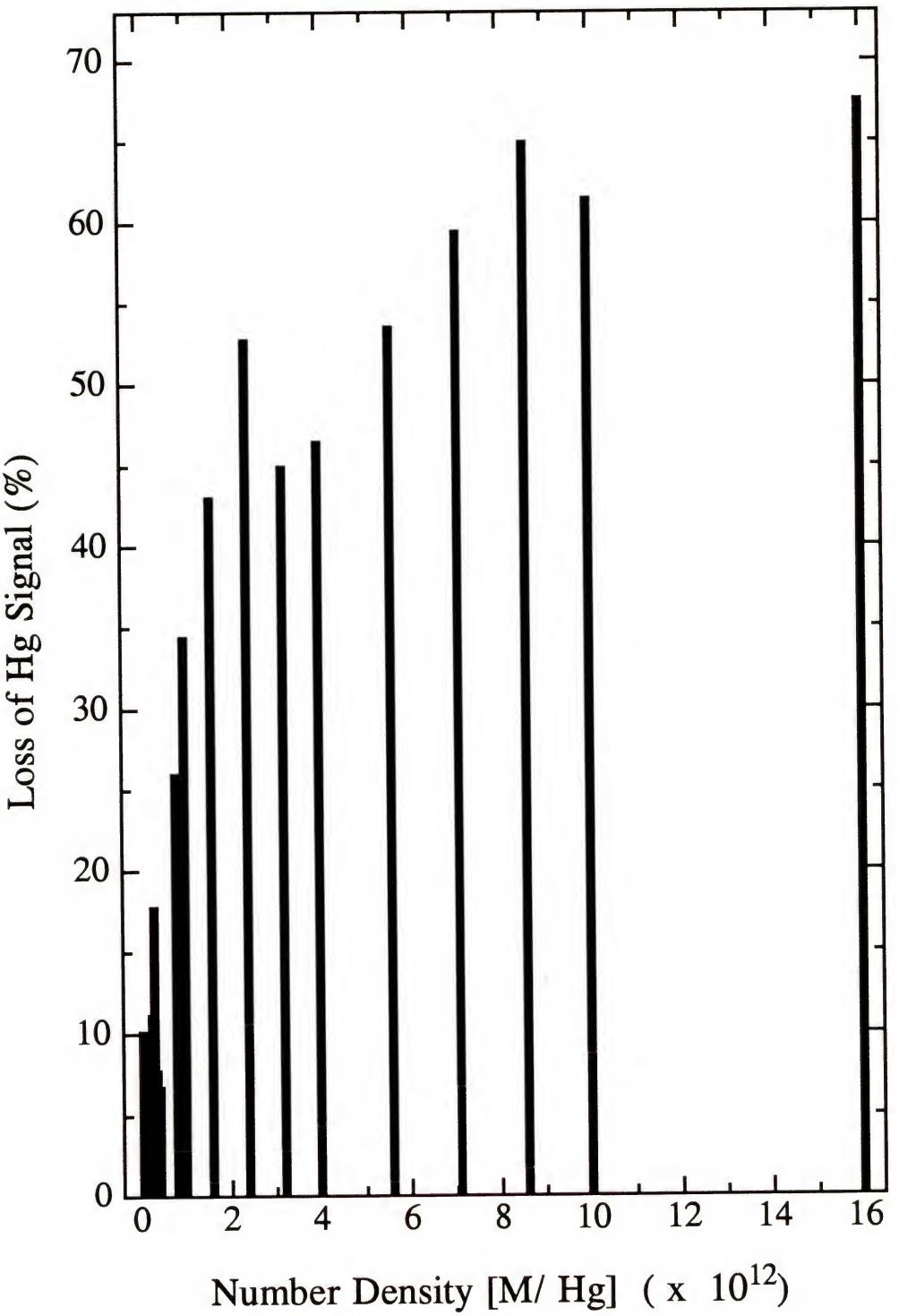

M = Na and K atoms

RSD = 16%

$$A^* + B \rightleftharpoons A + B^* \qquad \text{(Equation 8-1)}$$

where: A = ground state donor atom

A^* = excited state donor atom

B = ground state acceptor atom

B^* = excited state acceptor atom

This transfer of energy is likely to occur in systems where the difference between excited state levels, measured as ΔE, can be made up by the translational energy of relative motion of the colliding atoms, and where a large transfer cross section exists.

One of the most extensively studied systems involving this type of process is[130]:

$$Hg(6^3P_1) + M \rightarrow Hg(6^1S_0) + M^* \qquad \text{(Equation 8-2)}$$

where: M = metal atom (such as Na, Cd, K, Tl, In, Zn).

The case where M = Na will be used to illustrate this type of energy transfer system. The energy of the excited mercury level $Hg(6^3P_1)$ lies at 4.86 eV; whereas, excited levels of the sodium atom lie about 0.10 eV above the $Hg(6^3P_1)$ level. The largest transfer cross section of the sodium atom in this area is 38 $Å^2$ for the $Na(9^2S)$ level. The difference in energy for this sodium level and that of the excited mercury level is only 0.019 eV. Therefore, it is deduced that, as the number density of Na atoms increases, more Na atoms collide with the excited mercury atoms, and there is a transfer of energy that causes the de-excitation of mercury according to the equation:

$$Hg(6^3P_1) + Na^0 \rightarrow Hg^0 + Na(9^2S) \qquad \text{(Equation 8-3)}$$

The de-excitation of mercury results in the decrease of the fluorescence signal collected. Experimental studies have proven that collisions according to Equation 8-3 are

responsible for populating the Na(9^2S) level.[131,132,133,134,135,136,137] Several studies have also indicated that the probability of energy transfer is not influenced by the classical optical selection rules for transitions in the separate atoms.[138,139] For example, the transition from the sodium ground state to the 9^2S state is optically forbidden. However, the population of this level is greater than that of the Na(8^2P) level, which is optically allowed and has a similar ΔE of 0.01 eV. A conclusive theoretical explanation of these experimental results has not yet been formulated. An analogous argument for the decrease in mercury fluorescence signal upon the addition of KOH can be made with respect to the Na illustration.

The experimental rate constant for an energy transfer quenching process can be determined using Stern-Volmer analysis.[140,141] The premise of this study is that a reaction mechanism exists which involves a competition between the inherent decay of A^* and quenching by species Q. In terms of rate constants, the quantum yield of fluorescence, Y_f^0, in the absence of the quencher is given by:

$$Y_f^0 = \frac{k_f}{k_f + k_D} \qquad \text{(Equation 8-4)}$$

where: k_f = rate constant of fluorescence

k_D = rate constant of radiationless deactivation processes.

In the presence of a quenching species, Q, Equation 8-4 becomes:

$$Y_f = \frac{k_f}{k_f + k_D + k_Q[Q]} \qquad \text{(Equation 8-5)}$$

where: k_Q = rate constant of quenching ($M^{-1} \cdot s^{-1}$)

[Q]= concentration of quenching species (M).

The Stern-Volmer Equation is given by the ratio of the quantum yields in the absence and in the presence of the quencher:

$$\frac{Y_f^0}{Y_f} = \left(\frac{k_f}{k_f + k_D}\right)\left(\frac{k_D + k_f + k_q[Q]}{k_f}\right) = 1 + k_q \tau_f [Q] \qquad \text{(Equation 8-6)}$$

where: $\tau_f = (k_f + k_D)^{-1}$, the lifetime of the $Hg(6^3P_1)$ state.

The Stern-Volmer constant, K_{SV}, is given by:

$$K_{SV} = k_q \tau_f \qquad \text{(Equation 8-7)}$$

A plot of the relative efficiencies of fluorescence in the presence and absence of a quencher, $[(Y_f^0/Y_f) - 1]$, versus the concentration of the quencher, [Q], should yield a linear line with slope equal to $k_q\tau_f$ and an intercept of 0. Therefore, the rate constant of quenching, k_q, is equal to the slope of the line divided by the lifetime of the excited mercury state. It is usually more convenient to plot the response of the fluorescence detector than the actual quantum yields of fluorescence. In that case, $[(R^0/R) - 1]$ is plotted versus [Q], where R^0 and R equal the response of the detector in the absence and presence of the quenching species, respectively.

Figure 8-4 shows the Stern-Volmer plot for the interference observed between sodium and potassium atoms with mercury. At metal atom concentrations below 0.02 M and above 0.26 M, the reduction of mercury signal is due to processes independent of those discussed above. The linear portion of the curve from approximately 0.03 to 0.20 M gave a slope equal to 12.78 M^{-1} and an intercept of 0.96 (Figure 8-5). The

Figure 8-4: Stern-Volmer plot of mercury signal affected by sodium and potassium quenching.

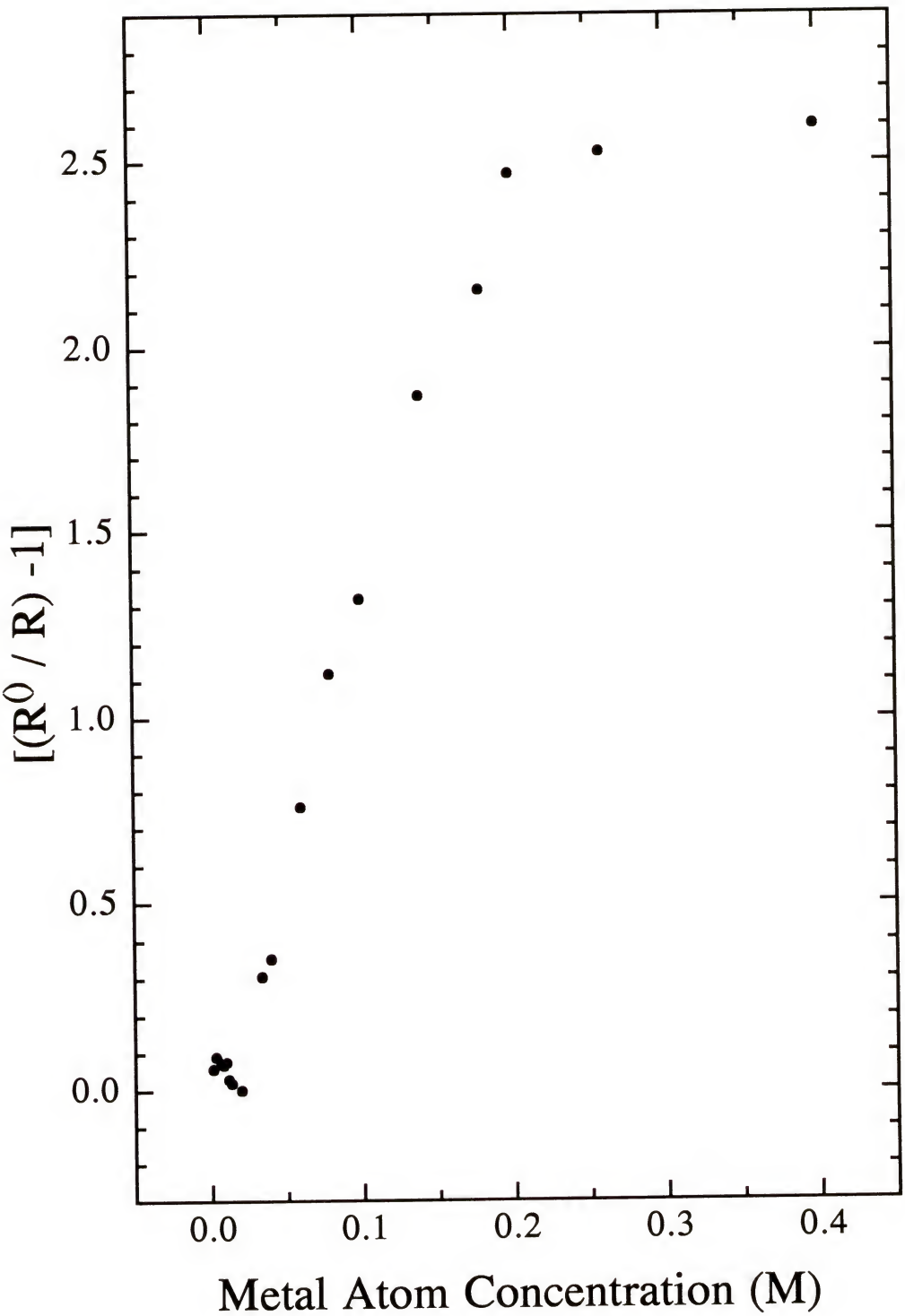
2.5
2.0
1.5
1.0
0.5
0.0
[(R^0 / R) -1]
0.0
0.1
0.2
0.3
0.4
Metal Atom Concentration (M)

Figure 8-5: Linear region of Stern-Volmer plot.

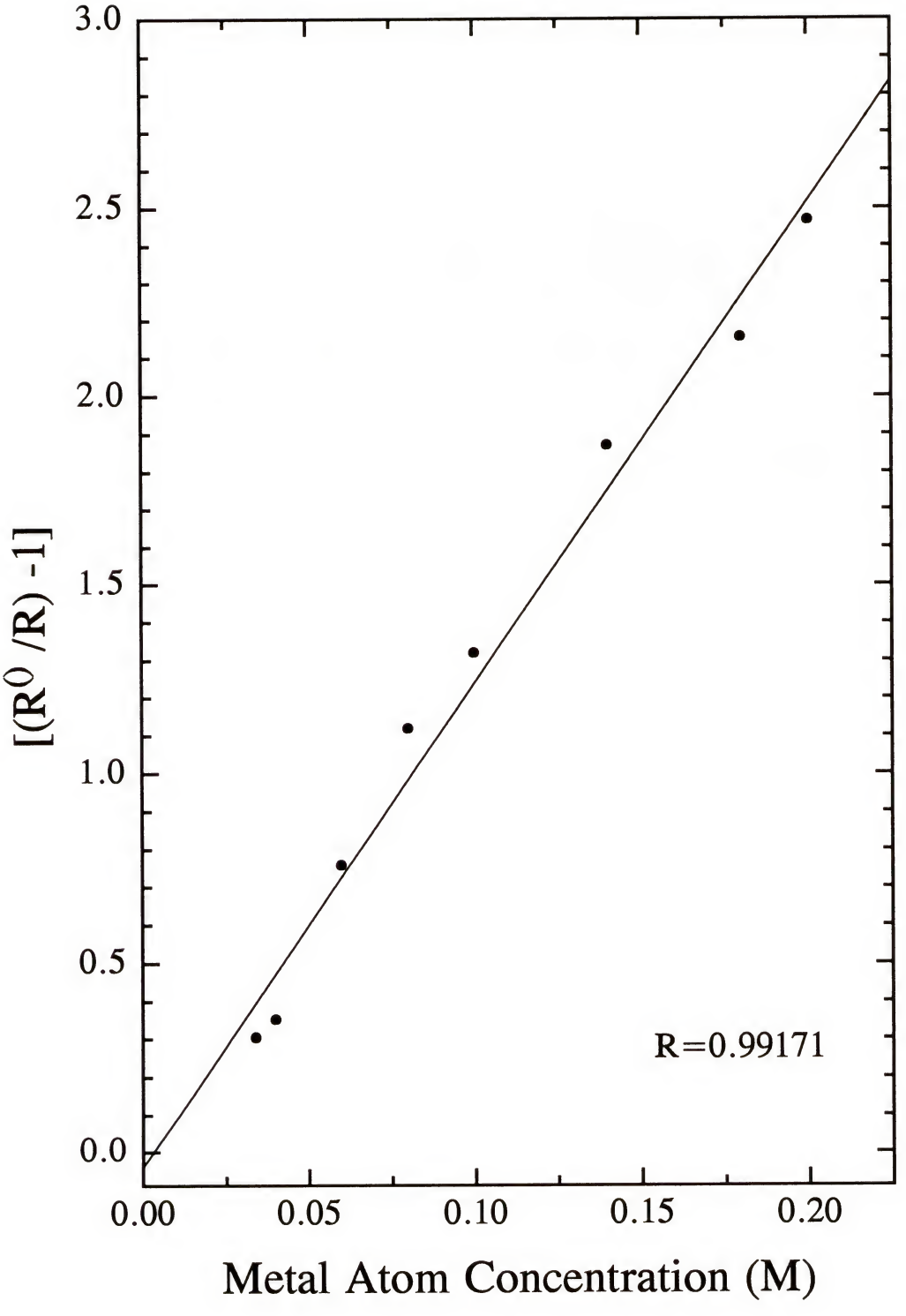
3.0
2.5
2.0
1.5
1.0
0.5
0.0
[(R0 /R) -1]
0.00
0.05
0.10
0.15
0.20
Metal Atom Concentration (M)
R=0.99171

lifetime of the $Hg(6^3P_1)$ excited state is approximately 1.2 x 10^{-7} s.[142] Therefore, the quenching rate constant in this system is given by:

$$k_q = \frac{K_{SV}}{\tau_f} = \frac{slope}{\tau_f} = \frac{12(M^{-1})}{1.2x10^{-7}(s)} = 1.0x10^8(M^{-1}\cdot s^{-1}) \qquad \text{(Equation 8-8)}$$

Experimental Results

The mercury standard solutions, sample solutions, and SRM solutions were sub-sampled from the solutions digested by EPA Method 245.5 for CVAAS analysis. The acidic solutions were neutralized with 0.250 mL of 0.25 M KOH. KOH was chosen over NaOH merely because potassium ions are already present in the solution from the digestion reagents used. The neutral pH of the resulting solutions was measured by visual inspection of pH paper spotted with the solutions.

Dye lasers λ_1 and λ_2 were operated at energies that ensured saturation of both mercury transition steps, with $Q_{\lambda 1} \approx 130\ \mu J$ and $Q_{\lambda 2} \approx 100\ \mu J$ at the furnace. The graphite furnace program used was slightly modified from the program used for aqueous mercury solutions. Twenty microliters of 1000 ppm $PdCl_2$ matrix modifier solution was injected in the furnace and dried at 110 °C for 35 s, after which it was atomized at 1200 °C for 5 s. Ten microliters of sample solution were then injected into the furnace and dried at 110 °C for 45 s, after which it was atomized at 1150 °C for 5 s. The change in analyte atomization temperature from 1200 to 1150 °C helped to minimize the interference by potassium atoms by reducing their atomization during signal collection.

A cleaning step of 2300 °C for 5 s was the final stage of the program. Data points were collected by a boxcar set at 10 averages with a sensitivity of 0.02 (V_i/V_o), and the signal collection gate width was set at 600 ns with a 10 ns delay to allow for the laser pulse to diminish before collection of signal. All data was saved to a computer using Stanford software (Stanford SR245, Stanford Research, Palo Alto, CA).

As with the CVAAS experiments, a calibration curve was generated by measuring the standard mercury solutions digested by the EPA method versus the weight of mercury in the sample volume (Figure 8-6). The data points in the plot are the average of at least three runs given in peak area relative to the boxcar intensity (RTBI). It can be seen from Figure 8-6 that as the weight of mercury increases, the absolute error in the measurement (given by one standard deviation unit from the average) also increases. This is not due to an inherent increase in noise with mass, but rather to the progressive degradation of the graphite tube and platform due to the high salt content of the samples. This degradation is visible upon inspection of the apparatus. When the tube and platform are changed, the error in the measurement decreases again, even with samples with higher masses of mercury present. The overall relative standard deviation (RSD) of analyses performed in non-degraded tubes was 3%. The typical signal collected for a digested standard mercury solution is illustrated in Figure 8-7.

After the calibration plot was prepared, the fourteen soil samples and control samples were analyzed, and their mercury concentrations were calculated using the

Figure 8-6: Calibration curve of mercury standards digested by EPA Method 245.5 and measured by LEAFS-ETA.

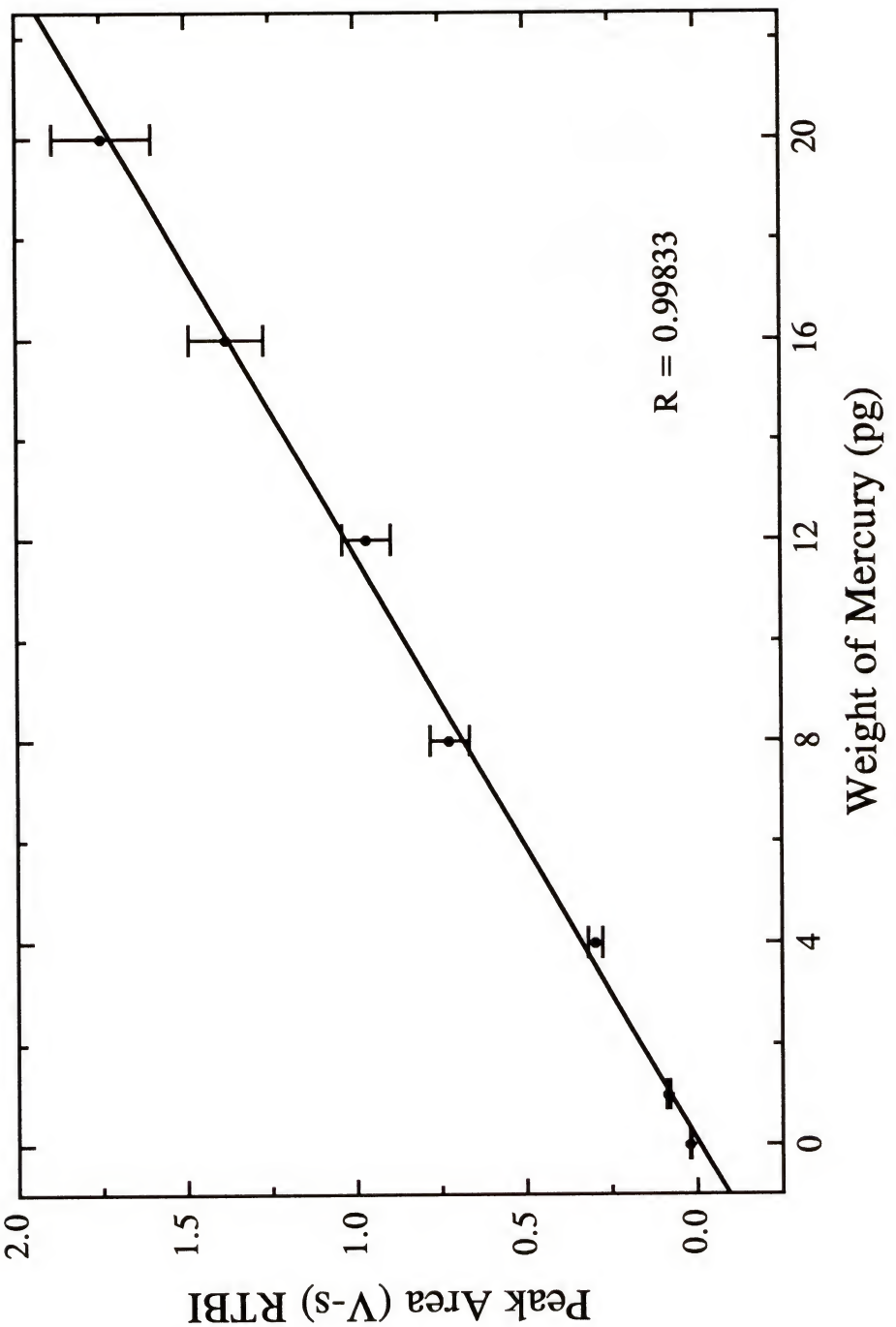
Peak Area (V-s) RTBI
2.0
1.5
1.0
0.5
0.0
0
4
8
12
16
20
Weight of Mercury (pg)
R = 0.99833

Figure 8-7: LEAFS-ETA signal of a 4 pg standard mercury solution digested by EPA Method 245.5.

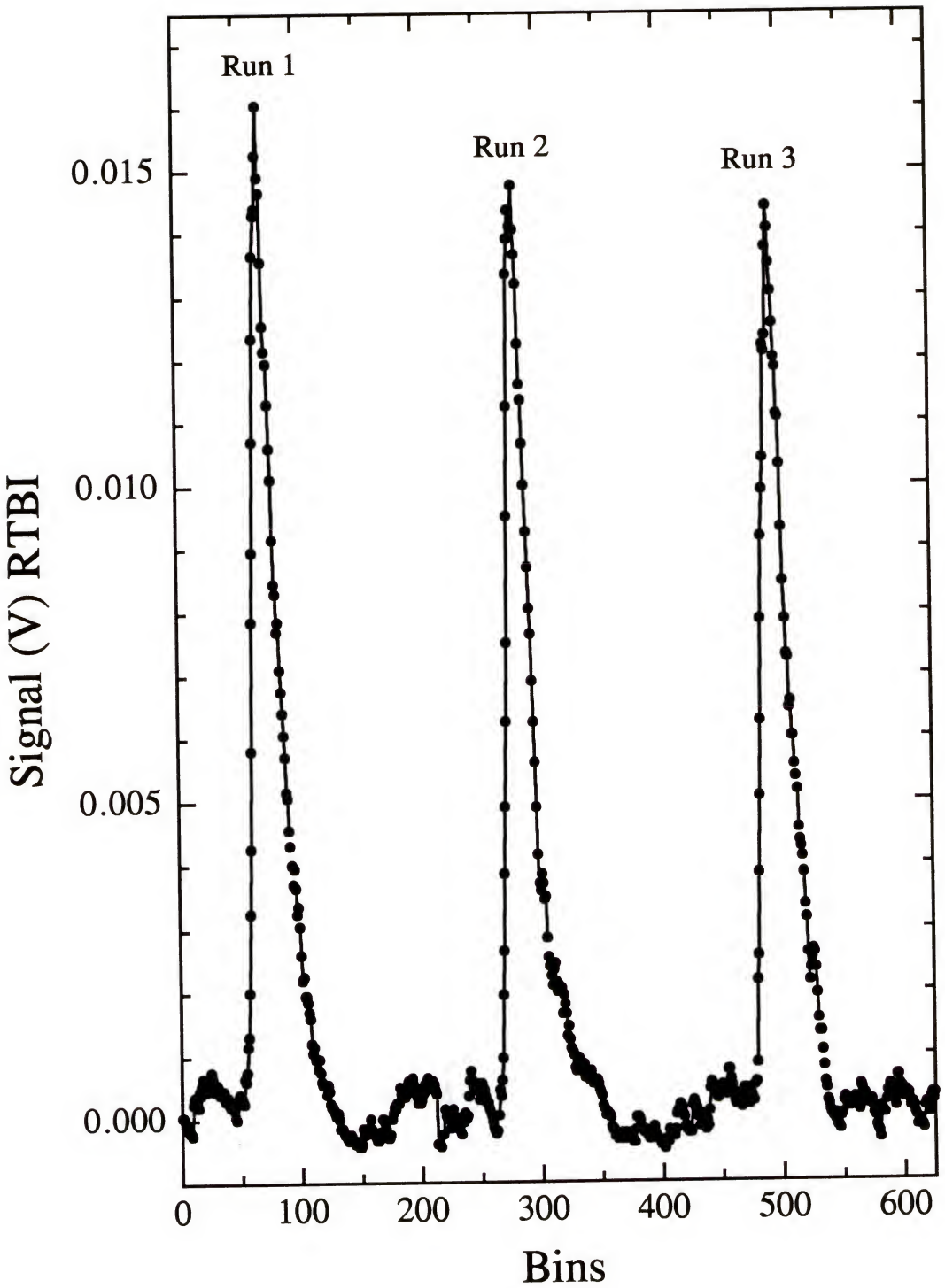
Run 1
Run 2
Run 3
0.015
0.010
0.005
0.000
Signal (V) RTBI
0
100
200
300
400
500
600
Bins

equation of the line from the calibration plot. Figure 8-8 shows a typical signal for a digested soil sample. Table 8-2 summarizes the results obtained by this method.

Discussion

Several observations can be made from the results shown in Table 8-2. First, the higher mercury concentrations present in the shallower soil depths show the same trend as the analysis by CVAAS. Second, the SRM value is again lower than its certified value of 60 ng Hg per g sample. This may be due to the factors discussed in the CVAAS results sub-section.

The similarity in the trends seen by LEAFS-ETA relative to the standard method of analysis by CVAAS suggests that LEAFS-ETA can be used as a viable method of mercury determination in soil.

LEAFS-ETA with Microwave Sample Digestion

Now that LEAFS-ETA had shown promise for the determination of mercury in soil, the simpler and more efficient microwave digestion method was formulated and used to decompose the samples. The LEAFS-ETA instrumental parameters outlined in the previous section were used for the analysis of the samples digested by the microwave method.

All standard solutions, sample solutions, and control solutions were digested in 10 mL of trace-metal certified 15.9 M nitric acid at a total power of 107.8 W for five minutes for two samples, as was described in detail in Chapter 5. Digestion under these

Figure 8-8: LEAFS-ETA signal of soil sample (core depth 12-14 cm) digested by EPA Method 245.5.

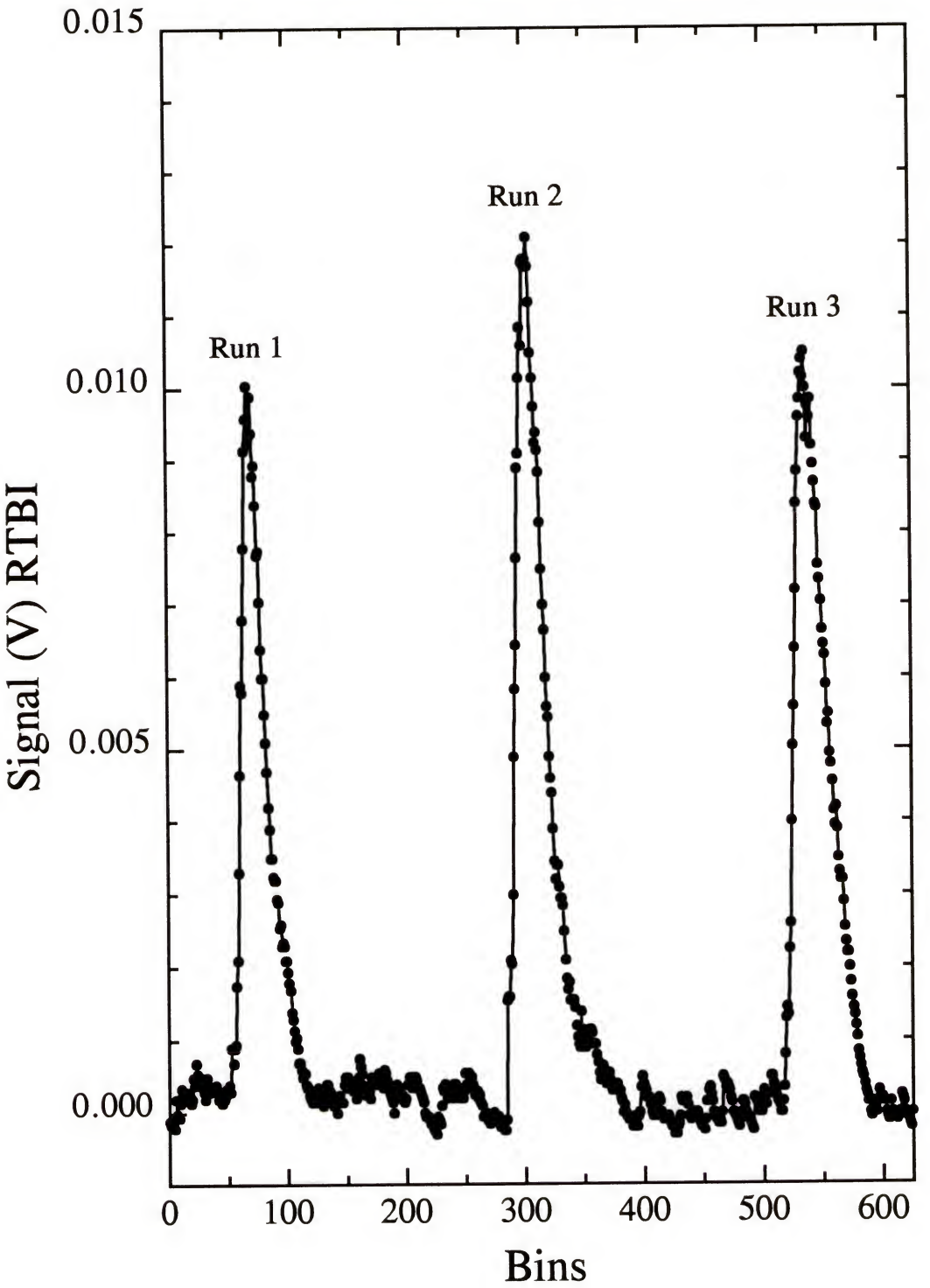
0.015
0.010
0.005
0.000
Signal (V) RTBI
Run 1
Run 2
Run 3
0
100
200
300
400
500
600
Bins

Table 8-2

Mercury in Soil Samples Digested by EPA Method 245.5
and Measured by LEAFS-ETA

Core Depth (cm)	Sample Mass (g)	Peak Area (V-s)	Mass of Hg Analyzed† (pg)	Conc. of Hg in Sample‡ (ng/g)
0-2	0.2507	0.4713	5.5	111
4-6	0.2515	0.4193	4.9	89
6-8	0.2538	0.5339	6.3	124
8-10	0.2577	0.7042	8.2	160
10-12	0.2503	0.3956	4.7	93
12-14	0.2529	0.3049	3.6	72
14-16	0.2514	0.2886	3.4	68
16-18	0.2495	0.2126	2.5	51
22-24	0.2495	0.1900	2.3	46
24-26	0.2520	0.1722	2.1	41
24-26	0.2483	0.1509	1.8	37
28-30	0.2520	0.1510	1.8	36
30-32	0.2496	0.1476	1.8	36
34-36	0.2500	0.1474	1.8	36
22-24(s)*	0.2524	0.3805	4.5	89
30-32(s)*	0.2566	0.2913	3.5	67
SRM 8406	0.2537	0.1999	2.4	47

* sample spiked with 20 ng Hg

† $Mass\ Hg(pg) = \frac{Signal(V\text{-}s) + 0.0076(V\text{-}s)}{0.08637(\frac{V\text{-}s}{pg})}$

‡ corrected for dilution factor of 5

conditions produces a final acid content of 20% in the solution.[53] Because the analyte is in a solution volume of only 10 mL with 20% acid, the solution can now be diluted to 25 mL to give a total acid content of 8%. This acid percentage is low enough to allow the direct injection of sample solution into the graphite furnace without the need for a neutralization step. With the least concentrated standard tested, this translated into the injection of 3 pg Hg which is readily and reliably measured by the LEAFS-ETA system.

Optimization

Before the sample digestions could progress, the parameters of microwave power and digestion time had to be optimized. Based on various microwave programs employed in industry and other research labs,[143,144,145] it was observed that a microwave power between 30 and 100 W per vessel was used to digest soil, sediment, and sludge samples. Because a home microwave oven unit with no safety features available was utilized in this work, a conservative power of 53.9 $W \cdot vessel^{-1}$ was used in the heating program. The time of digestion was optimized by heating 0.25 g samples of SRM 8406 with 10 mL of nitric acid at this power for one to six minutes. Figure 8-9 illustrates the peak areas obtained after analysis of these digested solutions by LEAFS-ETA. The design of the decomposition procedure was to leach all the mercury into the digested solution without loss due to vapor release upon overpressurization of the vessel. The loss of vapor was monitored by two methods. First, a small piece of damp neutral pH paper was fastened to the outer screw cap of the vessel near the pressure relief port.

Figure 8-9: Optimization of microwave digestion time for two SRM 8406 samples at 53.9 ($W \cdot vessel^{-1}$).

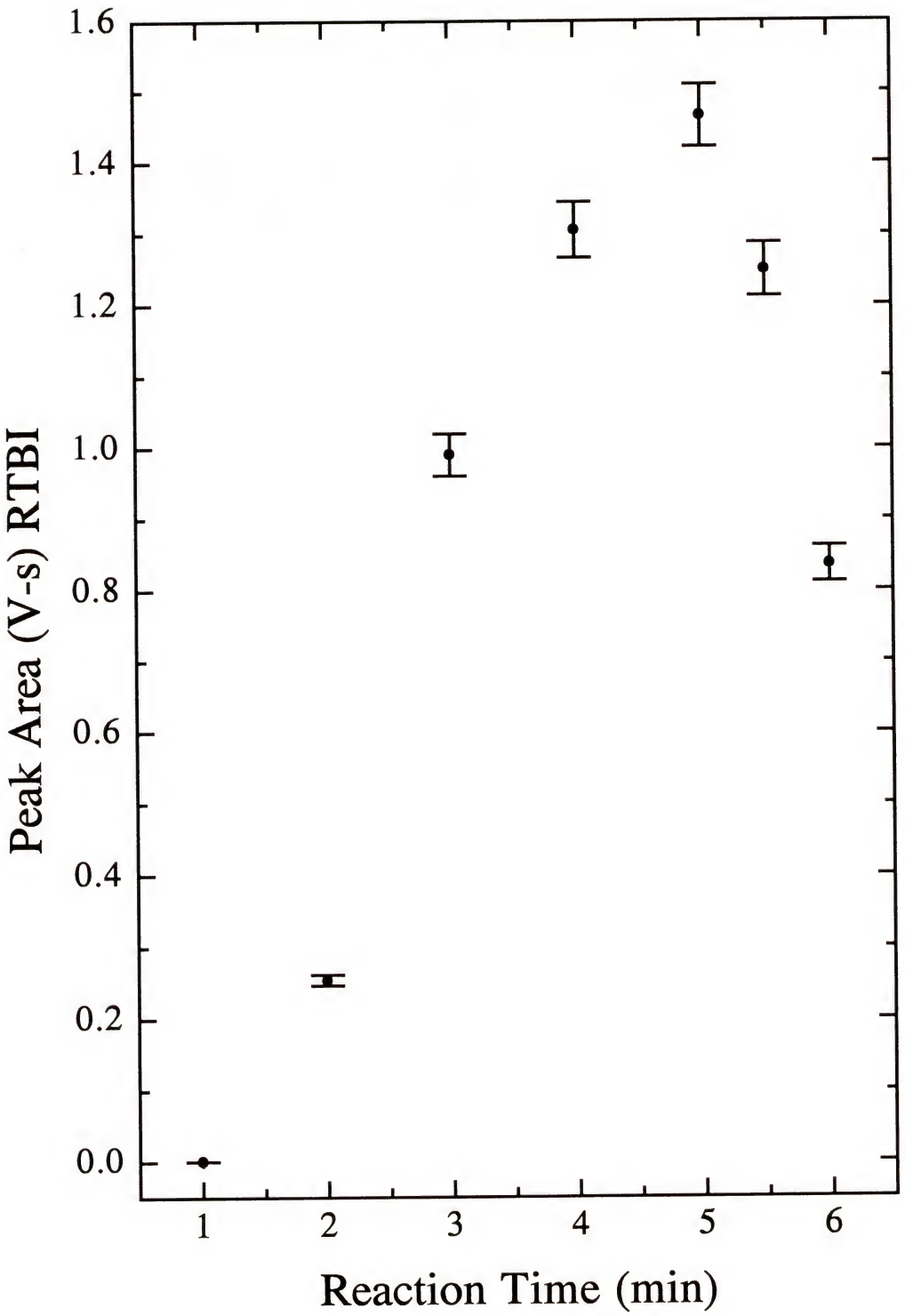
Peak Area (V-s) RTBI
1.6
1.4
1.2
1.0
0.8
0.6
0.4
0.2
0.0
1
2
3
4
5
6
Reaction Time (min)

When acid vapors were emitted, the paper turned a deep red color. Second, the inner Teflon cup and cover containing the sample and reagent were weighed before and after digestion. The weight loss should be conservatively no more than 0.5% after digestion. The maximum digestion time was determined to be 5 minutes for 53.9 $W \cdot vessel^{-1}$. For this time, the maximum mercury signal was obtained with only a 0.003% loss of mass.

Experimental Results and Discussion

The method of standard additions was used to determine if this microwave procedure produced quantitative results. Spikes were added to six samples of SRM 8406 before digestion so that 0, 6, 12, 18, 24, and 30 pg of added mercury were in the 10 μL samples analyzed. Figure 8-10 shows the signals collected for three of the spiked samples. Figure 8-11 shows the standard addition plot created by plotting the corrected peak area versus the weight of mercury in the analyzed sample. Using the equation for the line, converting from μL to mL, and compensating for dilution effects yielded a final weight of 14.60 ng Hg in the unspiked, undiluted sample. Based on the original weight of the dry sample of 0.2498 g, the final concentration of mercury in SRM 8406 was determined to be 58.45 (ng/g) with a RSD of 3.1%. This measured value was in good agreement with the certified value of 60 (ng/g).

Two different types of blank solutions were prepared. One consisted of 10 mL of nitric acid. The other consisted of 10 mL of nitric acid with 0.25 g of SRM 8406 that had been oven dried at 170 °C for three hours. Both blanks were digested according to the outlined microwave procedure. The second blank was prepared to determine if the

Figure 8-10: LEAFS-ETA signals for three SRM 8406 samples spiked with 6, 12, and 18 pg Hg digested by the microwave method.

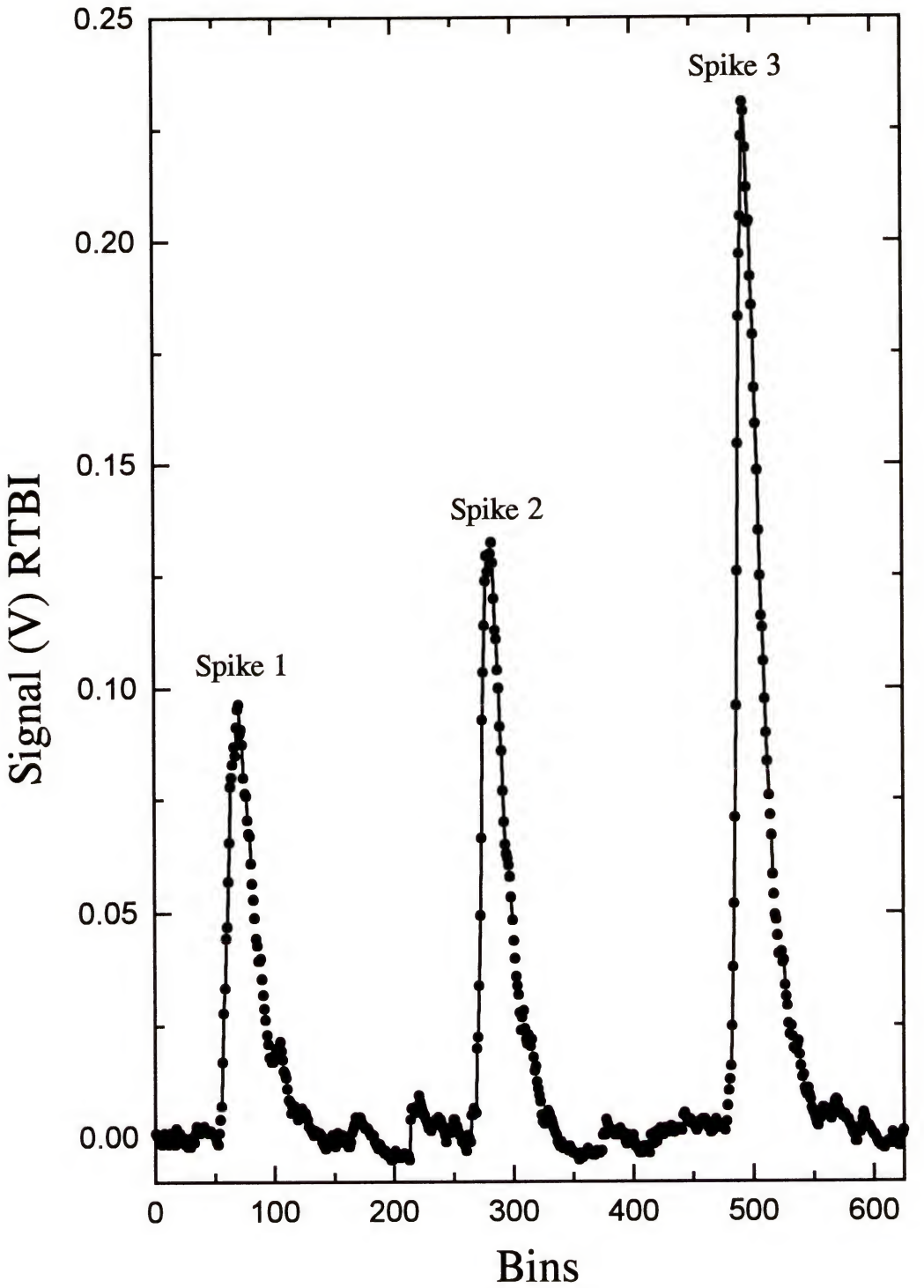
0.25
0.20
0.15
0.10
0.05
0.00
Signal (V) RTBI
Spike 1
Spike 2
Spike 3
0
100
200
300
400
500
600
Bins

Figure 8-11: Standard addition plot of microwave-digested SRM 8406 measured by LEAFS-ETA.

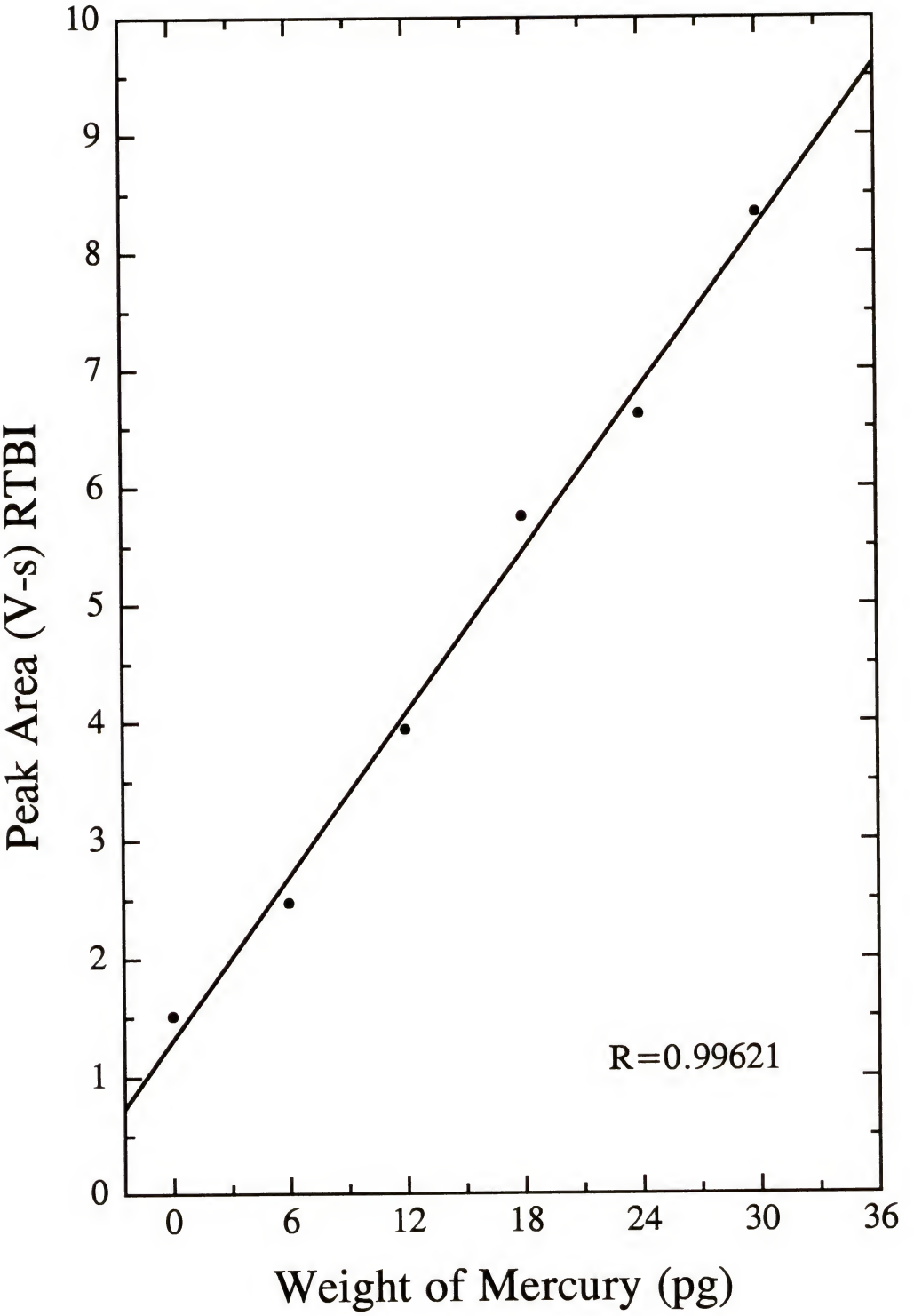
Peak Area (V-s) RTBI
Weight of Mercury (pg)
R=0.99621
0
1
2
3
4
5
6
7
8
9
10
0
6
12
18
24
30
36

background matrix of the sample contributed to the signal observed. However, no significant difference was found in the signals of the two blanks (Figure 8-12). Consequently, all remaining blanks used in this research consisted of 10 mL of nitric acid digested according to the microwave procedure.

Sixteen standards were prepared so that between 3 and 90 pg Hg were analyzed in the 10 μL sample injected into the graphite furnace. The results were used to prepare a calibration plot which was linear over the standard sample range, with R = 0.996348 (Figure 8-13). The fourteen soil samples, two soil samples spiked with 20 ng Hg, and SRM 8406 were digested by the microwave procedure. The equation of the line from the calibration plot was used to determine the concentration of mercury (pg/μL) in the injected sample. Conversion of this concentration from pg/μL to ng/mL and accounting for dilution by a factor of 2.5, the mass of mercury in the original sample volume of 10 mL was determined for all sample solutions. From the masses of samples digested, the mercury concentration in the original dry sample solid was determined. Table 8-3 summarizes the results obtained from the analysis of the microwave digested samples by LEAFS-ETA.

Comparison of Methods and Digestion Procedures

The results obtained for the concentrations of mercury found in the soil samples by EPA Method 245.5 digestion with CVAAS, EPA Method 245.5 digestion with LEAFS-ETA and microwave-assisted digestion with LEAFS-ETA are summarized in Table 8-4.

Figure 8-12: LEAFS-ETA signals of blanks prepared by microwave digestion:
A. 10 mL nitric acid
B. 10 mL nitric acid with 0.25 g SRM 8406 baked at 170 °C for 3 hours.

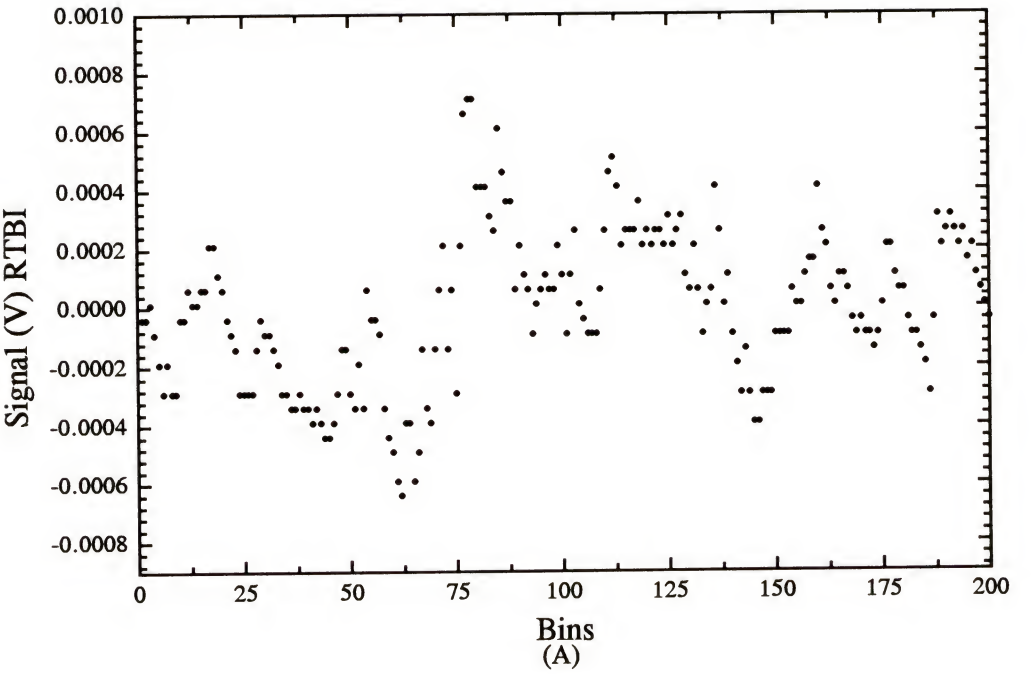
Signal (V) RTBI
0.0010
0.0008
0.0006
0.0004
0.0002
0.0000
-0.0002
-0.0004
-0.0006
-0.0008
0
25
50
75
100
125
150
175
200
Bins
(A)

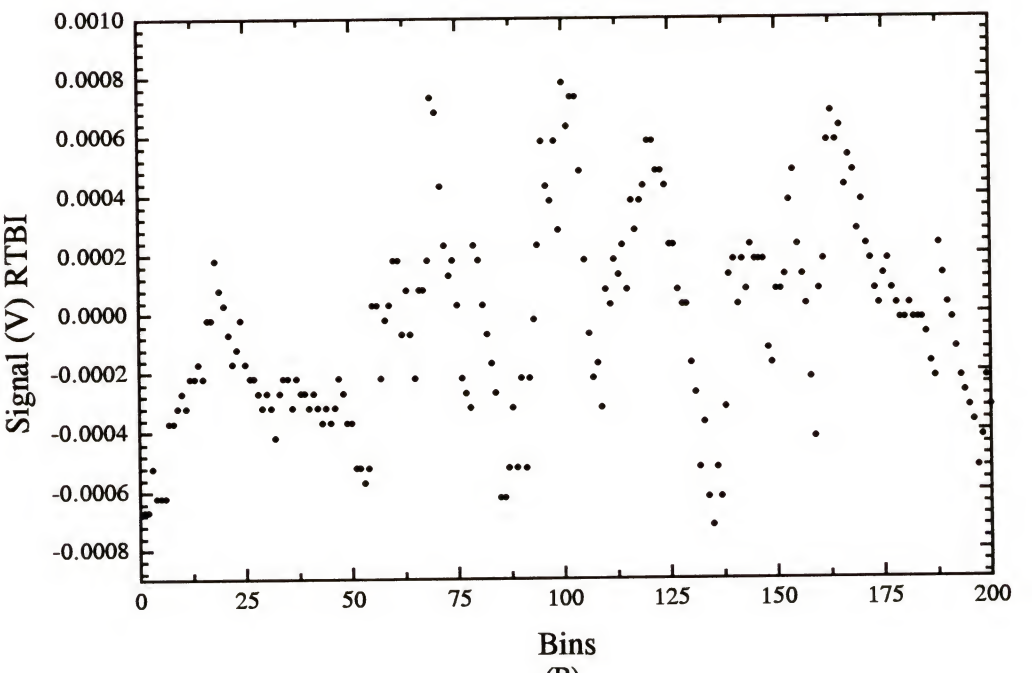
Signal (V) RTBI
0.0010
0.0008
0.0006
0.0004
0.0002
0.0000
-0.0002
-0.0004
-0.0006
-0.0008
0
25
50
75
100
125
150
175
200
Bins
(B)

Figure 8-13: Calibration curve of mercury standards digested by the microwave procedure and measured by LEAFS-ETA.

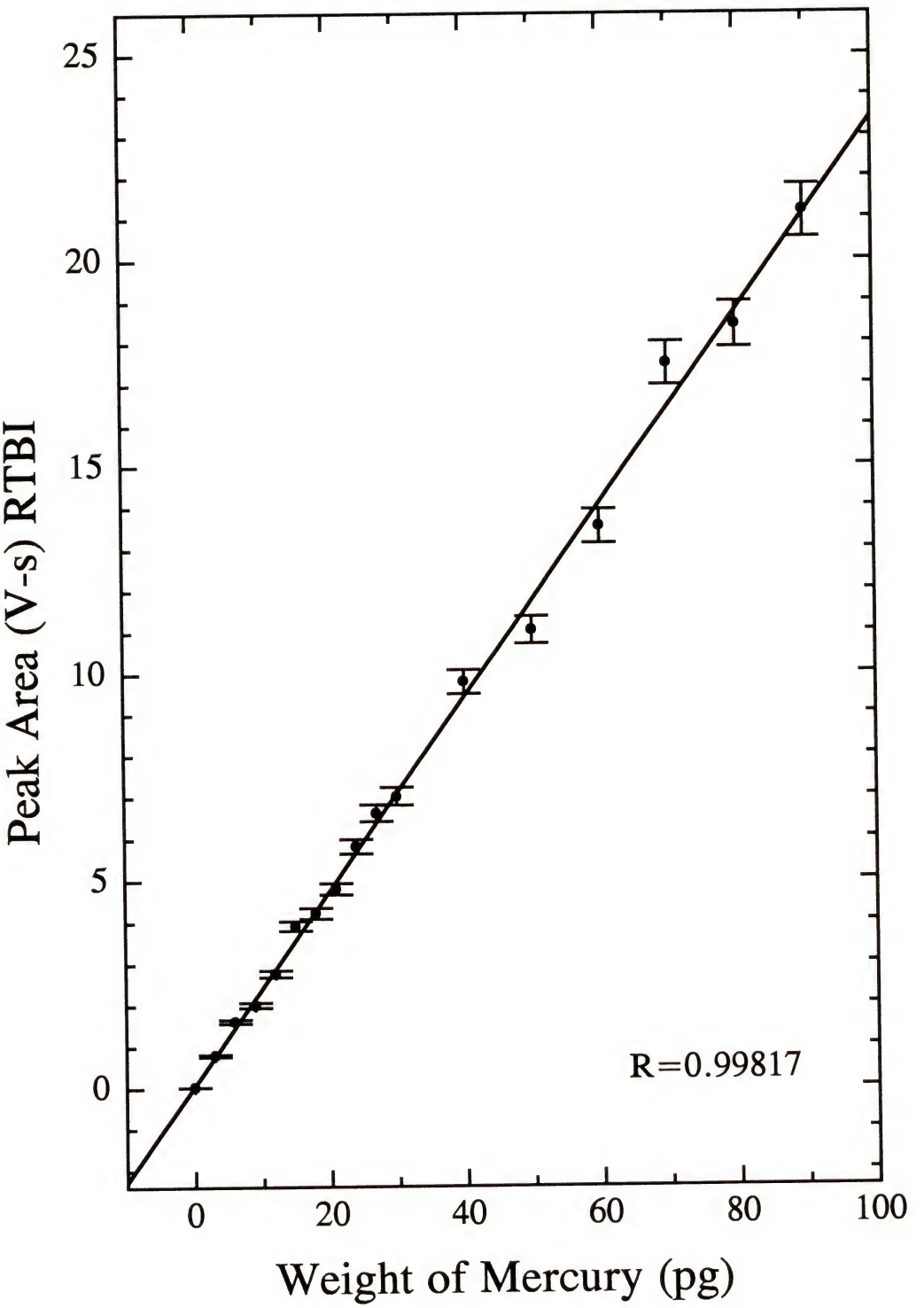
25
20
15
10
5
0
Peak Area (V-s) RTBI
0
20
40
60
80
100
Weight of Mercury (pg)
R=0.99817

Table 8-3

Mercury in Soil Digested by Microwave Method and Measured by LEAFS-ETA

Core Depth (cm)	Sample Mass (g)	Peak Area (V-s)	Mass of Hg Analyzed† (pg)	Conc. of Hg in Sample‡ (ng/g)
0-2	0.2413	7.4102	31	325
4-6	0.2509	6.9698	30	294
6-8	0.2488	3.7372	16	158
8-10	0.2475	4.7626	20	203
10-12	0.2526	2.5164	10	104
12-14	0.2480	2.1384	9.3	39
14-16	0.2507	1.8028	7.4	74
16-18	0.2489	1.6489	6.8	68
22-24	0.2305	0.9178	3.6	39
24-26	0.2288	0.8637	3.4	37
26-28	0.2309	0.7881	3.0	33
28-30	0.2301	0.6592	2.5	27
30-32	0.2317	0.7409	2.9	31
34-36	0.2496	1.0479	4.2	42
22-24(s)*	0.2518	2.6785	11	111
30-32(s)*	0.2494	2.5832	11	108
SRM 8406	0.2516	1.4578	5.9	59

* sample spiked with 20 ng Hg

† $$Mass\ Hg(pg) = \frac{Peak\ Area(V\text{-}s) - 0.069035(V\text{-}s)}{0.233831(\frac{V\text{-}s}{pg})}$$

‡ corrected for dilution factor of 2.5

Table 8-4

Comparison of Concentrations† of Mercury Found in Soil Samples

Core Depth (cm)	EPA 245.5 CVAAS‡	EPA 245.5 CVAAS	EPA 245.5 LEAFS-ETA	Microwave LEAFS-ETA
0-2	312	104	111	325
4-6	282	82	98	203
6-8	109	109	124	158
8-10	129	143	160	203
10-12	98	82	89	104
12-14	86	67	72	89
14-16	69	60	68	74
16-18	64	46	51	68
22-24	31	38	46	39
24-26	16	31	41	37
26-28	30	24	37	33
28-30	17	24	36	27
30-32	24	24	36	31
34-36	46	24	36	42
22-24(s)*	NR	74	89	111
30-32(s)*	NR	52	67	104
SRM 8406[a]	NR	45	47	59

† concentration in original, solid sample (ng/g)
‡ previous study[129]; NR = Not Reported
* sample spiked with 20 ng Hg
[a] certified value of 60 (ng/g)

The analysis of EPA Method 245.5 digested samples by CVAAS performed in a previous study, in which the control samples' values agreed with the acceptable EPA criteria, was used as the reference method for the studies performed in this work.

The results obtained for the EPA-method digested samples with CVAAS and EPA-digested samples with LEAFS-ETA can be used to compare the methods of CVAAS and LEAFS-ETA for the determination of mercury in soil samples. In all samples tested, the LEAFS-ETA values were approximately 11% higher than the CVAAS values. This can be attributed to several factors. In CVAAS, the mercury ions are atomized by addition of $SnCl_2$. Time is needed for the reaction to proceed and for the atoms to be swept into the absorption cell. There may be loss of mercury atoms during this transfer process from the sample cell to the absorption cell. Error may also occur because the absorbance peak height and not the area is measured. In samples containing a large mass of mercury, the peak height may not accurately reflect the concentration of mercury due to the transfer time necessary. In LEAFS-ETA, the mercury-containing solution is injected directly into the sample cell. The mercury is thermally atomized in a short period of time and contained in the small graphite tube volume while the fluorescence is measured as peak area. This is a more efficient and accurate method of atomization and signal measurement than that used in CVAAS. Another possibility is that when the EPA digested samples used in CVAAS were subsampled for the LEAFS-ETA analysis, the solutions may have been sufficiently inhomogeneous to cause the LEAFS samples to contain a higher concentration of mercury. However, because all the LEAFS-ETA values were consistently higher than the CVAAS values, this seems unlikely to account for the total effect.

The results obtained for the EPA-method digested samples with LEAFS-ETA and microwave-method digested samples with LEAFS-ETA can be used to compare the two methods of sample digestion for the determination of mercury in soil. At soil concentrations above 300 ppb Hg, the microwave digestion method gave values 66% higher than the EPA method. This suggests that some mercury must have been lost, or possibly incompletely digested, during the EPA decomposition procedure. For soil concentrations between 50 and 200 ppb Hg, the mercury concentrations found for the microwave digestion procedure were approximately 18% higher than for the EPA method of digestion. Again, this may be due to the reasons cited above. For soil concentrations between 30 and 50 ppb Hg, the EPA digestion method gave values 17% higher than the microwave digestion method. It is improbable that the microwave method incompletely digested these soil samples. This is based on the fact that the standard additions method showed there was complete digestion of SRM 8406 by accurately obtaining results of 60 ng/g for that standard. It is more probable that the digestion by the EPA method allowed contamination of the samples which becomes more apparent at lower concentrations of mercury.

An overall comparison of the results obtained by LEAFS-ETA with the microwave digestion to CVAAS with the EPA method of digestion whose control values were within the acceptable ranges shows good agreement. The microwave digestion with LEAFS-ETA analysis yielded overall values approximately 8% higher than the CVAAS method with EPA digestion. In four cases, however, the values of the former method were 40% higher than those of the latter. Again, this illustrates the variability of mercury loss from the samples digested according to the EPA method.

Based on current EPA criteria, the recovery of mercury from control samples is used as a gauge to measure the performance of a particular method. The per cent recovery of mercury from spiked samples is given by:

$$\%Recovery = \frac{(spiked\ sample\ result\ -\ sample\ result)}{spike\ added} \times 100 \quad \text{(Equation 8-10)}$$

The digested SRM 8406 is known as the laboratory control solid sample (LCSS), and its per cent recovery is given by:

$$\%Recovery = \frac{measured\ concentration}{certified\ concentration} \times 100 \quad \text{(Equation 8-11)}$$

The EPA's acceptable % Recovery range for these controls is between 75 and 125%, inclusive.

Table 8-5 summarizes the per cent mercury recovered from the control samples used in this work. The values obtained for the spiked samples digested by EPA Method 245.5 were low for both CVAAS and LEAFS-ETA analyses. The SRM 8406 gave per cent recoveries of 75 and 79%, respectively. These values fall within the low end of the EPA range. The microwave digestion with LEAFS-ETA analysis gave per cent recoveries of 94, 98, and 99% for the two spiked samples and the SRM 8406.

Figures of merit for the three techniques examined in this work are given in Table 8-6. The concentration limit of detection (LOD) was determined by multiplying 3 times the standard deviation of the blank and dividing by the slope of the line from the calibration curve. The absolute detection limit was obtained by multiplying the

Table 8-5

Per Cent Recovery† of Mercury from Control Samples

Control Sample	EPA 245.5 CVAAS (%R)	EPA 245.5 LEAFS-ETA (%R)	Microwave LEAFS-ETA (%R)
22-24(s)*	39	55	94
30-32(s)*	31	42	98
SRM 8406	75	79	99

† acceptable range is 75-125%, inclusive
* sample spiked with 20 ng Hg

Table 8-6

Figures of Merit for the Determination of Mercury in Soil

Technique	Concentration LOD	Absolute LOD	%RSD
EPA 245.5 CVAAS	135 pptr	7 ng	†
EPA 245.5 LEAFS-ETA	10 pptr	105 fg	3‡
Microwave LEAFS-ETA	1 pptr	14 fg	3

† cannot be determined because entire sample is sacrificed in analysis
‡ increases proportional to fast degradation of graphite tube

concentration LOD by the sample volume used in each technique. The microwave digestion of the soils produced a concentration LOD one order of magnitude lower than the EPA digestion method. Detection by LEAFS-ETA reduced the concentration LOD one order of magnitude lower than the detection limit by CVAAS. Overall, microwave digestion of soil coupled with analysis by LEAFS-ETA has a concentration LOD two orders of magnitude lower than the EPA 245.5 digestion of soil and detection by CVAAS. On an absolute basis, however, the LEAFS-ETA detection with microwave digestion has a limit of detection more than five orders of magnitude lower than that for CVAAS detection with EPA 245.5 digestion.

CHAPTER 9
CONCLUSIONS AND FUTURE WORK

Conclusions

It is clear from the data presented in this dissertation that the soil of the Florida Everglades is suffering from anthropogenic contamination from mercury. Methods of sample digestion and detection must constantly be improved to provide the reliable determination of lower concentrations of mercury in the environment. It is only with improvements in methodology and instrumentation that EPA maximum contaminant levels (MCL) can be reduced.

The method of Cold Vapor Atomic Absorption Spectrometry (CVAAS) is sensitive for the determination of mercury. However, it does have certain disadvantages. The choice of reduction reagent used is critical because it must react completely with the mercury ions in solution to form Hg(0). $SnCl_2$ will not reduce organo-mercurials, while $NaBH_4$ will. However, $SnCl_2$ works best in acidic solutions, while $NaBH_4$ operates most efficiently under alkaline conditions. The mercury atoms must be transferred from the sample cell to the absorption cell, and loss of atoms can result during this process. Also, if the transfer process is slow, more accurate results will be obtained by measuring the peak area rather than the peak height. Although the concentration LOD found with the CVAAS method was 135 pptr, a sizeable sample volume of 50 mL was used,

corresponding to an absolute LOD of 7 ng Hg. In some circumstances, a large sample volume may not be available; therefore, CVAAS may not be reliable to use in those cases.

The method of Laser-Excited Atomic Fluorescence Spectrometry with Electrothermal Atomization (LEAFS-ETA) combines the selectivity of a two-color excitation process, the sensitivity of fluorescence detection, and the high efficiency of atomization in a graphite tube to produce a highly sensitive technique for the determination of mercury. This method is extremely selective for the detection of mercury due to its two-color excitation scheme, and the two highly intense tunable dye laser excitation sources ensure that the excitation transitions are saturated. Detection by fluorescence measurement is more sensitive than the absorbance detected in CVAAS. The atomization in the graphite furnace is highly efficient and allows for the maximum number density of mercury atoms from the sample to be probed by the excitation sources. Also, optimization of the furnace program can be used to further minimize interferences by non-analyte species. The instrumentation for this system is expensive and complicated, however, and correct optical alignment is critical to maintain collection of the maximum signal possible. In analyses of small sample volumes or low concentrations of mercury, however, LEAFS-ETA is superior to CVAAS. In this work, LEAFS-ETA yielded a concentration LOD of 10 and 1 pptr depending on the sample digestion method used, which corresponded to 105 and 14 fg Hg absolute.

With improvements in instrumentation proceeding at a rapid pace, sample preparation methods must also be improved to lower overall detection limits. The EPA

Method 245.5 for the digestion of soil samples currently being used has many weaknesses. In the EPA method, numerous harsh chemicals are used to digest the soil which can ultimately contaminate the sample and the environment upon disposal. Furthermore, the volume of reagents added necessitates the decomposition of samples containing mercury in the nanogram range. Therefore, no less than 6 ng Hg can be detected in the 50 mL digested sample solution by CVAAS. The digested sample solution contains a high percentage of acid. Depending on the detection method used and the concentration of the sample, other pretreatment steps may be necessary before analysis, such as neutralization. The EPA digestion method employs a time-consuming hot water bath that is highly inefficient at transferring heat to the sample, and digestion can take several hours. Furthermore, the heating program cannot be controlled accurately. Although control samples are used to monitor the success of the digestion, mercury can be lost as inorganic or organic vapor during the decomposition process. In an actual EPA-regulated analysis, the soil samples digested by EPA Method 245.5 for analysis by CVAAS and LEAFS-ETA prepared in this work would have to be discarded and re-digested because the spiked samples and SRM values did not fall within the EPA %Recovery limits.

A faster, more reliable, and more accurate method of digesting soil samples is with microwave heating in a high-pressure closed digestion vessel. For mercury in soil, the only reagent necessary is nitric acid, and digestion is complete within five minutes. Furthermore, the heating program can be accurately controlled either by computer or by using condition prediction equations. There is less chance of contamination to the sample

or analyte loss through vapor escape, and the contamination to the environment is minimized. The %RSD for samples digested by this method was 3%, as it was for the EPA digestion method. However, the microwave-digested sample solutions had less added salt content and did not degrade the graphite tube and platform as fast as the EPA digestate did. Therefore, the RSD was more consistent than that for the samples digested by the EPA method. Also, no sample pretreatment procedure was necessary before analysis. The initial instrumental set-up cost for microwave digestion is high, but depending on the number of samples typically run, the cost of the system can be paid for in as little as nine months considering the cost per microwave digestion is approximately $2.03, whereas per hot plate digestion is $6.98.[146]

The combination of LEAFS-ETA analysis with a microwave-assisted sample digestion procedure provided the most accurate and reliable determination of mercury in soil. The concentration LOD found in this work was 1 pptr or 14 fg Hg absolute, with a RSD of 3%. This LOD is two orders of magnitude lower than the concentration LOD and more than five orders of magnitude lower than the absolute LOD of the most commonly used method of mercury detection by CVAAS of soil samples digested by an EPA-approved wet oxidation method.

Future Work

In terms of microwave digestion, the procedure used in this work could be used as a guideline to digest different types of samples such as sediments, sludges, and slags. The per cent of organics in the samples, however, must be taken into consideration when

altering the digestion procedure. Microwave digestion may be particularly important in preparing watery samples for analysis because they typically have a much lower mercury concentration than soil samples. Digestion in a closed vessel would reduce contamination to the sample and loss of the volatile analyte.

The samples digested by the microwave procedure could be analyzed routinely by CVAAS. The LOD may improve sufficiently to allow for the accurate analysis of samples containing smaller masses of mercury.

Instrumentally, the LEAFS-ETA system can be improved. The limiting background noise is stray light scatter from the laser beams. Any improvements to reduce this extrinsic noise would improve the LOD of the technique. One instrumental variation that can be investigated involves using only one dye laser tuned to 253.7 nm which would promote the mercury electrons from the 6^1S_0 level to the 6^3P_1 level. In an argon atmosphere, the fluorescence waveform produced persists for approximately 70 or 80 ns; whereas, the laser probe only lasts for approximately 10 ns. Using a monochromator with a grating blazed for 200 or 250 nm and a solar blind PMT which measures radiation below 320 nm, the laser probe scatter can be gated off and only the resonance fluorescence at 253.7 nm will be detected.

REFERENCES

1. Fujita, M., *Anal. Chem.*, 40(13), 2042, 1968.
2. Wilken, R., Hintelmann, H., *Water, Air, & Soil Pollution*, 56, 427, 1991.
3. Lee, Y., Iverfeldt, Å., *Water, Air, & Soil Pollution*, 56, 309, 1991.
4. Iverfeldt, Å., Lindquist, O., *Atm. Environ.*, 16, 2917, 1982.
5. Azzaria, L., Aftabi, A., *Water, Soil, & Air Pollution*, 56, 203, 1991.
6. Grobenski, Z., *Atomic Spectroscopy*, 6(4), 91, 1985.
7. Wheeler, B., *Spectroscopy*, 8(5), 34, 1993.
8. Okumura, M., *Fresenius J. Anal. Chem.*, 345, 570, 1993.
9. Resto, W., Two-Color Spectroscopic Studies of Mercury, dissertation, Department of Chemistry, University of Florida, Gainesville, Florida, 1993.
10. D'Itri, F., D'Itri, P., Mercury Contamination:A Human Tragedy, John Wiley & Sons, New York, 1977.
11. Troyer, W., No Safe Place, Clarke, Irwin, & Co. Ltd., Canada, 1977.
12. Nagel, M., *J. Chem. Ed.*, 802, 1987.
13. Organization for Economic Co-operation and Development, Mercury and the Environment, Paris, 1974.
14. D'Itri, F., The Environmental Mercury Problem, CRC Press, Columbus, Ohio, 1972.
15. Englender, S., *Archives of Environmental Health*, 35(4), 224, 1980.
16. Patterson, J., IIEQ Doc., 75-10, 45, Illinois, 1975.
17. Schneider, M., *J. Am. Dent. Assoc.*, 89(5), 1092, 1974.
18. Shapiro, I., *Lancet*, 1(8282), 114750, 1982.

19. Smart, E., *Rev. Environ. Health*, 5(1), 59, 1985.

20. Siblerud, R., *Toxic Subst. J.*, 10(4), 425, 1990.

21. Kabata-Pendia, A., Pendia, H., Trace Elements in Soils and Plants (2nd Ed.), CRC Press, Boca Raton, Florida, 1992.

22. Davies, B., Applied Soil Trace Elements, John Wiley & Sons, New York, 1980.

23. Meij, R., *Water, Air, & Soil Pollution*, 56, 21, 1991.

24. Mukherjee, A., *Water, Air, & Soil Pollution*, 56, 35, 1991.

25. Pacyna, J., Münch, J., *Water, Air, &* Soil Pollution, 56, 51, 1991.

26. Maserti, B., Ferrara, R., *Water, Air, & Soil Pollution*, 56, 15, 1991.

27. Gonzalez, H., *Water, Air, & Soil Pollution*, 56, 83, 1991.

28. Glass, G., *Environ. Sci. Technol.*, 24(7), 1059, 1990.

29. Schuster, E., *Water, Air, & Soil Pollution*, 56, 667, 1991.

30. Dryssen, D., Wedborg, M., *Water, Soil, & Air Pollution*, 56, 507, 1991.

31. Wang, J., *Water, Soil, & Air Pollution*, 56, 533, 1991.

32. Mierle, G., Ingram, R., *Water, Air, & Soil Pollution*, 56, 349, 1991.

33. Xu, H., Allard, B., *Water, Air, & Soil Pollution*, 56, 705, 1991.

34. Allard, B., Arsenie, I., *Water, Air, & Soil Pollution*, 56, 457, 1991.

35. Kerry, A., *Water, Air, & Soil Pollution*, 56, 565, 1991.

36. Hutchinson, T., Meema, K., Lead, Mercury, Cadmium, and Arsenic in the Environment, John Wiley & Sons, New York, 1987.

37. Matilainen, T., *Water, Air, & Soil Pollution*, 56, 595, 1991.

38. Bately, G., Trace Element Speciation: Analytical Methods & Problems, CRC Press, Boca Raton, Florida, 1989.

39. Rasmussen, P., *Water, Air, & Soil Pollution*, 56, 379, 1991.

40. Browne, C., Fang, S., *Plant Physiology*, 61, 430, 1978.

41. Basett, R., Cravey, R., Disposition of Toxic Drugs in Man (3rd Ed), YBM Publishers, New York, 1989.

42. Scientific & Technical Assessments of Environmental Pollutants Panel on Mercury, An Assessment of Mercury in the Environment, National Academy of Sciences, Washington, D.C., 1978.

43. Zakrzewski, S., Principles of Environmental Toxicology, ACS, D.C., 1991.

44. Grosser, Z., *Environmental Testing & Analysis*, 24, 1992.

45. Carter, M., Soil Sampling & Methods of Analysis, Lewis Publishers, Boca Raton, Florida, 1993.

46. Anderson, R., Practical Statistics for Analytical Chemists, VNR Company, New York, 1987.

47. Florida National Parks & Monuments Association, Inc., Homestead, Florida, *Everglades National Park Slide/Cassette Program*, Finley Holiday Film Corp., Hollywood, California.

48. Bendicho, C., de Loos-Vollebregt, M., *J. Anal. At. Spectr.*, 6, 353, 1991.

49. Ali, A., Smith, B., Winefordner, J., *Talanta*, 36(9), 893, 1989,

50. Wagner, R., Yogis, G., Guide to Environmental Analytical Methods, Genium Publishing Corporation, New York, 1992.

51. Leeman Labs, *Leeman Letter*, #23, 1992.

52. Knapp, G., *Analytical Proceedings*, 27, 112, 1990.

53. Kingston, H., Jassie, L., Introduction to Microwave Sample Preparation: Theory and Practice, ACS, Washington, D.C., 1988.

54. Von Hippel, A., Dielectric Materials & Applications, John Wiley, New York, 1954.

55. Miller-Ihli, N., *Spectroscopy*, 7(9), 20, 1992.

56. Parr Instrument Company, "Operating Instructions for Parr Microwave Acid Digestion Bombs," #243M, Illinios, 1989.

57. Abu-Samra, A., Morris, J., Koirtyohann, S., *Anal. Chem.*, 47, 1475, 1975.

58. Carius, G., *Ann. Chem.*, 136, 1, 1860.

59. Jackwerth, E., Gomišček, S., *International Union of Pure & Applied Chem.*, 56(4), 479, 1984.

60. Kingston, H., Jassie, L., *Anal. Chem.*, 58, 2534, 1986.

61. Kingston, H., *Spectroscopy*, 7(9), 20, 1992.

62. Binstock, D., Grohse, P., Gaskill, Jr., A., Sellers, C., Kingston, H., Jassie, L., *J. Assoc. Off. Anal. Chem.*, 74(2), 360, 1991.

63. Mateo, M., Sabaté, S., *Anal. Chim. Acta*, 279, 273, 1993.

64. *Federal Register*, 56(207), 55410, 1991.

65. Scheuhammer, A., Bond, D., *Biol. Trace Elem. Res.*, 31(2), 119, 1991.

66. Horvat, M., Lupsina, V., Pihlar, B., *Anal. Chim. Acta*, 243(1), 71, 1991.

67. Kuldvere, A., *Analyst*, 115(5), 559, 1990.

68. Adeloju, S., Mann, T., *Anal. Lett.*, 20(7), 985, 1987.

69. Dumarey, R., Van Ryckeghem, M., Dams, R., *J. Trace Microprobe Tech.*, 5(2-3), 229, 1987.

70. Hon Way, L., *Analyst*, 108(1292), 1313, 1983.

71. May, J., Sih, J., Mustafa, A., *J. Biol. Stand.*, 6(4), 339, 1978.

72. Toth, J., Ingle, Jr., J., *Anal. Chim. Acta*, 92(2), 409, 1977.

73. Agemian, H., Chau, A., *Anal. Chem.*, 50(1), 13, 1978.

74. Dassani, S., MCClellan B., Gordon, M., *J. Agric. Food Chem.*, 23(4), 671, 1975.

75. Yamamoto, Y., Kumamaru, T., Shiraki, A., *Fresnius' Z. Anal. Chem.*, 292(4), 273, 1978.

76. Capelli, R., Fezia, C., Franchi, A., Zanicchi, G., *Analyst*, 104(1245), 1197, 1979.

77. Welz, B., Schubert-Jacobs, M., *Fresnius' Z. Anal. Chem.*, 331(3-4), 324, 1988.

78. Daniels, R., Wigfield, D., *J. Anal. Toxicol.*, 13(4), 214, 1989.

79. Bailey, B., Lo, F., *J. Ass. Offic. Anal. Chem.*, 54(6), 1447, 1971.

80. Lidums, V., *Chem. Scr.*, 2(4), 159, 1972.

81. Lopez-Escobar, L., Hume, D., *Anal. Lett.*, 6(4), 343, 1973.

82. Ramelow, G., Balkas, T., *At. Absorpt. Newsl.*, 15(2), 55, 1976.

83. Kothandaraman, P., Dallmeyer, J., *At. Absorpt. Newsl.*, 15(5), 120, 1976.

84. Christmann, D., Ingle, Jr., J., *Anal. Chim. Acta*, 86(1), 53, 1976.

85. Lawrence, K., White, M., Potts, R., Bertrand, R., *Anal. Chem.*, 52(8), 1391, 1980.

86. Chou, S., Naleway, C., *Anal. Chem.*, 56(9), 1737, 1984.

87. De Andrade, J., Pasquin, C., Baccan, N., Van Loon, J., *Spectrochim. Acta, Part B*, 38B(10), 1329, 1983.

88. Chakraborty, D., Das, A., *At. Spectrosc.*, 9(6), 189, 1988.

89. Kuldvere, A., *Analyst*, 107(1280), 1343, 1982.

90. Sun, F., Julshamn, K., *Spectrochim. Acta, Part B*, 42B(7), 889, 1987.

91. Christmann, D., Ingle, Jr., J., *Anal. Chim. Acta*, 86(1), 285, 1976.

92. Marshall, G., Midgley, D., *Anal. Chem.*, 53(12), 1760, 1981.

93. Welz, B., Melcher, M., *At. Spectrosc.*, 5(2), 59, 1984.

94. Temmerman, E., Dumarey, R., Dams, R., *Anal Lett.*, 18(A2), 203, 1985.

95. Lee, S., Jung, K., Lee, D., *Talanta*, 36(10), 999, 1989.

96. Ure, A., Shand, C., *Anal. Chim. Acta.*, 72(1), 63, 1974.

97. Agemian, H., Chau, A., *Anal. Cim. Acta*, 75(2), 297, 1975.

98. Jirka, A., Carter, M., *Anal. Chem.*, 50(1), 91, 1978.

99. Randlesome, J., Aston, S., *Environ. Technol. Lett.*, 1(1), 3, 1980.

100. Kennedy, K., Crock, J., *Anal. Lett.*, 20(6), 889, 1987.

101. Van Delft, W., Vos, G., *Anal. Chim. Acta*, 209(1-2), 147, 1988.

102. Wigfield, D., Daniels, R., *J. Anal. Toxicol.*, 13(3), 191, 1989.

103. Ingle, Jr., J., Crouch, S., Spectrochemical Analysis, Prentice Hall, Englewood Cliffs, New Jersey, 1988.

104. Omenetto, N., *Spectrochim. Acta*, 44B, 131, 1989.

105. Neumann, S., Kriese, M., *Spectrochim. Acta*, 29B, 127, 1974.

106. Falk, H., Tilch, J., *J. Anal. At. Spectrom.*, 2(6), 527, 1987.

107. Wei, G., Dougherty, J., Preli, Jr., F., Michel, R., *J. Anal. At. Spectrom.*, 5(3), 249, 1990.

108. Preli, Jr., F., Dougherty, J., Michel, R., *Anal. Chem.*, 59(14), 1784, 1987.

109. Vera, J., Stevenson, C., Smith, B., Omenetto, N., Winefordner, J., *J. Anal. At. Spectrom.*, 4(7), 619, 1989.

110. Vera, J., Leong, M., Stevenson, C., Petrucci, G., Winefordner, J., *Talanta*, 36(12), 1291, 1989.

111. Bolshov, M., Zybin, A., Koloshnikov, V., Mayorov, I., Smirenking, I., *Spectrochim. Acta, Part B*, 41B(5), 487, 1986.

112. Bolshov, M., Zybin A., Koloshnikov, V., Smirenkina, I., *Spectrochim. Acta, Part B*, 43B(4-5), 519, 1988.

113. Bolshov, M., Boutron, C., Zybin, A., *Anal. Chem.*, 61(15), 1758, 1989.

114. Bolshov, M., Koloshnikov, V., Boutron, C., Patterson, C., Barkov, N., *Optoelectron. Environ. Sci.*, 54, 185, 1991.

115. Bolshov, M., Koloshnikov, V., Rudnev, S., Boutron, C., Gorlach, U., Patterson, C., *J. Anal. Atom. Spectrom.*, 7, 99, 1992,

116. Remy, B., Verhaeghe, I., Mauchien, P., *Appl. Spectrosc.*, 44(10), 1633, 1990.

117. Liang, Z., Wei, G., Irwin, R., Walton, A., Michel, R., Sneddon, J., *Anal. Chem.*, 62(14), 1452, 1990.

118. Sjöström, S., *Spectrochimica Acta Reviews*, 13(6), 407, 1990.

119. Wiese, W., Martin, G., Wavelengths and Transition Probabilities for Atoms and Atomic Ions, NIST, Washington, D.C., 1980.

120. Butcher, D., Dougherty, J., Preli, Jr., F., Walton, A., Wei, G., Irwin, R., Michel, R., *J. Anal. At. Spectrom.*, 3, 1059, 1988.

121. Dittrich, K., Stärk, H., *J. Anal. At. Spectrom.*, 1, 237, 1986.

122. Welz, B., Schlemmer, G., Ortner, H., Wegscheider, W., *Prog. Analyt. Spectrosc.*, 12(2), 111, 1989.

123. Wu, S., Chakrabarti, C., Rogers, J., *Prog. Analyt. Spectrosc.*, 10(2/3), 111, 1987.

124. Katskov, D., *Spectrochimica Acta Reviews*, 14(6), 409, 1991.

125. Styris, D., Redfield, D., *Spectrochimica Acta Reviews*, 15(2), 71, 1993.

126. Holcombe. J., Rayson, G., *Prog. Analyt. Atom. Spectrosc.*, 6(3), 225, 1983.

127. Tsalev, D., Slaveykova, V., Mandjukov, P., *Spectrochimica Acta Reviews*, 13(3), 225, 1990.

128. Falk, H., *Prog. Analyt. Atom. Spectrosc.*, 5(213), 205, 1982.

129. Delfino, J., Department of Environmental Engineering Sciences, University of Florida, Gainesville, Florida, 32611.

130. Alkemade, C., Hollander, Tj., Snelleman, W., Zeegers, P., Metal Vapours in Flames, Pergamon Press, The Netherlands, 1982.

131. Callear, A., Photochemistry and Reaction Kinetics, The University Press, Oxford, UK, 1967.

132. Kraulinya, E., The Sensitized Fluorescence of Metal Vapor Mixtures, Publishing House of State University of Latvin, Latvin, USSR, 1968.

133. Massey, H., Burhop, E., Gilbody, H., Electronic and Ionic Impact Phenomenon Volume 3, Clarendon, UK, 1971.

134. Gilmore, F., Bauer, E., Mc Gowan, J., *J. Quant. Spectrosc. Radiat. Transfer*, 9, 157, 1969.

135. Krause, L., The Physics of Electronic and Atomic Collisions, North-Holland, Amsterdam, 1972.

136. Krause, L., The Excited State in Chemical Physics, Interscience-Wiley, New York, 1975.

137. Elbel, M., Progress in Atomic Spectroscopy, Part B, Plenum, New York, 1979.

138. Callear, A., *Appl. Opt.*, Supplement No. 2, 145, 1965.

139. Czajkowski, M., Skardis, G., Krause, L., *Can J. Phys.*, 51, 334, 1973.

140. Turro, N., Modern Molecular Photochemistry, Benjamin/Cummings Co., Inc., Meulo Park, California, 1978.

141. Cundall, R., Gilbert, A., Photochemistry, ACC, New York, 1970.

142. Benck, E., Lawler, J., *J. Opt. Soc. Am. B*, 6(1), 11, 1989.

143. Application notes: OS-14 (1991), GM-1 (1988), GM-13 (1989), OS-15 (1991), CEM Corporation, P.O. Box 200, Matthews, N.C., 28106.

144. Ryan, D., Department of Chemistry, University of Massachusetts Lowell, Lowell, Massachusetts, 01854.

145. Walker, G., Environmental Science Trace Metal Lab, University of Massachusetts Boston, Boston, Massachusetts.

146. Questron Corporation, P.O. Box 2387, Princeton, NJ, 08543.

BIOGRAPHICAL SKETCH

Stefanie T. Pagano was born in Passaic, New Jersey, on December 20, 1966. In 1972, she moved to Jacksonville, Florida, with her mother, brother, and sister. In Jacksonville, she attended Bishop Kenney High School, where she attained the rank of Lieutenant in the Naval J.R.O.T.C. program and received the American Legion Award before receiving her diploma suma cum laude in 1984.

In 1984, while pursing her interest in Naval R.O.T.C., she attended George Washington University in Washington, D.C., as a political science major. After an athletic injury ended a future with the Navy, she moved back to Jacksonville and attended Florida Junior College as a business major. She received her Associate of Arts degree with High Honors in 1986. In 1987, she entered the University of Florida as a chemistry major and was Secretary of the U.F. Chemistry Society from 1987 to 1988 and President from 1988 to 1989. After receiving her Bachelor of Science degree in chemistry in 1989, she entered the Graduate School at the University of Florida, where she conducted research under Dr. James D. Winefordner. In the summer of 1992, she worked as an intern for the agricultural firm Viljavuuspalvelu Oy in Helsinki, Finland.

She is a member of the American Chemical Society, Society for Applied Spectroscopy, American Association for the Advancement of Science, Phi Theta Kappa, American-Scandinavian Foundation, and Amnesty International.

I certify that I have read this study and that in my opinion it conforms to acceptable standards of scholarly presentation and is fully adequate, in scope and quality, as a dissertation for the degree of Doctor of Philosophy.

James D. Winefordner, Chair
Graduate Research Professor of Chemistry

I certify that I have read this study and that in my opinion it conforms to acceptable standards of scholarly presentation and is fully adequate, in scope and quality, as a dissertation for the degree of Doctor of Philosophy.

Vaneica Young
Associate Professor of Chemistry

I certify that I have read this study and that in my opinion it conforms to acceptable standards of scholarly presentation and is fully adequate, in scope and quality, as a dissertation for the degree of Doctor of Philosophy.

Martin Vala
Professor of Chemistry

I certify that I have read this study and that in my opinion it conforms to acceptable standards of scholarly presentation and is fully adequate, in scope and quality, as a dissertation for the degree of Doctor of Philosophy.

David Powell
Associate Scientist of Chemistry

I certify that I have read this study and that in my opinion it conforms to acceptable standards of scholarly presentation and is fully adequate, in scope and quality, as a dissertation for the degree of Doctor of Philosophy.

Cheng Wei
Professor of Food Science & Human Nutrition

This dissertation was submitted to the Graduate Faculty of the Department of Chemistry in the College of Liberal Arts and Sciences and to the Graduate School and was accepted as partial fulfillment of the requirements for the degree of Doctor of Philosophy.

April, 1994

_____

Dean, Graduate School